Fall 2013

Smooth Muscle-Specific Removal of Brain-Derived Neurotrophic Factor Results in Increased Vagal Afferent Innervation to the Intestine and Increased Satiation in Mice

Jessica Erin Biddinger
Purdue University

Graduate School ETD Form 9
(Revised 12/07)

PURDUE UNIVERSITY
GRADUATE SCHOOL
Thesis/Dissertation Acceptance

This is to certify that the thesis/dissertation prepared

By Jessica Erin Biddinger

Entitled

Smooth Muscle-Specific Removal of Brain-Derived Neurotrophic Factor Results in Increased Vagal Afferent Innervation to the Intestine and Increased Satiation in Mice

For the degree of Doctor of Philosophy

Is approved by the final examining committee:

Edward Fox
Chair

Kimberly Kinzig

Terry L. Powley

Edward Bartlett

To the best of my knowledge and as understood by the student in the *Research Integrity and Copyright Disclaimer (Graduate School Form 20)*, this thesis/dissertation adheres to the provisions of Purdue University's "Policy on Integrity in Research" and the use of copyrighted material.

Approved by Major Professor(s): Edward Fox

Approved by: Christopher R. Agnew 11/6/13
Head of the Graduate Program Date

SMOOTH MUSCLE-SPECIFIC REMOVAL OF BRAIN-DERIVED NEUROTROPHIC FACTOR RESULTS IN INCREASED VAGAL AFFERENT INNERVATION TO THE INTESTINE AND INCREASED SATIATION IN MICE

A Dissertation

Submitted to the Faculty

of

Purdue University

by

Jessica Erin Biddinger

In Partial Fulfillment of the

Requirements for the Degree

of

Doctor of Philosophy

December 2013

Purdue University

West Lafayette, Indiana

ACKNOWLEDGEMENTS

I would like to thank everyone who made this dissertation possible. Without the help of all of you along the way, I would have never been able to achieve this goal. Dr. Ed Fox, you have been the most amazing mentor I could have ever asked for. I have the highest respect for you both personally and professionally. I will never forget the good times we shared and the rough spots we somehow made it through. Thank you to the rest of my committee members: Drs. Terry Powley, Kim Kinzig, and Ed Bartlett, for your helpful comments during my meetings and presentations. Your input has improved my project and my scientific thinking, and made me a better scientist. Thank you to my friends - I could not have made it out alive without you guys. I also want to thank my parents, for always being there for me and for listening to my never ending worries. And to my husband, Jon, you already know. I can't express in words how grateful I am for your support. I could have never done this without you.

Thank you, everyone, for being there for me. I hope I have made you proud.

TABLE OF CONTENTS

Page

Page

LIST OF TABLES

LIST OF FIGURES

Appendix Figure Page

Appendix Figure Page

Appendix Figure Page

LIST OF ABBREVIATIONS

Ach = acetylcholine

ANOVA = analysis of variance

AP = area postrema

ARC = arcuate nucleus of the hypothalamus

BDNF = brain-derived neurotrophic factor

BrdU = bromodeoxyuridine

CCK = cholecystokinin

CGRP = calcitonin gene-related peptide

Chopper = cytoplasmic juxtamembrane death domain

CNS = central nervous system

CTF = C-terminal fragment

DMH = dorsomedial nucleus of the hypothalamus

DMV = dorsal motor nucleus of the vagus

DRG = dorsal root ganglion

E = embryonic day

EPSP = excitatory postsynaptic potential

GDNF = glial cell line-derived neurotrophic factor

GI = gastrointestinal

GLP-1 = glucagon-like peptide-1

ICC = interstitial cells of Cajal

IGLE = intraganglionic laminar ending

IMA = intramuscular array

KI = knockin

KO = knockout

LH = lateral hypothalamic area

LTP = long-term potentiation

NA = nucleus ambiguus

NGF = nerve growth factor

NT-3 = neurotrophin-3

NT-4 = neurotrophin-4

NT-6 = neurotrophin-6

NT-7 = neurotrophin-7

NTS = nucleus of the solitary tract

P = postnatal day

PBN = parabrachial nucleus

PFA = paraformaldehyde

PNS = peripheral nervous system

PVN = periventricular nucleus of the hypothalamus

PYY = peptide YY

QPCR = quantitative polymerase chain reaction

RT-PCR = reverse-transcriptase polymerase chain reaction

SAM = slowly-adapting mechanoreceptor

SCG = superior cervical ganglion

SDA = subdiaphragmatic deafferentation

Sema 3D = semaphorin 3D

SF-1 = steroidogenic factor-1

SM = smooth muscle

Trk = tyrosine kinase

TS = solitary tract

TUNEL = terminal deoxynucleotidyl transferase dUTP nick end labeling

WGA-HRP = wheatgerm agglutinin – horseradish peroxidase

WT = wild type

ABSTRACT

Biddinger, Jessica Erin. Ph.D., Purdue University, December 2013. Smooth Muscle -Specific Removal of Brain-Derived Neurotrophic Factor Results in Increased Vagal Afferent Innervation to` the Intestine and Increased Satiation in Mice. Major Professor: Ed Fox.

Vagal afferents transmit signals regarding food-derived stimuli in the gastrointestinal (GI) tract to the brain. Vagal mechanoreceptors called intraganglionic laminar endings (IGLEs) innervate the smooth muscle wall of GI organs and detect stretch and tension to regulate GI reflexes and satiation. Brain-derived neurotrophic factor (BDNF) is expressed in the smooth muscle of developing GI organs when vagal afferents from the nodose ganglion begin to innervate the GI tract. Therefore, it was hypothesized BDNF is necessary for development of vagal afferents that innervate this tissue. Targeted smooth muscle-specific BDNF homozygous knockout (BDNF SM -/-) mice were generated and .vagal afferent innervation and analysis of feeding behavior were compared to wild type (wt) mice. IGLEs and axons in the GI tract were labeled by injection of the nerve tracer horseradish peroxidase conjugated to wheatgerm agglutinin (WGA-HRP) into the nodose ganglion. Nodose ganglion neurons were also quantified to investigate the contribution of vagal sensory neurons to IGLE density. Meal pattern and microstructure analyses were used

to determine if any underlying changes in the mechanisms that regulate feeding were associated with altered vagal function. Contrary to expectations for knockout (KO) of a growth factor gene, BDNF SM -/- mice showed increased IGLE density in the intestine compared to controls, whereas those supplying the stomach exhibited normal density. BDNF SM -/- mice showed an increase in total vagal sensory neuron number compared to wild-type (wt) mice as well as increases in the number of larger-diameter longitudinal axon bundles in the intestine. BDNF SM -/- mice exhibited decreases in meal duration and meal size compared to wt mice, suggesting food is more satiating in BDNF SM -/- mice compared to controls. Mutants also showed increased satiety ratio, suggesting a given amount of food produced greater satiety. Consistent with vagal afferent mediation of increased satiation in mutants, initial rate of food intake was similar in mutants and controls, but the subsequent sustained intake rate over min 6-30 was reduced in mutants. The increase in vagal sensory neuron and axon bundle numbers in BDNF SM -/- mice suggests GI BDNF may normally suppress survival of vagal GI afferents.

INTRODUCTION

Metabolic homeostasis is a complex process that involves coordinated networks of several neural and hormonal interactions in both the central (CNS) and peripheral nervous systems (PNS) to maintain energy balance. In the PNS, the control of visceral functions primarily occurs through the autonomic nervous system. Many of these visceral functions, such as regulation of heart rate, breathing, perspiration, and digestive functions, operate below the level of consciousness and are critical to sustaining life. There are two main subdivisions that comprise the autonomic nervous system: the sympathetic branch, which controls visceral functions during stress, and the parasympathetic branch, which regulates visceral functions at rest. The vagus nerve is part of the parasympathetic branch of the autonomic system, and innervates visceral organs such as the heart, lungs, kidneys, liver, stomach, intestine, and bladder, among others. As such, the vagus nerve is important for many of the visceral functions necessary to maintain life. In particular, vagal innervation of the GI tract is critical for proper regulation of digestive functions such as nutrient absorption, gastric motility, secretion, and detection of toxins and inflammation, all of which influence food intake.

Vagal Circuit Involved in the Regulation of Food Intake

Vagal satiation signaling occurs through integration of peripheral satiety signals from the GI tract with CNS inputs to regulate food intake. The vagus nerve is composed of both sensory and motor components that are important for digestion and can influence food intake through regulation of gastrointestinal reflexes. In general, the sensory component of the vagus sends signals to the brain regarding the nutritional status of food in the GI tract and contributes to the regulation of digestive vago-vagal reflexes, whereas the vagal efferent innervation to the GI tract is the final common pathway that integrates peripheral sensory and CNS inputs to effect motor outputs that also control digestive functions such as reflexes and motility.

After food ingestion, information about the chemical and mechanical stimuli derived by the food are detected by sensory receptors in the GI tract and are then sent through vagal afferents carried by the solitary tract (TS) in the hindbrain. From the TS, excitatory glutamatergic projections continue on to the dorsal vagal complex, which is composed of two sensory nuclei, the nucleus of the solitary tract (NTS) and the area postrema (AP), and the dorsal motor nucleus of the vagus (DMV). The NTS distributes the sensory signals that arise from the gut throughout the rest of the brain, primarily through connections to the paraventricular nucleus of the hypothalamus (PVN), although there are less prominent connections from the NTS to other hypothalamic areas, such as the arcuate nucleus (ARC), dorsomedial nucleus (DMH), and lateral hypothalamic area (LH). From the PVN, the sensory signals

are sent throughout the rest of the hypothalamus and higher reward centers in the brain. Sensory information from the NTS also reaches the hypothalamus through the parabrachial nucleus (PBN). After sensory information has been processed throughout the brain, motor output responses are generated to regulate reflexes that contribute to food intake.

Vagal Regulation of Short-Term Food Intake

In addition to its many roles in digestion, the vagus primarily regulates short-term controls of food intake. The short term unit of food intake is a meal; therefore, vagal regulation of ingestive behavior occurs through meals, rather than the overall amount of food intake (Smith 1996). Many manipulations to test the role of the vagus in the regulation of food intake have generally not affected long-term food intake or body weight, particularly sensory-specific vagal manipulations (Berthoud 2008; Fox 2013). For example, rats with vagal subdiaphragmatic deafferentation (SDA) ingested larger meals; however the animals compensated for the increased meal size with a decrease in meal frequency, which resulted in no net change in total amount of food consumed (Schwartz et al., 1999). In addition, sensory vagotomy resulted in decreased suppression of food intake after intestinal nutrient infusion (Walls et al., 1995). These results suggest vagal deafferentation leads to decreased negative feedback signaling to the brain. Consistent with this, rats with chemical deafferentation using the neurotoxin capsaicin showed increased short term food intake and reduced suppression of food intake after CCK administration (Ritter & Ladenheim 1985). Capsaicin, the active ingredient in red chili

peppers, is a selective neurotoxin that destroys small-diameter sensory neurons, which make up a large portion of sensory innervation to the gut: approximately 50% of neurons in the nodose ganglion that project to the stomach and 70% of those innervating the duodenum are responsive to capsaicin (Peters et al., 2006). In addition to surgical and chemical manipulation of vagal afferents to study the contribution of the vagus in regulation of food intake, genetic ablation that interferes with vagal signaling also leads to changes in meal termination, or satiation, rather than more hedonic or motivational controls of food intake. For example, neutrophin-4 (NT-4) knockout mice showed a 90% loss of vagal mechanoreceptors in the intestine, which was associated with decreased satiation, as demonstrated by increased meal size on a liquid diet and increased meal duration on a solid diet. These effects were compensated for by trends toward decreased meal frequency and decreased feeding rate, resulting in no change in total food intake or body weight (Fox et al., 2001a).

In contrast to the sensory-specific approaches used to determine the role of vagal afferents in food regulation, total vagotomy methods that lesion both sensory and motor components of vagal innervation to the gut have resulted in altered total food intake. Total vagotomy surgeries have resulted in a counterintuitive decrease in total food intake that is associated with a loss of body weight in both humans and rodents (Faxen et al., 1979; Mordes et al., 1979; Laskiewicz et al., 2003; Kral et al., 2009). Animals with total vagotomy also show a decrease in abdominal body fat (Stearns et al., 2012), suggesting

vagal innervation may also play a role in long-term control of body adiposity. The decrease in food intake and body adiposity may be due to damaged motor innervation that interferes with gastric motility or reflexes, although this is unclear (Fox 2013). Manipulations that ablate both sensory and motor vagal innervation make it difficult to disentangle the independent roles of each component of vagal GI innervation to the regulation of food intake.

Characterization of Vagal Innervation to the Gut

Vagal efferents arise from the nucleus ambiguus (NA) and DMV in the brainstem, while vagal afferents originate from the nodose ganglion. The majority of total vagal innervation is sensory, as it has been reported that up to 73% of the total vagal fibers are afferent, and the remaining fibers efferent (Fox & Powley 1985; Prechtl & Powley 1985, 1990). Abdominal vagal innervation is also primarily sensory, although there appears to be more motor innervation than originally thought (Prechtl & Powley 1985, 1990).

Vagal afferents innervating the GI tract terminate in sensory receptors called chemoreceptors and mechanoreceptors, which are located in the mucosal/lamina propria and smooth muscle/myenteric plexus walls of the GI tract, respectively. These receptors detect chemical and mechanical stimuli from food in the GI tract to regulate digestion functions and feeding through GI reflexes and negative feedback to the CNS. However, it is not clear how sensory information is encoded and transduced by these receptors, as the rapidly-adapting mechanoreceptors in the mucosa also have chemoreceptive

properties, in contrast to the mechanoreceptors located in the smooth muscle, which are slowly-adapting mechanoreceptors.

Chemoreceptors detect the chemical components of food and peptides and neurotransmitters released by the presence of food. Signals detected by chemoreceptors include hormones released from the GI tract. These hormones act as nutritional signals regarding the contents of the gut and relay this information back to the brain to effect a response (Schwartz et al., 1991; Peters et al., 2006; Berthoud 2008; Zhang et al., 2010; Chu et al., 2013). Some of the more well-characterized gut hormones that regulate satiety include cholecystokinin (CCK), glucagon-like-peptide-1 (GLP-1), and Peptide YY (PYY). All of these hormones are released in response to a meal and act to decrease short-term food intake through vagal signaling (Schwartz et al., 1991; Abbott et al., 2005; Koda et al., 2005; Peters et al., 2006; Rüttimann et al., 2009). In contrast, ghrelin is the only known appetitive hormone and is secreted by the stomach to increase food intake (Bowers et al., 1984; Kojima et al., 1999; Wren et al., 2001). Like the satiety hormones released by the GI tract, ghrelin also acts via vagal afferent signaling, and there is evidence that ghrelin functions to increase food intake by decreasing the sensitivity of vagal afferents (Page et al., 2007). There are two primary pathways circulating GI hormones utilize to effect responses on digestive functions: (1) hormones released by the gut travel through the blood to act directly in the CNS, and (2) receptors located in the gut respond to GI hormones and these signals travel to the NTS through vagal afferents. The relative importance and consequences of

these two divergent pathways is not clear. For example, there are CCK receptors on vagal terminals in the GI tract and on the smooth muscle, but CCK receptors are also present in the brain, including the NTS (Hill et al., 1987; Wank et al., 1992; Ritter et al. 1994; Broberger et al., 2001). Therefore, it is unknown exactly how CCK contributes to regulation of food intake, as there are multiple pathways used to effect a response.

Three main types of vagal afferent chemoreceptors have been identified: crypt and villus afferents, which are located in the lamina propria within the intestinal mucosa and innervate crypts and villi, respectively (Berthoud et al., 1995; Powley et al., 2011), and the more recently identified antral gland afferent, located in the antrum of the stomach (Powley et al., 2011). Villus afferents and their terminals are located in close proximity to enterocytes, by which they are thought to indirectly detect chemical signals secreted from these cells through a paracrine mechanism (Li et al., 2001; Powley et al., 2011). Crypt afferents encircle mucosal crypts in a ring-like fashion and have been proposed to have many different functions, including relay of paracrine signaling, chemoreception, and mobilization of reflexes. The mucosal antral gland afferents are located along the antral wall of the stomach and form terminals just below the epithelium of the lumen. Interestingly, antral gland afferents appear to function as both chemo- and mechanoreceptors, as these afferents that innervate the antral mucosa of the stomach are responsive to both pH and light mechanical stimulation, although not to the same extent as manipulations that produced greater tension and stretch that activate

mechanoreceptors in the smooth muscle (Clarke & Davison 1978; Powley et al., 2011).

Mechanoreceptors in the smooth muscle wall have been proposed to detect stretch and tension, which contribute to satiation through regulation of GI reflexes (Phillips & Powley 2000; Fox et al., 2001a; Zagorodnyuk et al., 2001). Two main types of presumptive vagal mechanoreceptor endings have been identified: intramuscular arrays (IMAs) and intraganglionic laminar endings (IGLEs).

The IMA ending type is located primarily in the longitudinal and circular muscle layers of the forestomach and the circular layer of the esophageal and pyloric sphincters (Berthoud & Powley 1992; Wang & Powley 2000; Fox et al., 2000). They have also been identified in the intestine, although very rarely. The terminals of IMAs are arranged in a rectilinear fashion, parallel to muscle fibers and to each other as they course through the smooth muscle. The morphology and location of IMAs suggests they serve as stretch and length detectors, as they are located almost exclusively where stretching occurs, which include the forestomach where food is collected, and the sphincters, which regulate the movement of food through the GI tract and prevent reflux of digested food back up through the alimentary canal. Mice lacking interstitial cells of Cajal (ICCs), also called c-Kit mutant mice, display a selective reduction in IMA density compared to wild type (wt) mice, suggesting ICCs are required for normal development of IMAs (Fox et al., 2001b). The ICCs are important for peristaltic reflexes in the GI tract, as they serve as pacemaker cells that generate slow

waves to contract the muscles of the GI tract wall. The ligand for c-Kit receptors, steel factor, is also necessary for normal development of IMAs, as mice lacking steel also show decreased IMA density and decreased ICC number. Steel factor mice ate smaller meals but compensated for decreased meal size by increased meal frequency, which resulted in normal daily food intake (Fox et al., 2002). The ICC mutations appear to be selective for IMAs, as both c-Kit and steel mutant mice displayed normal IGLE structure, distribution, and density (Fox et al., 2001b, 2002). Therefore, ICCs have a trophic effect on the development or maintenance of IMAs. Electrophysiological evidence detailing the function of IMAs has thus far been lacking, but the few studies that have attempted to characterize the function of presumptive IMAs are consistent with the proposed function of muscle length and stretch receptors (Blackshaw et al., 1987; Page & Blackshaw 1998, 1999).

The other class of vagal afferent mechanoreceptors, the IGLEs, have a much greater distribution than IMAs and are located throughout the esophagus, stomach, and intestine. The IGLE ending type was first identified by Nonidez in the esophagus of the dog in 1946, and was further characterized by others (Nonidez 1946; Rodrigo et al., 1975; Neuhuber 1987; Berthoud & Powley 1992; Berthoud et al., 1997; Wang & Powley 2000; Fox et al., 2000; Zagorodynuk et al., 2001). The IGLEs are the most numerous mechanoreceptor class in both the stomach and intestine. They are found most densely in the stomach, but also in very high densities in the proximal duodenum and decrease caudally down the length of the intestine. IGLEs are

found in the myenteric plexus, between the circular and longitudinal layers of the smooth muscle in the GI tract wall. These terminals consist of flattened aggregates of terminal puncta in close apposition to myenteric ganglia. It has been proposed that IGLEs, due to their morphology and their location in the myenteric plexus between the two tissues that comprise the smooth muscle, detect the shearing forces between these two muscle layers (Neuhuber & Clerc 1990). Zagorodynuk et al. (2001) showed vagal afferents to the gut are slowly-adapting C-fibers that terminate in IGLEs, which respond to muscle tension and contraction.

Functions of Brain-Derived Neurotrophic Factor

There are many factors that shape the development of vagal afferents innervating the GI tract and can therefore influence their function. Function of vagal afferents could be impacted through altered development or by altered function directly during adulthood. One family of growth factors that is critical to the survival of vagal sensory neurons and their projections are the neurotrophins. Neurotrophins are important for the growth, differentiation and survival of new neurons in development, and the survival and maintenance of existing neurons in adulthood. The family of neurotrophins includes nerve growth factor (NGF), brain-derived neurotrophic factor (BDNF), neurotrophin-3 (NT-3), NT-4/5, neurotrophin-6 (NT-6), and neurotrophin-7 (NT-7). All of the neurotrophins are structurally similar, as they share a high degree of sequence similarity. Neurotrophins are small homodimeric polypeptides that are composed of 120 amino acid residues (McDonald et al. 1991) and signal

through the tyrosine kinase (Trk) family of receptors. Each neurotrophin signals through a particular high-affinity receptor, with NGF, NT-6, and NT-7 signaling through the TrkA receptor, BDNF and NT-4 sharing the TrkB receptor, and NT-3 signaling through the TrkC receptor. In addition to these specific high-affinity receptors, all of the neurotrophins can signal through the promiscuous low-affinity nerve growth factor receptor p75. One primary mechanism of action of the neurotrophins is their ability to regulate the survival of neurons and their axonal projections through regulation of their expression in the target tissue (Levi-Montalcini & Angeletti 1968; Lindsay 1988). The target tissue produces a certain level of neurotrophic factors that allow for survival of a finite density of axons and axon terminals. An overabundance of axons and terminals are produced during development; however, precise combinations and levels of neurotrophic factor expression allows for the survival of the strongest connections to the target tissue, while the remaining weaker innervation is pruned (Sanes & Lichtman 1999; Reichardt 2006; Johnson et al., 2007).

One neurotrophic factor of particular importance is BDNF. It has many functions, which include its well-known role in development as a growth and survival factor, but it has also been shown to function as a neurotransmitter and a neuromodulator, as BDNF has the ability to modulate other neurotransmitters or act as a neurotransmitter itself. A well-known role for BDNF is emerging as a mediator of synaptic modifications through activity-dependent mechanisms (Caleo et al., 2000; Pezet et al., 2002; Kuczewski et al., 2009; Tyler & Pozzo-Miller 2010; Huang et al., 2012). For example,

application of BDNF resulted in an increase in synaptic vesicles in excitatory presynaptic terminals on dendritic spines in the CA1 region of the hippocampus. The frequency of AMPA receptor-mediated excitatory postsynaptic potentials (EPSPs) in CA1 neurons in the hippocampus also increased upon BDNF exposure (Tyler & Pozzo-Miller 2010). In addition, Zhang & Poo (2002) showed an increase in acetylcholine (ACh) neurotransmitter secretion when BDNF was applied to the presynaptic axon. The ACh potentiation was associated with an increase in $[Ca^{2+}]_i$ in the axon. Also, BDNF and its TrkB receptor are involved in the plasticity of synaptic connections involved with learning and memory, as mice heterozygous for the BDNF gene have impaired long-term potentiation (LTP) (Korte et al., 1995).

In addition to the well-known roles of BDNF in development and learning and memory, BDNF is also becoming increasingly implicated as a hormone-like satiety factor important for feeding behavior and energy balance. Removal of BDNF genetically has repeatedly shown hyperphagia and obesity (Lyons et al., 1999; Kernie et al., 2000; Rios et al., 2001; Xu et al., 2003; Coppola & Tessarollo 2004; Fox & Byerly 2004; Unger et al., 2007; Camerino et al., 2012; Liao et al., 2012; Fox et al., 2013). The first report of a potential role for BDNF in the regulation of food intake and body weight was accidental, as researchers noticed attenuated weight gain in rats that were administered BDNF to test the role of BDNF on the function of presynaptic cholinergic hippocampal neurons (Lapchak & Hefti 1992; Vanevski & Xu 2013). Global-heterozygous BDNF KO

(BDNF +/-) mice were initially used as a genetic model to study the contribution of BDNF to intracellular regulatory pathways that control development and influence LTP. These BDNF +/- mice showed increased body weight, increased adipocyte density, and they were also insulin and leptin resistant, suggesting the mice were obese and diabetic (Lyons et al., 1999; Kernie et al., 2000). Infusion of BDNF or NT-4 into the third ventricle reversed the obesity in these mice and their body weights reverted to wt body weight. After this initial accidental discovery of a role for BDNF in regulation of body homeostasis, many other studies repeated these findings and expanded upon them. As a result, many genetic and pharmacological approaches have consistently found that removal of BDNF results in hyperphagia and obesity (Rios et al., 2001; Xu et al., 2003; Fox & Byerly 2004; Unger et al., 2007; Liao et al., 2012) and infusion of BDNF or TrkB both centrally and peripherally have consistently reduced food intake and body weight gain in mice and rats (Pelleymounter et al., 1995; Bariohay et al., 2009; Toriya et al., 2010; Spaeth et al., 2012), indicating BDNF is emerging as an important mediator of food intake and body weight regulation.

BDNF and Vagal Sensory Innervation

The majority of vagal sensory neurons depend on BDNF for survival, as 60% of neurons in the nodose ganglion are lost in global homozygous BDNF KO mice, compared to 41% and 43% losses in NT-3 and NT-4 KO mice, respectively (Erickson et al., 1996; ElShamy & Ernfors 1997). BDNF is widely distributed throughout the brain, in both neurons and glia. However, it is also

expressed at high levels in peripheral tissues that are innervated by vagal afferents in both embryonic and adult stages of development. Peripheral organs with high BDNF mRNA and protein levels are composed of smooth muscle layers, including the stomach, small intestine, large intestine, blood vessels and epithelial tissues. In fact, the lungs, heart, stomach, duodenum, colon, liver, and pancreas all have higher protein BDNF levels than the brain in mice at 2 months of age (Lommatzsch et al., 1999). In addition, the receptor for BDNF, TrkB, is also expressed in the nodose ganglion and in the enteric neurons of the GI tract (Zhuo & Helke 1996), indicating that BDNF can bind to and interact with its receptor on vagal afferent terminals to effect a response in GI tissues. However, importantly, neither TrkB nor p75 are present in the smooth muscle itself (Lommatzsch et al., 1999). This indicates BDNF cannot bind to its receptors to mediate a response in the GI smooth muscle.

BDNF expression is initiated in GI tissues innervated by vagal afferents in embryonic development, when vagal afferents begin to reach their target destinations in the GI tract, indicating that BDNF may be necessary for the proper development of vagal afferents into the GI tract. The nodose ganglion begins to develop between embryonic day (E) 10-E12 (Rinaman & Levitt 1993; ElShamy & Ernfors 1997), and initiation of BDNF expression in the embryonic GI tract begins to occur at E12 (Fox et al., 2013). Vagal sensory fibers are first observed extending into the embryonic gut at approximately E12 (Murphy & Fox 2007) while efferent preganglionic fibers arrive in the GI tract at E13 (Sang & Young 1998; Rinaman & Levitt 1993). Precursors of sensory and motor vagal

nerve terminals begin to develop in the GI tract between E15-E16.5 and have reached a mature pattern between postnatal day (P) 8-P10 (Swithers et al., 2002; Murphy & Fox 2007). As stated before, BDNF is important for the survival of vagal sensory neurons (ElShamy & Ernfors 1997). Consistent with a role for BDNF in the development of vagal GI afferents, Murphy & Fox (2010) showed mice lacking both copies of BDNF had disrupted vagal afferent innervation at P0, with a 50% decrease in IGLE density in the stomach compared to wild type mice.

In addition to its role in the development of the gut and the vagal afferents innervating it, BDNF may also be important for the function of vagal sensory innervation to mechanoreceptors in the GI tract. For example, Carroll et al. (1998) showed slowly-adapting mechanoreceptors (SAMs) innervating the skin in juvenile BDNF KO mice had impaired neuronal responses, as these mice demonstrated decreased mean afferent impulses that were caused by a reduction in mechanical sensitivity. Since a majority of vagal afferents innervating the smooth muscle of the GI tract important for feeding are also SAMs, it is possible the function of vagal afferents that signal back to the brain regarding the nutritional status of the GI tract would also be altered by loss of BDNF-like mechanoreceptors in the skin.

Rationale and Hypotheses

Based on the concomitant spatial and temporal pattern of BDNF expression and development of vagal afferents extending into the GI tract, in this project, I hypothesized GI BDNF is necessary for the development of vagal

afferent innervation in the GI tract, which would subsequently affect ingestive behavior. This hypothesis was tested using a genetic approach, since the use of transgenic animals to knock out the function of the BDNF gene in a tissue-specific manner allows for deconstruction of how GI BDNF contributes to the development of vagal afferents in the smooth muscle of the GI tract and how this potentially impacts feeding behavior. Additionally, because BDNF is found throughout the brain and periphery, including the nodose ganglion and CNS sites important for the regulation of energy balance, it is important to determine the contribution of GI BDNF in the smooth muscle to these processes.

Targeting BDNF knockout to the smooth muscle allows for determination of the impact of BDNF on the development of IGLEs, as these vagal afferent mechanoreceptors are located in the smooth muscle layer of the GI tract wall. In this project, both BDNF alleles are removed from the smooth muscle in order to determine the effect of GI BDNF on the development of the vagus nerve and how it contributes to feeding behavior. Mice with a targeted knockout of BDNF to the smooth muscle should theoretically have BDNF removed from only the smooth muscle with BDNF remaining present in all other tissues.

Because BDNF is hypothesized to be necessary for the development of GI vagal afferents, I predicted loss of GI BDNF would lead to a decrease in vagal afferent innervation in the GI tract in the mutant mice. The decrease in vagal sensory innervation of the GI tract would result in decreased IGLE density in GI organs such as the stomach and intestine. Loss of BDNF from the

smooth muscle would also lead to a decrease in vagal afferent fibers and bundles innervating the GI tract. IGLEs in the stomach and intestine could be decreased through several different ways: they may fail to survive, axons projecting outward from the nodose ganglion may fail to reach their final target destinations in the GI tract, or the neurons and/or terminals may fail to differentiate as a result of BDNF deficiency in GI smooth muscle.

Just as the density of vagal afferents is hypothesized to be altered due to loss of GI BDNF, function of vagal afferents in the GI tract could also be disrupted by smooth muscle-specific removal of BDNF. Vagal afferent function could be affected indirectly through developmental changes, which could subsequently lead to changes in vagal signaling, or the development of vagal afferents could remain intact, and function itself could be directly affected by BDNF. Furthermore, even if no differences in density emerge, then it is predicted that there could still be changes in function, because it has previously been shown that although mechanoreceptors in the skin did not have any morphological disruptions due to BDNF KO, they did show significantly decreased mechanical sensitivity (Carroll et al., 1998). As mechanoreceptors in the skin have similar mechanosensitive properties to IGLEs in the GI tract, negative vagal feedback signaling from the gut to the brain could be altered in mice missing BDNF from the smooth muscle.

Because I am predicting loss of BDNF from the smooth muscle leads to a decrease in IGLE density and/or function in the GI tract, I also predicted feeding behavior of the animals would subsequently be altered. Changes in

feeding behavior were studied through meal pattern and microstructure analyses, since these analyses serve as functional assays to test if there are changes in food ingestion that could be associated with changes in vagal function. This is important because any changes in meal patterns or meal microstructure help pinpoint mechanisms underlying any potential changes in food intake. For example, ingestion of larger meals may result from a lack of negative feedback signaling. Therefore, I predicted mutant mice missing GI BDNF would demonstrate increased meal size.

I also predicted BDNF smooth muscle knockout mice will not show any changes in total food intake or body weight, based on previous reports of the role of the vagus in regulation of food intake and body weight, as selective vagal deafferentations have repeatedly shown short-term changes in food intake but not long-term changes in total food intake that would impact body weight (Schwartz et al., 1999; Fox et al., 2001; Berthoud 2008; Fox 2013). For example, short term changes in food intake could occur in the mutant mice which would indicate alterations in vagal satiation feedback signaling, such as increased meal size. However, other compensatory changes could occur such that the mice ultimately maintain normal daily food intake and a stable, wild-type like body weight. This has been previously shown in other studies that have employed genetic and SDA manipulations and more specifically, neurotrophin transgenic mice, in order to study feeding patterns (Schwartz et al., 1999; Kelly et al., 2000; Fox et. al, 2001a; Chi et al., 2004; Powley et al., 2005; Fox et al., 2013).

An additional benefit of knocking out BDNF to study the role of the vagus is the ability to also separate out the sensory and motor components of vagal innervation to the GI tract. Although both vagal afferents and efferents are important for proper regulation of digestion, disentangling their respective roles has been difficult. This genetic approach is a sensory-specific manipulation, in contrast to surgical methods such as vagotomies, which eliminate or damage motor innervation in addition to sensory (Fox 2013). Deletion of BDNF from the smooth muscle selectively targets sensory vagal innervation, because Jones et al. (1994) showed BDNF is important for the survival and differentiation of sensory neurons, but is not essential for development of motor neurons. For example, there were no differences in neuron number between wild type and global homozygous BDNF KO mice (BDNF -/-) in several populations of motor neurons, including the DMV. However, in almost every sensory neuron population examined, BDNF -/- mice showed significant neuron loss at P15. These included the trigeminal, geniculate, vestibular and petrosal-nodose ganglia (Jones et al., 1994). In fact, the petrosal-nodose complex showed a 44% loss of neurons in BDNF -/- mice compared to controls (Jones et al., 1994). Additionally, BDNF -/- mice showed normal development of efferent innervation and myenteric neurons while sensory terminals in the GI tract showed a significant 50% loss (Murphy & Fox 2010). Therefore, in the GI tract, BDNF appears to selectively support the survival of vagal afferent innervation.

Complete knockout of BDNF results in perinatal lethality, so an approach that bypasses the tissues responsible for the lethal defects in respiratory function must be utilized in order to understand the function of this protein in adulthood (Erickson et al., 1996; Balkowiec & Katz 1998; Katz 2005). Therefore, this project utilized the cre-lox system to target removal of BDNF from the smooth muscle. The fatal respiratory defect observed in global homozygous KO mice is spared and the mice are viable.

METHODS

Animals

To generate a knockout of BDNF that is specific to the smooth muscle, the cre-lox system was used (Figure 1). In order to successfully employ the cre-lox strategy to remove BDNF from the smooth muscle, the following breeding strategy was utilized (Figure 2): First, SM22α$^{cre/cre}$ (also called transgelin^{cre}; Tg (TagIn-cre) 1Her/J) mice were obtained from Jackson Laboratories (cat no. 004746; Bar Harbor, ME). These are transgenic mice that express the enzyme cre recombinase only in smooth muscle. The strain was generated and maintained on a mixed background of 129S5/SvEvBrd, C57BL6 and SJL mice. Cre efficiency in these SM22α$^{cre/cre}$ mice was previously reported to be 100% recombination in the stomach, and 90% in the intestine (Lepore et al., 2005). These mice were then mated with floxed BDNF mice: these animals have the coding region of the BDNF gene surrounded by cre recombinase target sites called loxP sites (BDNF $^{lox/lox}$). Cre recombinase specifically recognizes loxP sites and has been shown to effectively mediate the excision of DNA located between loxP sites. These matings (SM22α$^{cre/cre}$; BDNF$^{+/+}$ x SM22α$^{+/+}$; BDNF$^{lox/lox}$) result in all of the offspring being double heterozygotic transgenic mice needed for the next round of mating (SM$^{cre/+}$; BDNF $^{+/lox}$).

These mice are then mated among themselves ($SM^{cre/+}$; $BDNF^{+/lox}$ x $SM^{cre/+}$; $BDNF^{+/lox}$) to produce the experimental groups of mice. This breeding strategy results in six different genotypic possibilities (Fig 2). These six genotypes generated are:

(1) $SM22\alpha^{+/+}$; $BDNF^{+/+}$ (wild type).

-These mice are the primary control group and are not missing any BDNF from the smooth muscle. These mice have normal levels of BDNF, with neither allele floxed, nor do they have the cre transgene.

(2) $SM22\alpha^{cre/+;}$ $BDNF^{+/+}$ (cre only)

-These mice do not have any floxed BDNF alleles; although they do have the cre recombinase transgene. However, because there are no loxP sites present, cre cannot bind, and therefore, no knockout will occur.

(3) $SM22\alpha^{+/+}$; $BDNF^{lox/lox}$ (double lox)

-These mice have both BDNF alleles floxed, but because they are missing the cre transgene, no DNA should be recombined between the lox sites, and all of the BDNF in the animal should remain present. It has been shown that insertion of lox P sites do not impact affect body weight (Rios et al., 2001).

(4) SM22α$^{+/+}$; BDNF$^{+/lox}$ (single lox)

-These mice have one floxed BDNF allele and do not have the cre transgene, therefore, just as with the animals in (3), will not have BDNF KO.

(5) SM22α$^{cre/+}$; BDNF$^{+/lox}$ (BDNF SM +/-)

-These mice are targeted heterozygotes, because while they have the cre transgene, they only have one floxed BDNF allele, so therefore approximately 50% of BDNF will be removed from the smooth muscle.

(6) SM22α$^{cre/+}$; BDNF$^{lox/lox}$ (BDNF SM -/-)

-These mice are the primary group for comparison to wt mice. They are targeted homozygotes that are missing both copies of BDNF from the smooth muscle and should have normal BDNF levels in the rest of the body.

The breeding strategy utilized in this study resulted in the generation of a total of 400 mice. A total of 20 Generation 1 mice (10 SM22α$^{cre/cre}$; BDNF$^{+/+}$ and 10 SM22α$^{+/+}$; BDNF$^{lox/lox}$) from the two founder strains maintained in the lab were used to breed Generation 2. These 10 matings of Generation 1 resulted in 74 Generation 2 pups. A total of 26 of these Generation 2 mice (13 males and 13 females) of the double heterozygous mice (SM$^{cre/+}$; BDNF $^{+/lox}$ x

$SM^{cre/+}$; $BDNF^{+/lox}$) were bred together to generate a total of 306 Generation 3 pups.

The percentages of pups obtained from each genotype are similar to predicted ratios according to Mendelian genetics. The distribution and number of pups generated from each genotype in Generation 3 is as follows:

wild-type: 26 pups, 8.5%

cre only: 58 pups, 18.95%

double lox: 22 pups, 7.19%

single lox: 48 pups, 15.69%

BDNF SM +/-: 101 pups, 33.01%

BDNF SM -/-: 51 pups, 16.66%

We have previously identified sites of SM22α cre-mediated recombination using Rosa26 and $BDNF^{lox\text{-}lacZ}$ reporter mice (Fox & Biddinger 2012; Fox et al., 2013). These mice allow for visualization of the KO location in the GI tract using a LacZ reporter. Rosa 26 reporter mice contain a floxed stop sequence in front of the LacZ gene. When cre recombinase binds to the lox sites, the stop sequence is removed and this allows for transcription of the β-galactosidase gene which can then be stained with X-gal. The $BDNF^{lox\text{-}lacZ}$ reporter mice allow for visualization of the KO by a method similar to that for the Rosa26 reporter mice. These experiments showed SM22α cre-mediated recombination occurs in the smooth muscle of blood vessels and mesentery in the GI tract at the same developmental age as GI afferents begin developing

into the GI tract (E12), making the SM22α cre suitable promoter to effectively KO BDNF from the smooth muscle.

All animals were genotyped at weaning using tail tips. Primer sequences used for genotyping were: BD3: 5' GGC TTC ATG CAA CCG AAG TAT G 3', BD ln1: 5' TGG GAT TGT GTT TCT GGT GAC 3', Cre 800: 5' GCT GCC ACG ACC AAG TGA CAG CAA TG 3', Cre 1200: 5' GCT GCC ACG ACC AAG TGA CAG CAA TG 3'. Amplified genomic DNA was visualized by gel electrophoresis on a 2% agarose gel with ethidium bromide added. All mice were maintained on a 12:12 hr light:dark cycle at 23°C with ad libitum access to a chow diet (Rodent Diet 5001; Purina, St. Louis, MO) and tap water, except during meal pattern and meal microstructure data collection periods. All procedures were conducted in accordance with the American Association for Accreditation of Laboratory Animal Care guidelines and were approved by the Purdue University Animal Care and Use Committee.

RNA Extraction and cDNA Synthesis

BDNF mRNA was extracted in order to verify the specificity of the KO of BDNF from smooth muscle organs. Wild type (n = 10) and BDNF SM -/- (n = 10) mice were sacrificed by cervical dislocation at 3-4 month of age. Prior work clearly showed BDNF was removed from GI tissues using the SM22α cre promoter at embryonic ages (Fox & Biddinger 2012; Fox et al., 2013), however it is unclear if cre-mediated recombination also occurs in the adult. Therefore, mice were sacrificed at 3-4 months old for RNA extraction in order to coincide with the anatomical and behavioral experiments in this study. Hypothalamus,

prefrontal cortex, whole ventral stomach, and the first 2 cm of duodenum were dissected and homogenized in Trizol (Invitrogen, Carlsbad, CA). Next, RNA was extracted by first separating the aqueous phase containing the RNA from the DNA-containing organic layer using choloroform. Then, the RNA was precipitated out with isopropyl alcohol and washed in 75% ethanol. The RNA concentration was determined from the optical density at 260 nm absorbance, and the purity of the RNA was calculated by the ratio of the 260 nm/280 nm absorbance. Each 1 µg RNA sample was incubated with DNase1 (Invitrogen) to remove genomic DNA and first-strand cDNA was synthesized using the Maxima enzyme mix (Thermo Scientific, Barrington, IL) in 20 µl PCR reactions. The PCR protocol for cDNA synthesis is as follows: 25°C for 10 min, 50°C for 15 min, and then the reaction was terminated by heating at 85°C for 5 min. This product was used in further RT-PCR and QPCR experiments to visualize and quantify BDNF mRNA expression (see below).

Qualitative Reverse Transcriptase Polymerase Chain Reaction (RT-PCR)

To visualize BDNF mRNA, qualitative RT-PCR was performed. After cDNA synthesis and DNase treatment, 2 µL cDNA was amplified using the *Taq* PCR_x DNA polymerase kit (Invitrogen). The PCR protocol used to amplify the cDNA was: 94°C for 3 min and 35 cycles with 94°C for 45 s, 55°C for 30 s, and 72°C for 90 s followed by 72°C for 10 min. Primer sequences employed were (Kawakami et al., 2002, Zermeno et al., 2009): BDNF forward: 5' GAA GAG CTG CTG GAT GAG GAC 3', BDNF reverse: 5' TTC AGT TGG CCT TTT GAT ACC 3', β-actin forward: 5' TGG TGG GTA TGG GTC AGA AGG ACT C 3',

β-actin reverse: 5' CAT GGC TGG GGT GTT GAA GGT CTC A 3'. β-actin cDNA from each sample was also amplified to assess the integrity of the isolated total RNA and reverse transcriptase was omitted in negative controls after Dnase treatment to confirm the removal of genomic DNA. Total PCR products were visualized by gel electrophoresis on a 2% agarose gel with ethidium bromide added.

Quantitative Reverse Transcriptase Polymerase Chain Reaction (QPCR)

In order to quantify the extent of BDNF mRNA loss from the smooth muscle, quantitative RT-PCR was performed. Amplification of 1μg cDNA from the first-strand reaction was performed in triplicate using the following PCR protocol: 95^{o}C for 10 min and 45 cycles with 95^{o}C for 30 s, 60^{o}C for 30 s, and 72^{o}C for 30 s (Unger et al., 2007; Cordeira et al., 2010). Primer sequences employed were (Cordeira et al., 2010): BDNF forward: 5’ GAA AGT CCC GGT ATC CAA AG 3’, BDNF reverse: 5’ CCA GCC AAT TCT CTT TTT 3’, β-actin forward: 5’ GGC TGT ATT CCCC TCC ATC G 3’, β-actin reverse: 5’ CCA GTT GGT AAC AAT GCC ATG T 3’. For each primer set, melt curve analysis was used to determine the appropriate concentration mRNA and to confirm the absence of primer dimers. These curves were created using serial dilutions and the PCR efficiency was calculated (Cordeira et al., 2010; Fox et al. 2013). All primers were optimized such that the correlation coefficient was 0.99–1.0 and the PCR efficiency was 95–100%. Real-time PCR amplification was performed using an iCycler and the iQ SYBR Green Supermix (BioRad, Hercules, CA).

Body Weight

Male and female mice were weighed once a week on the same day each week, except when mice were weighed daily during meal pattern and microstructure experiments. Body weight measurements of all genotypes generated were initiated at weaning, when the animals were 3 weeks of age, until meal pattern collection began at 3-4 months of age. Sample sizes included in the long-term body weight measurements are: males: wt (*n* = 7), cre only (*n* = 10), SM22α$^{+/+}$; single lox (*n* = 4), double lox (*n* = 6), BDNF SM +/- (*n* = 10), BDNF SM -/- (*n* = 10). Females: wt (*n* = 7), cre only (*n* = 10), single lox (*n* = 10), double lox (*n* = 2), BDNF SM +/- (*n* = 10), BDNF SM -/- (*n* = 10). Some of these same animals were included in the body composition and meal pattern analyses in order to be as efficient as possible with the transgenic mice. Mice in the body weight measurements described above that were also included in the body composition and meal pattern analyses were 7 male and 6 female wt mice and 7 male and 8 female BDNF SM -/- mice.

Body Composition

Fat and lean body masses were determined in wt (*n* = 13; 7 males, 6 females) and BDNF SM -/- (*n* = 15; 7 males, 8 females) mice using an EchoMRI whole-body composition analyzer (EchoMRI-900, Echo Medical Systems, LLC, Houston, TX) in live mice without anesthesia (Taicher et al., 2003; Tinsley et al., 2004). This quantitative nuclear magnetic resonance instrument was utilized to obtain precise measurements of body composition parameters, including total body fat, lean mass, body fluids, and total body

water. Fat and lean mass were calculated as total grams and also as a percent of total body mass. Body composition was measured on the day before meal pattern testing was initiated, prior to fasting, when the animals were 3-4 months of age. All of the mice used in the body composition analysis were the same mice used for the meal pattern analysis experiment.

Tracer Injections Into the Nodose Ganglion

To visualize vagal afferent innervation and vagal nerve terminals in the GI tract of BDNF SM -/- mice (n = 9; 5 males, 4 females) and controls (n = 12; 4 males, 8 females), the nerve tracer horseradish peroxidase conjugated to wheatgerm agglutinin (WGA-HRP) was injected into the nodose ganglion. This method was utilized because to date it is the only tracer that labels nearly the entire population of sensory vagal axons and their terminal endings (Mesulam 1978; Fox et al., 2000; Wang & Powley 2000). Mice were anesthetized with intraperitoneal (i.p.) injections of a ketamine hydrochloride (Ketaset, Fort Dodge IA, 33. 34 mg/mL) - xylazine (Anased, Lloyd Laboratories, Shenandoah, IA, 100 mg/mL) mixture. The left nodose ganglion was exposed and WGA-HRP (Vector Laboratories Inc., Burlingame, CA; 0.5 µL, 4%) was pressure-injected (PicoSpritzer Iid; General Valve Corporation, Fairfield, NJ; 40 p.s.i., 4 msec) into the ganglion using a glass micropipette (inner diameter, 25 mm).

Tissue Processing

Twenty-twenty two hours after nodose ganglion injection, mice were anesthetized using Brevital sodium (JHP Pharmaceuticals, Rochester, MI, 500mg/mL) or ketamine (Ketaset, Fort Dodge IA, 33. 34 mg/mL) - xylazine

(Anased, Lloyd Laboratories, Shenandoah, IA, 100 mg/mL) mixture. Mice were perfused for 5-10 minutes with warm 0.9% saline until the liver cleared, and then fixed with 3% paraformaldehyde (PFA)/0.75% gluteraldehyde at 4mL/min. The dorsal and ventral halves of the stomach and the first 8 cm of the intestine were processed as wholemounts. The smooth muscle and mucosal layers of the GI tract wall were separated by sharp dissection using Dumont #7 forceps. The tissues were processed using tetramethylbenzidine according to the protocol by Mesulam (1978) and mounted on gelatin coated slides. Next, the tissues were flattened by placing weights on a slide covering the tissue for 30 min. They were then air-dried overnight and cleared with xylene the following day. The slides were then coverslipped using D.P.X. mounting medium (Sigma Aldrich, St. Louis, MO).

IGLE Quantification

The IGLEs in the ventral stomach and first 8 cm of duodenum in BDNF SM -/- mutants and controls were quantified using a previously characterized method. This quantification method was first utilized by Wang & Powley (2000) in the rat, and was later modified for use in the mouse by Fox and colleagues (2000). First, the area of the stomach was determined. Then, a sampling grid that adjusts for the area of the stomach was used to locate sites in the stomach and intestine to be sampled and quantified. Next, a 1 X 1 cm^2 counting grid that consists of one hundred 1 mm^2 squares was placed in the ocular of the microscope. This allows for quantification of IGLEs at the calculated sampling sites. Criteria for IGLE identification were as previously determined: an IGLE

must consist of a laminar aggregate of fine terminal puncta within the neuropil of a myenteric ganglion, and must cover all or part of the myenteric ganglion (Rodrigo et al., 1975; Rodrigo et al., 1982; Neuhuber 1987; Fox et al., 2000).

Counting of IGLEs was conducted at 100X magnification. Occasionally, 200X magnification was used to verify the presence of IGLEs. However, once an IGLE was identified at 200X, counting was done at 100X. Because it can be difficult to distinguish individual IGLEs, the squares of the counting grid that contained IGLEs were counted. This method of quantification resulted in 48 different areas of each stomach half sampled, which accounts for approximately 13% of the total stomach area. IGLE density is defined as the number of squares of the sampling and counting grid containing IGLE terminal puncta per mm^2. Density of IGLEs in the stomach was also analyzed by stomach compartment. Stomach compartments were determined by dividing the width of the stomach into 8 equidistant columns based on the sampling sites calculated from the area of the tissue, and closely approximating how many vertical columns constituted each compartment. IGLEs in the three columns nearest the fundus of the stomach were counted as the forestomach, the middle three columns as the corpus, and the two columns nearest the pyloric sphincter as the antrum. The nerve tracer and method of quantification employed in this study do not clearly distinguish terminal size and number, each of which contributes to terminal density. Potential implications of this are discussed in the discussion section.

To quantify IGLEs in the duodenum, the same counting grid as described above was used. The duodenum was sampled and quantified as follows: starting near the anterior end where tissue is intact, the counting grid was aligned at one lateral edge of the duodenum and all squares of the counting grid containing IGLEs at each sampling site were quantified. The grid was moved sequentially along the entire width of the intestine and squares of the grid containing IGLEs were counted at each of the sampling sites. This was repeated every 5 mm moving caudally along the length of the first 8 cm of duodenum. This method of quantifying IGLEs in the duodenum resulted in approximately 80 different sampling sites, resulting in quantification of approximately 20% of the total area of the intestine.

The total area of the stomach, the width of the duodenum at the pyloric sphincter, width of the intestine just before the cecum, and the length of the intestine did not differ between BDNF SM -/- mice and controls. The area sampled in the stomach and intestine also did not differ between BDNF SM -/- mice and controls.

Wholemounts were not included in the analyses if vagal afferent innervation could not be adequately observed. For example, large portions of the stomach or intestine with unlabeled labeled fibers indicate an incomplete injection. Also, sometimes vagal afferent fibers cannot be visualized due to dense artifact that can occur with this method and these cases were also not included in the analyses (Mesulam 1978). In this study, 70% of the animals injected were included in the analysis (15 controls and 12 mutant animals were

injected with WGA-HRP, but 3 controls and 3 BDNF SM -/- mice were dropped, resulting in final sample sizes of n=12 for controls and n=9 BDNF SM -/- animals). There were no differences in IGLE density between males and females; therefore their data were combined.

Axon Bundle Density Quantification

In addition to quantification of IGLE density, other aspects of vagal innervation were further investigated by quantification of circular and longitudinal individual fibers and fiber bundles in the intestine of BDNF SM -/- mice (n = 9) and controls (n = 9). A fiber is defined as a single axon that is not contained within a vagal fiber bundle. A bundle is defined as two or more axons coursing together in parallel and in close apposition. Vagal elements were quantified using the same sampling sites as described above for the intestine (see IGLE quantification) and magnification (100X). Each time a circular or longitudinal axon fiber or axon bundle crossed the top or left sides of the squares of the counting grid at each sampling site it was counted. Axons crossing the right and bottom sides of the grid were not counted to ensure no axons were counted twice as the squares at each sampling site were analyzed for axon crossings. This process was repeated at each sampling site as the grid was moved along the intestine.

Bundle Diameter

The diameters of circular and longitudinal fiber bundles in the intestine of BDNF SM -/- mice and controls were measured and quantified. This was done using the same sampling sites and magnification (100X) used for

quantification of IGLE density in the intestine and vagal axon bundle density as described above. Axon bundles were measured by placing a micrometer scale onto the same counting grid in the ocular of the microscope as described above, projecting a ruler onto the field of view of each sampling site. Every axon bundle that crossed the top and left sides of each square of the counting grid was counted and measured. Bundle diameters were measured to the nearest 0.5 μm, as this was the smallest observable diameter bundle using the WGA-HRP nerve tracer. Because the bundles were measured to the nearest 0.5 μm, they were grouped into 0.5 μm-diameter bins.

Nodose Ganglion Cell Counts

Right and left nodose ganglia were removed from wt (*n* = 9) and BDNF SM -/- mice (*n* = 14). After dissection, the ganglia were postfixed in 4% PFA for 48 hr and then transferred to 10% buffered formalin for a minimum of 7 days. The ganglia were then embedded in paraffin, sectioned at a thickness of 10 μm and stained with cresyl violet. The first section that contained substantial stained neurons was counted, followed by every subsequent tenth section containing stained neurons that spanned the entire ganglion. Counting was done at 200X magnification to ensure only neurons that contained a clearly identified nucleolus were counted. The raw numbers obtained were then multiplied by the total number of sections per ganglion to ensure accurate estimation of the total number of neurons per ganglion.

Meal Pattern Analysis

Wt (*n* = 13) and BDNF SM -/- mice (*n* = 15) at 3–4 months of age were housed individually in plastic cages equipped with computerized pellet dispensers (Coulbourn Instruments, Allentown, PA) for collection and analysis of eating patterns. Each automated pellet dispenser was equipped with infrared photobeam sensors that detected beam breaks every 100 ms. When a mouse removed a pellet, the beam break was detected and another pellet was dispensed. Raw data was analyzed using Graphic State software (v2.0; Coulbourn Instruments). Meal patterns were collected using a balanced pellet diet (20 mg dustless 380 precision pellets, Bio-Serv, Frenchtown, NJ), which is similar to chow. The macronutrient composition of the pellet diet used in the automated feeding machines is 22% protein, 66% carbohydrate, and 12% fat, with a caloric density of 3.623 kcal/g. This is comparable to the chow diet which is composed of 28% protein, 60% carbohydrate, and 12% fat, with a caloric density of 3.04 kcal/g. To become acclimated to the test cages and diet before the experiment, mice were adapted to the test room and cages for a minimum of 1 week before the start of meal pattern collection. During that week, animals received three limited pre-exposures to the test diet, each consisting of 10 of the Bio-Serv precision pellets, to prevent neophobia at the start of testing. All animals used in the experiment ate all 10 pellets during each pre-exposure. Intake patterns were monitored 18 h each day and animals were fasted the remaining 6 h, during which time cage maintenance was performed and mice were weighed. Each daily session began at the start of the dark phase of the

light cycle (lights out at 5:00 pm) and extended 6 h into the light phase, and meal pattern data were collected for 22 consecutive days. Mice of each genotype were tested in parallel to control for any inadvertent variations in the testing conditions.

Meal Criteria

Meal initiation was defined as a minimum of seven pellet removals with a minimum of 20 min between responses. Once a meal was initiated, meal termination was defined as the onset of a 20-min interval with no food intake. The criteria for meal onset (time interval between pellet removals and number of pellet removals) were determined by systematically varying them and examining the effect on meal number (Fox & Byerly 2004). These data were used to identify the range of criteria that exhibited the greatest stability in estimates of meal numbers, and the specific set of criteria chosen was drawn from the middle of this range. These criteria were applied to the raw data using the Graphic State software to identify the times of onset and termination of each meal, which were used to calculate several meal parameters. These were considered to be good estimates based on the observation that mice consumed all or almost all of each pellet, as evidenced by the minute amount of spillage present on cage floors.

Meal Microstructure

The first meal of each daily test session (defined as spontaneous food intake during the first 30 min after mice gained access to the food at the start of the session) was subjected to microstructural analysis to characterize changes

in food intake rate over the course of this first meal after six hours of food deprivation (Davis, 1998; Fox & Byerly 2004). Meal microstructure data was collected at the same time and using the same animals as in the meal pattern analysis. Initial intake rate and changes in this rate across the 30-min feeding session were estimated by determining the amount of food consumed during each minute of the first 30 min of food intake. Analysis of meal microstructure allows for deconstruction of the initial or oropharyngeal and postingestive contributions to food intake which drive ingestive behavior. The initial rate of food intake is influenced by taste or other oropharyngeal factors that represent motivational or hedonic controls of food intake. The latter part of the meal represents the rate of decrease in intake rate, which is mainly influenced by postingestive controls of food intake, such as vagal negative feedback signals activated by the accumulation of food in the GI tract as the animals become satiated.

Statistical Analysis and Graphical Display of Data

Changes in BDNF mRNA levels between controls and BDNF SM -/- mice were determined by comparing changes in the constitutively expressed housekeeping gene, β-actin, and BDNF. This was done using the Livak and Schmittgen method (2001). Briefly, the difference in gene expression between BDNF and β-actin in the tissues was calculated and then compared using one-way analysis of variance (ANOVA). Levels of BDNF mRNA normalized to β-actin in controls were set at 100%. Animals with the cre transgene only (no floxed BDNF) or the lox transgene only (no cre) did not differ from wt mice in

any variable tested, and were therefore combined with wt in some cases for more efficient animal use. Values are presented as means ± SEM (standard error of the mean). Body weight and body composition in BDNF SM -/- mice mutants and controls were tested using one-way ANOVA. Differences in IGLE density, and vagal fibers and bundles between controls and BDNF SM -/- mice were determined using one-way ANOVA. Nodose ganglion counts were compared between genotypes using one-way ANOVA. All counting in this study was performed by the same experimenter (J.E.B.) and done blind to genotype. Meal pattern variables were tested in wt and BDNF SM -/- mice using repeated-measures ANOVA across days 5-22. Meal microstructure was analyzed using TongueTwister software (v1.45, Tallahassee, FL). Food intake between wt and BDNF SM -/- mice during meal microstructure analysis was tested using one-way ANOVA for individual time points and repeated-measures ANOVA over multiple days. Statistics were tested using Statistica software (v6.0, StatSoft, Tulsa, OK). P-values less than 0.05 were considered significant. Graphs were constructed with GraphPad Prism (v4.0, GraphPad Software, Inc.) software. Figure layouts were organized using Photoshop (v6.0 Adobe Sytems, Mountain View, CA). Photoshop was also used to adjust brightness and contrast on photomicrographs, and to apply scale bars and text to images.

RESULTS

Verification of BDNF SM -/- KO Mice

In order to verify BDNF KO in the smooth muscle, two different types of RT-PCR were performed. Qualitative RT-PCR was first performed to verify RNA integrity. Quantitative RT-PCR was performed to quantify the extent to which BDNF RNA was decreased in the stomach and intestine in BDNF SM -/- mice compared to controls. Qualitative RT-PCR showed bands of BDNF from the hypothalamus, prefrontal cortex, ventral stomach and first 2 cm of duodenum at the expected 332 bp. Bands of β-actin mRNA from the hypothalamus, prefrontal cortex, ventral stomach and first 2 cm of duodenum were observed at the expected location of 266 bp (Zermeno et al., 2009).There were no bands visible in PCR products made from mRNA that had not been reverse transcribed, indicating no DNA contamination.

Quantitative RT-PCR showed trends toward decreased BDNF mRNA levels in the ventral stomach and first 2 cm of duodenum in BDNF SM -/- mice compared to controls, as shown in Figure 3. Levels of BDNF mRNA were decreased by 82% in the intestine of BDNF SM -/- mutants compared to controls, and decreased by 54% in the ventral stomach of BDNF SM -/- mice compared to controls. Levels of BDNF mRNA in hypothalamus and cortex were

similar in mutants and controls, which implies the KO is specific to the GI tract, as high levels of BDNF remain in the CNS. The decrease in BDNF mRNA levels in BDNF SM -/- mice compared to controls appeared to be greatest in the intestine, indicating the intestine as the primary site of cre-mediated recombination, although there was also a substantial decrease in BDNF mRNA levels in the stomach. Relative % of BDNF mRNA levels in BDNF SM -/- mutant mice compared to controls in each tissue were: 79.87 ±12.43 % in the hypothalamus (p = 0.310), 85.02 ± 36.28% in the prefrontal cortex (p = 0.369), 45.99 ± 24.55% in the ventral stomach (p = 0.294), and 17.95 ± 13.21% in the first 2 cm of intestine (p = 0.117).

Body Weight

The breeding strategy employed to generate BDNF SM -/- mice and the relevant control groups resulted in six different genotypes. The body weights of males of all genotypes are shown in Figure 4A and females of all genotypes are shown in Figure 4B. Body weights are shown from weaning at 3 weeks of age until adulthood at 4 months of age. All animals showed a normal, wt-like body weight and typical growth curves. There were no differences in body weight between any of the genotypes in either males or females at any age. Importantly, mice expressing either the cre transgene or lox transgene alone showed no body weight phenotype, suggesting the transgenes themselves have no effects on body weight.

Density of Vagal Afferent Innervation in the Stomach and Intestine

IGLE Morphology and Density in the Stomach

Vagal afferent innervation and IGLEs were labeled in the stomach and intestine of control and BDNF SM -/- mice in order to determine the role of BDNF on the development of sensory innervation and nerve endings in the smooth muscle. IGLES observed in the stomach displayed the characteristic pattern of innervation as shown in both genotypes in Figure 5. Vagal afferent fibers and bundles terminate in groups of IGLEs, which can be seen as aggregates of fine terminal puncta. Images of IGLEs in the stomach of control mice are shown in Figure 5A, while BDNF SM -/- are shown in Figure 5B. Morphology of IGLEs in both the stomach of controls and BDNF SM -/- mice appeared to be normal. Shape, size, and distribution of IGLEs appeared to be normal in the forestomach, corpus, and antrum compartments of the stomach in both groups of mice, and also appeared very similar to those observed in other studies (Fox et al., 2000; Fox et al., 2001a; Powley et al., 2005) and other strains of mice (Fox et al., 2000).

IGLE density was quantified as the average IGLE density of the ventral wall (Fig 6A) and also in each of the stomach compartments of the ventral wall (Fig 6B). Similar IGLE densities were observed in each stomach compartment (Fig 6B). There were no differences detected in total IGLE density between any of the genotypes in the stomach (Fig 6A: control: 3.23 ± 0.46 IGLEs/mm^2; BDNF SM -/-: 4.01 ± 0.79 IGLEs /mm^2; $p > 0.05$), or between any of the stomach compartments (Fig 6B: control forestomach: 2.84 ± 0.49 IGLEs / mm^2;

BDNF SM -/- forestomach: 3.68 ± 1.05 IGLEs /mm^2; control corpus: 3.58 ± 0.58 IGLEs / mm^2; BDNF SM -/- corpus: 4.60 ± 0.54 IGLEs /mm^2; control antrum: 3.33 ± 0.93 IGLEs / mm^2; BDNF SM -/- antrum: 3.71 ± 1.10 IGLEs /mm^2; $p >$ 0.05 for all comparisons). These values are similar to those observed in previous studies (Fox et al., 2001a). Although nonsignificant, there was a trend toward increased IGLE density in BDNF SM -/- mutants compared to controls. This trend was observed across all three stomach compartments.

IGLE Morphology and Density in the Duodenum

Like IGLE morphology in the stomach, control and BDNF SM -/- mice appeared to have qualitatively normal looking IGLEs, as shown in Figure 7. Morphology of IGLEs in the duodenum representative of controls are demonstrated in Fig 7A, while representative BDNF SM -/- IGLEs are shown in Fig 7B. Shape of IGLEs appeared to be normal in the duodenum in both groups of mice, and also appeared very similar to those observed in other studies (Fox et al., 2000; Fox et al., 2001a; Powley et al., 2005) and other strains of mice (Fox et al., 2000). Vagal afferent fibers and bundles can be seen giving rise to the IGLE nerve terminal endings. The innervation pattern of axons seen here was previously described (Fox et al., 2000) as a lattice pattern formed by the perpendicular branching of bundles that follows the organization of the myenteric plexus. IGLEs of both genotypes displayed this characteristic pattern of innervation and morphology in the duodenum.

Although IGLEs in the duodenum appeared to have a normal morphology in control and BDNF SM -/- mice, surprisingly, there was an

increase in IGLE density in BDNF SM -/- mice compared to controls in the intestine. This increase in IGLE density of mutants can be observed in Figure 7, which shows IGLE density at high-magnification in the duodenum of control (Fig 7A) and BDNF SM -/- mice (Fig 7B). Figure 8 also shows an increase in IGLE density in the duodenum of BDNF SM -/- mutant mice (Fig 8B) compared to controls (Fig 8A), shown as photomontages composed of approximately 50 images each at a decreased magnification.

The increase in IGLE density in the duodenum of BDNF SM -/- mice compared to controls was statistically significant at a 40% increase, as shown in Figure 9 (IGLE density for total 0-8 cm: control: 5.61 ± 0.71 IGLEs/mm^2; BDNF SM -/-: 7.78 ± 0.72 IGLEs/mm^2; p <0.05). This finding was unexpected, as the original hypothesis was that knocking out a growth factor would lead to a decrease in neuron outgrowth and vagal afferent endings as shown in other studies (Fox et al., 2001a; Raab et al. 2003; Murphy & Fox 2010) and more specifically, that BDNF SM -/- mice would show a decrease in IGLE density. The increase in IGLE density in the BDNF SM -/- mice appears to be consistent across the entire 0-8 cm duodenum, as both the 0-4 and 4-8 portions of the intestine showed this increase, however only the total average IGLE density (0-8 cm) described above was statistically significant (0-4 cm: control: 5.36 ± 0.81 IGLEs/mm^2; BDNF SM -/-: 7.76 ± 0.80 IGLEs/mm^2, p = 0.053; 4-8 cm: control: 5.35 ± 0.64 IGLEs/mm^2; BDNF SM -/-: 7.33 ± 0.82 IGLEs/mm^2, p = 0.071). The density of IGLEs determined across the first 8 cm

of the duodenum in this study represents a novel finding, as there are nearly identical IGLE densities in the first 4 cm (0-4 cm) as in the 2nd 4 cm (4-8 cm).

Vagal Element Density

In order to further investigate the contribution of BDNF to the development of vagal sensory innervation of the GI tract, several vagal elements were quantified in control and BDNF SM -/- mice: the density of individual longitudinal axon fibers, longitudinal axon bundles, individual circular axon fibers, and circular axon bundles was determined. Figure 10 shows the density of these vagal elements across the entire 0-8 cm of duodenum sampled (A), the first 4 cm of duodenum sampled (B), and the next 4-8 cm of duodenum sampled (C). See Table 1 for values ± SEM. Consistent with previous studies, the first 4 cm of duodenum displayed much higher density of vagal afferent innervation compared to more caudal parts of the intestine (Berthoud et al., 1997; Fox et al., 2000; Fox et al., 2001a). The first 4 cm of duodenum showed increased innervation compared to the 4-8 cm duodenum in all vagal elements quantified except individual circular fibers, although there was a trend towards increased 0-4 circular fiber density compared to 4-8 cm circular fiber density in both genotypes. In general, there tended to be increased axon bundle density in both longitudinal and circular orientations compared to individual free axon density across both genotypes. Additionally, there tended to be increased longitudinal fibers and bundles compared to circular fibers and bundles, as has been seen in prior reports (Fox et al, 2000). These trends were observed at all parts of the duodenum sampled. There were

no statistically significant differences in the density of any of the vagal elements quantified between BDNF SM -/- mice and controls, at any part of the duodenum sampled. However, there was a trend toward increased axon bundle density in BDNF SM -/- mice in both the longitudinal and circular orientations compared to controls, across all parts of the duodenum. Interestingly, the percent increases in longitudinal and circular bundles in BDNF SM -/- mice compared to controls in the total (BDNF SM -/- longitudinal bundle increase: 36%; BDNF SM -/- circular bundle increase: 39%), 0-4 (BDNF SM -/- longitudinal bundle increase: 35%; BDNF SM -/- circular bundle increase: 37%), and 4-8 (BDNF SM -/- longitudinal bundle increase: 69%; BDNF SM -/- circular bundle increase: 44%) cm of duodenum are almost identical in the total and 0-4 cm duodenum, and increased in the 4-8 cm duodenum. However, although the percent increase in longitudinal bundles is larger in BDNF SM -/- mice compared to controls in the 4-8 cm duodenum, there is a trend toward increased average longitudinal bundle density compared to circular bundle density in the 0-8 and 0-4 cm duodenum. Quantification of individual longitudinal and circular fibers revealed almost identical densities in BDNF SM -/- and control mice (Table 1). Percent change of individual axon fibers in BDNF SM -/- mice compared to controls: 2.7% decrease in total 0-8 cm longitudinal fibers; 15% increase in total 0-8 cm circular fibers; 0.6 % decrease in 0-4 cm longitudinal fibers; 7% increase in 0-4 cm circular fibers; 0.7% increase in 4-8 longitudinal fibers; 38% increase in 4-8 cm circular fibers.

Bundle Diameter

In order to further refine the contribution of vagal bundle innervation in the intestine, diameter of axon bundles were measured to the nearest 0.5 μm in both the longitudinal and circular orientations in control and BDNF SM -/- mice. Figure 11 and Table 2 show axon bundle diameter measured in controls and BDNF SM -/- mice in the longitudinal orientation (A) and the circular orientation (B). In general, there were increased numbers of longitudinal axon bundles compared to circular bundles in both wt and BDNF SM -/- mice. The largest-diameter bundles (4.5 – 6.0 μm), were rarely observed in either the longitudinal and circular orientations in either genotype. In control mice, there was an inverse dose-response function observed, such that there were decreased axon bundles observed at each subsequent increase in diameter. This was observed in both longitudinal and circular bundles of the control mice. This same inverted dose-response function was generally observed in BDNF SM -/- mice as well, except for the number of longitudinal and circular bundles in the 1.5 – 2.0 μm diameter range. In the smallest diameter longitudinal bundles observed, the 0.5 – 1.0 μm diameter range, there were no differences between control and BDNF SM -/- mice (Figure 11A). However, at the 1.5 – 2.0 μm diameter range, BDNF SM -/- mice showed a greater number of longitudinal bundles compared to control mice ($p < 0.05$). In the 2.5 – 3.0 μm diameter range, there were no differences in longitudinal bundle number between control and BDNF SM -/- mice, although there was a near significant ($p = 0.071$) trend for BDNF SM -/- mice to show an increased number of

longitudinal axon bundles. At the 3.5 – 4.0 μm and 4.5 – 5.0 μm diameter ranges, BDNF SM -/- mice showed a statistically significant increase in the number of longitudinal bundles compared to control mice ($p < 0.05$). There were very few longitudinal axon bundles of the largest diameter observed, 5.5 – 6.0 μm, either in control or BDNF SM -/- mice, and there were no differences in axon bundle density at these large diameters (Table 2).

The increase in number of bundles at larger diameters observed in BDNF SM -/- mice compared to controls was specific to axon bundles in the longitudinal orientation, as there were no differences observed in number of bundles at any diameter in the circular orientation between BDNF SM -/- mice and controls (Figure 11B; Table 2). There was a trend toward increased circular bundle number in BDNF SM -/- mice compared to controls in all but the 5.5 – 6.0 μm diameter range bundles; however this trend was not statistically significant at any diameter measured.

Nodose Ganglion Counts

Vagal sensory neuron number was quantified in control and BDNF SM -/- mice. This was done in order to aid in distinguishing if the increases shown in IGLE density and larger-diameter axon bundle number were due to increased neuron survival or increased axon branching. Increased IGLE density in BDNF SM -/- mice could result from an increase in the proliferation or survival of vagal sensory neurons in these animals. If there is an increase in the number of neurons, then the axonal projections from these neurons could result in an increase in the number of terminal endings in the intestine. Alternatively, the

density of vagal sensory neurons may remain normal in the mutants, but the axons that give rise to IGLEs could demonstrate increased branching, which could also result in an increase in IGLE density in the intestine. Figure 12 shows cresyl-violet stained nodose ganglion neurons in control (A) and BDNF SM -/- mice (B) and quantification of nodose ganglion neurons in control and BDNF SM -/- mice, including the left and right sides, and the total nodose ganglion neuron numbers summed from both sides (C). Consistent with the increased vagal innervation in the GI tract, there was a statistically significant 47% increase in total nodose ganglion number in BDNF SM -/- mice compared to controls (Fig 12C: control: 3615.45 ± 315.90; BDNF SM -/- : 5324.16 ± 487.64, p = 0.012, as shown in Table 3). The increase in vagal sensory neuron number suggests increased survival of these neurons. This increase in total neuron number was achieved through a trend in increased neuron number in BDNF SM -/- mice compared to controls in the left side (p = 0.129) and a significant increase in the right side (p = 0.017; Table 3).

Food Intake, Body Weight and Body Composition During Meal Pattern Collection

Food Intake

Daily food intake was measured at the time of meal pattern collection, in young adulthood at 3-4 months of age on a balanced pellet diet. Daily food intake is shown in Figure 13A. There were no differences in daily food intake between the genotypes (wt: 3.19 ± 0.11 g; BDNF SM -/-: 2.96 ± 0.10 g). The food intake observed in this study (~ 3.0 g/day) is consistent with many other

studies and is the typical amount of chow a normal, wt mouse eats daily (Kernie et al., 2000; Fox et al., 2001a; Biddinger & Fox 2010; Krashes et al., 2013). There were also no differences in daily food intake between males or females, therefore their data were combined (Table 4).

Body Weight

Daily body weights observed on days 1-22 of meal pattern collection are shown in Figure 13B. The body weights observed during meal pattern collection are consistent with those shown in the long-term body weight curves in Figure 4. There were no differences in body weight at any time point between any of the genotypes during meal pattern collection.

Body Composition

Body composition was determined the day prior to meal pattern collection, before fasting. Body composition was analyzed as the total grams of body fat, total grams of lean mass, body fat as a percent of total body mass, and lean mass as a percent of body mass, in both males and females. Figure 14 shows total fat mass and total lean mass in male (A) and female (B) BDNF SM -/- mutants and control mice. There were no differences between the genotypes in either fat mass or lean mass, in either males or females. There were also no differences observed in fat mass or lean mass in males and females, although males tended to have slightly more lean mass compared to females. Figure 15 shows fat mass and lean mass calculated as a percent of total body mass in male (A) and female (B) BDNF SM -/- mutants and controls. There were no differences between any of the genotypes in either fat mass or

lean mass as a percent of total body mass, in either males or females. There were also no differences observed in the percent of fat or lean mass in males and females, although females tended to have slightly more fat mass as a percent of their body mass compared to males.

Meal Pattern and Meal Microstructure Analyses

Meal Patterns

Analysis of meal patterns is a behavioral assay that can be used to study any potential changes in the function of vagal afferent signaling. If vagal satiation signaling is impaired, this could be detected by changes in meal patterning. There were no differences in meal pattern parameters between males and females (Table 4); therefore their meal pattern data were combined. Changes in several meal pattern parameters were observed that are consistent with increased satiation and satiety in BDNF SM -/- mutants compared to controls. Significant decreases in both total and average meal duration was observed in BDNF SM -/- mice compared to wt mice (Figure 16A and B). Total meal duration (Fig 16A), which is the total time spent eating throughout the 18 hr meal collection period was significantly decreased in the mutants compared to controls (wt: 174.83 ± 23.7 min; BDNF SM -/-: 93.44 ± 22.08 min; $p < 0.05$). Additionally, the average meal duration (Fig 16B), which is the total time spent eating throughout the 18 hr meal collection period divided by the total number of meals taken during this time period was also significantly decreased in mutant BDNF SM -/- mice compared to wt mice (wt: 22.07 ± 3.65 min; BDNF SM -/-: 9.10 ± 3.94 min; $p < 0.05$). The decreases observed in meal duration

translate to a 47% decrease in the total meal duration and a 60% decrease in the average meal duration, respectively, in BDNF SM -/- mice compared to wt.

This significant decrease in meal duration contributed to a 20% decrease in meal size in BDNF SM -/- mice compared to wt mice, as shown in Figure 16C (wt: 0.359 ± 0.018 g; BDNF SM -/-: 0.286 ± 0.017 g; $p < 0.05$). The decrease in meal duration combined with the decrease is meal size is consistent with the interpretation that food is more satiating to BDNF SM -/- mice than wt, which could be due to an increase in vagal satiation signaling through increased negative feedback from the gut to the brain.

In addition to meal pattern changes in BDNF SM -/- mice that are associated with increased satiation, there were also changes in the feeding behavior of the mutants that are consistent with increased satiety. The intermeal interval (IMI) is the time spent between meals not eating. The IMI can be used as an indicator of satiety, as the mouse's state of satiety affects the length of time between meals. There was a significant 20% increase in total IMI in BDNF SM -/- mice compared to wt, and although not statistically significant, the average IMI was trending toward an increase in BDNF SM -/- mice compared to wt mice (total IMI $p < 0.05$; average IMI $p = 0.090$). Figure 17 shows total (A) wt: 596.94 ± 37.15 min; BDNF SM -/-: 715.56 ± 34.59 min and average (B) wt: 62.50 ± 2.77 min; BDNF SM -/-: 68.55 ± 2.58 min IMI values. BDNF SM -/- mice also demonstrated an 27% increase in satiety ratio compared to control mice, as shown in Figure 17C (wt: 193.2 ± 3.83 min/g; BDNF SM -/-: 244.63 ± 4.27 min/g; $p < 0.05$). The satiety ratio is a calculated

meal pattern parameter derived through the ratio of the IMI and the preceding meal size, which provides an estimate of how effective a given amount of food is at producing satiety.

Although BDNF SM -/- mice showed decreased meal duration and decreased meal size, which suggest increased satiation, and increased IMI and satiety ratio which suggest increased satiety, the mutant mice did not demonstrate any changes in overall food intake. Therefore, these short-term changes in feeding behavior were compensated for by other changes in meal pattern parameters to maintain normal food intake. This occurred through an increased eating rate and a trend toward an increase in meal frequency in mutant mice, which are depicted in Figure 18. The BDNF SM -/- mutants showed a significant 40% increase in intake rate (Fig. 18A, wt: 1.36 ± 0.23 g/min; BDNF SM -/-: 2.04 ± 0.21 g/min; $p < 0.05$). BDNF SM -/- mice also compensated for increased satiation and satiety with a trend toward increased meal number compared to wt mice (Fig 18B). They ate approximately one more meal during the 18 hr meal pattern collection period than wt mice (wt: 9.53 ± 0.46 meals; BDNF SM -/-: 10.81 ± 0.43 meals. Together, the meal pattern data are consistent with the known role of vagal afferents in the short-term control of food intake, as there were changes in the feeding behavior of BDNF SM -/- mice indicative of increased satiation, but no long-term change in total food intake that would influence body weight.

Meal Microstructure

Like meal patterns, meal microstructure analysis can also be used as a functional assay to observe any changes in the feeding behavior of the animals that could be associated with any changes in vagal signaling. The initial rate and changes in intake rate over the first 30 minutes of food intake provides a way to discriminate between oropharyngeal and postingestive contributions to eating (Davis 1998). Rate of food intake across the first 30 min meal after a 6 hr fast and averaged across days 5-22 are shown in Figure 19. This is depicted by each minute across the 30 min time period (A) and averaged across the entire 30 min (inset, B). Both wt and BDNF SM -/- mice show a very high initial intake rate as shown in minute 1 due to mild food deprivation (Fig 19A). During this first meal, the initial rate of food intake was similar in mutants and controls. As expected, there is a rapid decay of food intake rate as the animals of both genotypes start to become satiated during minutes 2-5 (Fig 19A). However, starting at minute 6, the BDNF SM -/- mice begin to show increased suppression of food intake compared to the controls. At around minute 20, BDNF SM -/- begin to initiate their second eating bout of the night, which is slightly before controls. During the next minute they start to decrease their food intake again, before wt mice become satiated. These time frames are consistent with the average meal duration as shown in Figure 16B during meal patterns.

The rate of food intake across minutes 6-30 is shown in Figure 20. This is depicted as the food intake rate per minute (A) and also as the average food

intake across minutes 6-30 (B). Consistent with vagal afferent mediation of increased satiation in mutants, the subsequent sustained intake rate across minutes 6-30 was reduced by 40% in mutants compared to control mice (wt: 0.0957 ± 0.000362 g/min; BDNF SM -/- : 0.0581 ± 0.000362 g/min; $p < 0.05$). However, also consistent with increased vagal satiation signaling, the mutant mice compensated for this increase such that there was no difference in overall food intake across the 1st 30 min of feeding between controls and BDNF SM -/- mice (Fig 19B, wt: 0.251 ± 0.0032 g/min; BDNF SM -/- : 0.240 ± 0.0037 g/min). This compensation was due to small, non-significant trends toward increased average food intake during minutes 1 and 2 after the six hour fast in BDNF SM -/- mice compared to wt mice (Fig 19A), which resulted in a trend toward the overall food intake across min 1-30 to be decreased in BDNF SM -/- mice compared to wt (Fig 19B).

DISCUSSION

Smooth muscle-specific removal of BDNF resulted in a significant increase in vagal innervation of the GI tract compared to controls, which was demonstrated by an increase in IGLE density in the intestine and an increase in number of larger-diameter longitudinal axon bundles, while IGLEs in the stomach displayed normal density. This increase in GI vagal innervation in the intestine could be due to increased vagal sensory neuron number. In addition, the increased IGLE density in BDNF SM -/- mice was associated with increased satiation and satiety that occurred through decreased meal duration and meal size, and increased IMI and satiety ratio in BDNF SM -/- mice compared to controls. The increases in satiation and satiety in BDNF SM -/- mice were compensated for by increased daily feeding rate and a trend toward increased meal number to maintain normal food intake. Consistent with the increased satiation demonstrated by BDNF SM -/- mice, analysis of meal microstructure revealed increased suppression of food intake during the postingestive phase of food intake.

The increase in IGLE density and longitudinal bundles observed in the intestine of BDNF SM -/- mice was surprising. It was originally predicted that smooth-muscle specific KO of BDNF would result in a decrease of vagal

afferent innervation, including decreased density of IGLEs and vagal fibers and bundles. There are several reports demonstrating that KO of neurotrophic factors leads to decreased mechanoreceptor density in the smooth muscle of the GI tract (Fox et al., 2001a; Raab et al., 2003; Murphy & Fox 2010). The reverse has also been observed, such that knockin (KI) of NT-4 leads to increased IGLE density (Chi et al., 2004).

Characterization of BDNF SM -/- KO Mice

Qualitative and quantitative PCR were utilized to verify and quantify the extent of the KO in GI tissues of adult BDNF SM -/- mice compared to controls. Qualitative PCR verified RNA integrity, indicating the RNA was not degraded. Quantitative PCR (QPCR) revealed trends towards decreases in BDNF mRNA levels in the ventral stomach (54% decrease) and first 2 cm of the duodenum (82% decrease) in BDNF SM -/- mice compared to controls. There was minimal BDNF removed in the CNS regions analyzed, as there were only 20 and 15% decreases in the hypothalamus and prefrontal cortex, respectively, in BDNF SM -/- mutants compared to controls, indicating the BDNF KO is restricted to the GI tract.

Although not statistically significant, BDNF was lost to a greater extent in the small intestine than in the stomach in BDNF SM -/- mice. This greater loss of BDNF in the intestine compared to the stomach is consistent with previous findings from our laboratory. Previous work in our lab provided a characterization of the expression of the SM22α promoter crossed to the BDNF promoter, essentially allowing for visualization of the BDNF SM -/- KO location

(Fox et al., 2013). The region where two independent events occur is the location of the KO: First, the enzyme cre recombinase needs to be present in high enough levels to recombine the DNA between the lox sites surrounding the BDNF exon. This is determined by the activity of the SM22a promoter in a given cell type. Additionally, there also needs to be high enough levels of the BDNF promoter activity in order to visualize the LacZ reporter expression that becomes activated when cre recombinase removes the BDNF coding sequences. These studies showed overlapping expression of the two promoters primarily in the smooth muscle of blood vessel walls in the GI tract, indicating this as the primary site of the KO. As the same two promoters were utilized in the present study, it is likely the location of the KO in the BDNF SM -/- mice in this study is the same or similar to the previous experiments in the Fox et al. (2013) study.

Although an 82% decrease in BDNF mRNA levels in the intestine of BDNF SM -/- mice compared to controls is large, there are several reasons why the decrease did not reach statistical significance. The GI tract wall is composed of several layers, and the smooth muscle is just one of them. The mucosa and myenteric plexus are additional layers of the GI tract wall which contain high levels of BDNF (Lommatzsch et al., 1999; Fox 2006; Grider et al., 2006; Boesmans et al., 2008). It is possible the remaining BDNF in the mucosa/lamina propria and myenteric plexus layers obscured the ability to detect the difference in BDNF mRNA levels in the smooth muscle layers. In embryonic stages of development, there are low levels of BDNF in the mucosa

(Fox & Murphy 2008). However, over time the mucosa shows increased levels of BDNF expression, and by adulthood there are high levels of BDNF in the mucosa (Lommatzsch et al., 1999). Because BDNF mRNA levels were measured in adulthood, it is possible BDNF in the mucosa layers of the GI tract impeded measurement of BDNF mRNA levels in the smooth muscle layers. Measurement of BDNF mRNA levels in BDNF SM -/- embryos, before BDNF expression in the mucosa becomes apparent, may show a more clear decrease.

Additionally, because both BDNF alleles were knocked out in the smooth muscle using the cre-lox methodology, there is the risk of increased variability in cre expression. The cre recombinase enzyme is not expressed uniformly in all cell types. A limitation of using cre-lox technology is variability in the expression patterns of cre transgenes and recombination efficiency (Chien 2001; Schmidt-Supprian & Rajewsky 2007). The original report which presented the generation of SM22α cre mice reported cre efficiency to range between 50-80% (Holtwick et al., 2002). Cre efficiency in the present study is likely to be similar. The variability in cre efficiency can in turn create variability in the extent of the KO in BDNF SM -/- mice. Although the mean decrease in BDNF mRNA levels in BDNF SM -/- mice is 82%, the error is large which limits the ability to reveal a statistically significant decrease in BDNF levels in the mutants compared to controls.

The significance of the restriction of the BDNF SM KO to the blood vessels and its contribution to the feeding effects as described in the present

study is unknown. Vagal axons grow alongside the blood supply in the GI tract, indicating these axons may be the axons primarily impacted in the BDNF SM -/- mice. This could potentially impact the satiation and satiety of the mutant mice, as they could be more susceptible to GI hormones in the blood supply, such as CCK, which could lead to increased satiation in the BDNF SM -/- mice. However, unpublished results in our laboratory showed expression of the BDNF promoter using the LacZ reporter dissipates in the blood vessels after birth, while expression remains in the rest of the tissues in adults (Fox, unpublished results). This time course and pattern of expression suggests the KO is restricted to development, and there are no additional functional changes that emerge in adulthood due to BDNF removal from blood vessel walls during embryonic development.

Consistent with the QPCR data showing BDNF was knocked out to the greatest extent in the intestine, effects on vagal afferent innervation demonstrated by BDNF SM -/- mice appear to be specific to the intestine as well, as the IGLEs in the intestine of the mutant mice were increased compared to controls, while the IGLEs innervating the stomach displayed normal density. As many other visceral organs innervated by vagal afferents are composed of smooth muscle, it is highly likely that BDNF was removed from these other organs. Therefore, if BDNF is removed from other organs innervated by vagal afferents such as the lungs, heart, kidneys, etc., this loss could potentially impact feeding behavior of the mice. However, it remains likely that the observed changes in feeding behavior are specific to BDNF removal from the

GI tract. Although BDNF is important for the development of many organs, changes in these organs may not change the feeding behavior of the animals. Alterations in vagal innervation and function of the lungs, for example, would be unlikely to lead to increased satiation and satiety. In addition, there were no changes in body weight or body composition which would suggest the development and/or function of other GI or visceral organs was affected by the BDNF SM KO.

Possible Mechanisms Underlying the Effects of Reduced BDNF in the Smooth Muscle on Increased Vagal Sensory Innervation

There are several explanations for why the counterintuitive increase in IGLE density and vagal bundles was observed. Increased IGLE density, increased number of larger-diameter vagal fiber bundles and increased vagal sensory neurons in the nodose ganglion of BDNF SM -/- mice suggests BDNF in GI smooth muscle may normally function to suppress survival (or proliferation or axon guidance) of vagal GI afferents. A balance of promoting and suppressive biological processes is necessary for proper development, and it appears BDNF in the smooth muscle is important for suppression of IGLE growth or survival. Although it is surprising the removal of a growth factor results in an increase in axon diameter and mechanoreceptor density, similar effects have been observed in other peripheral nervous systems.

Increased sympathetic innervation to hair follicles was previously demonstrated in homozygous global knockout of BDNF (BDNF -/-) mice compared to controls (Rice et al., 1998). Additionally, BDNF -/- mice, at 2

weeks of age, which is prior to the lethal respiratory deficit, demonstrated an increase in density of mechanoreceptors that innervate Merkel cells in the skin (Fundin et al., 1997). Mice deficient in BDNF (BDNF -/-) have also shown an increase in the extracellular matrix glycoprotein Reelin. These mice showed disorganized organization of cajal-retzius cells with aberrant axon fibers entering the cortical plate (Ringstedt et al., 1998). Application of BDNF antagonists also led to an increase in regeneration of forepaw mechanosensory innervation in the rat after spinal cord deafferentation, indicating BDNF has a suppressive effect on mechanosensory primary afferent axons (Ramer et al., 2007). As ablation of BDNF has led to increases in sensory innervation in other peripheral nervous systems, it is possible a similar role for BDNF on the development of vagal sensory innervation to mechanoreceptors in the GI tract has been uncovered.

Although counterintuitive, there are several reasons why the removal of a growth factor might lead to an increase in axon growth. As there are several processes underlying development, it is unclear what developmental aspects of vagal afferent innervation in the smooth-muscle are impacted by BDNF in this study. There are several important features of neuronal development that could be affected by BDNF. These include the birth or neurogenesis of new neurons, the differentiation of totipotent neuronal stem cell precursors into specific cell types, neuronal proliferation, axonal outgrowth of new neurons to their final target destination, and synapse formation of IGLEs with myenteric neurons. Several possible explanations involving these processes are discussed below.

Increased Neuron Survival in BDNF SM -/- Mutant Mice

The increase in vagal sensory neurons in the nodose ganglion observed in BDNF SM -/- mice compared to controls suggests there is increased survival of these neurons. An increase in the number of sensory neurons is consistent with the increase in longitudinal bundles and IGLE mechanoreceptor density found in the intestine of BDNF SM -/- mutants. As the number of vagal sensory neurons increases, it follows that a corresponding net increase in axons would result, and subsequently an increase in IGLEs.

As neurotrophic factors can influence the development of sensory neurons and their survival, there is also evidence that neurotrophic factors can subsequently influence several additional aspects of sensory innervation through alterations in sensory cell density. Elements of sensory innervation that can be impacted through alteration of neurotrophic factors and their effects on sensory neurons are density and function of sensory receptors in the periphery, and number of axon fibers, which can subsequently affect diameter of axon bundles. The increase in neuron number demonstrated by BDNF SM -/- mutant mice compared to controls is also consistent with the increase in number of larger-diameter longitudinal bundles, as these axons are sending longer nerve fibers innervating the length of the intestine. These longer fibers to the intestine could be responsible for the increase in IGLE density observed. If there is an increase in vagal sensory neurons in the nodose ganglion, there may be an increase in the axons projecting from these neurons which could result in an increase in nerve endings.

A direct relationship between sensory neuron number and density of peripheral nerve fibers and terminals has been observed (Krimm et al., 2004; Fox et al., 2001a; LeMaster et al., 1999; Stuckey et al., 1999; Davis et al., 1997; Albers et al., 1996; Jhaveri et al., 1996). For example, overexpression of NT-3 in the mouse epidermis resulted in an increase in many different cell types that innervate this tissue: these mice displayed increases in dorsal root ganglia sensory neurons, trigeminal sensory neurons, and sympathetic neurons (Albers et al., 1996). The mutant mice also displayed an increased number of the associated peripheral targets for these neurons, which are the Merkel cells in the skin, and showed enlargement of touch dome mechanoreceptor units and increased density of piloneural circular endings (Albers et al., 1996).

In addition to an increase in IGLE density in BDNF SM -/- mice, these mutants also demonstrated an increase in number of larger-diameter longitudinal bundles. Growth factors have been shown to impact axon bundle diameter in other sensory systems. Artemin, a member of the glial cell line-derived neurotrophic factor (GDNF) family, has been shown to lead to an increase in axon bundle diameter. Overexpression of artemin in the tongue resulted in an increase in dorsal root ganglion (DRG) neurons and increased axon bundle diameter of trigeminal sensory afferents (Elitt et al., 2008).

Overexpression of BDNF in taste cells located in the gustatory epithelium of circumvallate papillae results in increased taste bud size and increased gustatory nerve fiber innervation as determined by the expression of

the purinergic receptor P2X3 (Nosrat et al., 2012). It appears BDNF in the GI smooth muscle modulates the development of IGLEs through a different mechanism than NT-3 in the skin and BDNF in taste cells, because BDNF in the GI smooth muscle is knocked-out, while NT-3 in the skin and BDNF in taste buds are overexpressed. Nevertheless, in many circumstances there seems to be a direct relationship between sensory neuron numbers and density of peripheral nerve fibers and terminals (Krimm et al., 2004; Fox et al., 2001a; LeMaster et al., 1999; Stuckey et al., 1999; Davis et al., 1997; Albers et al., 1996; Jhaveri et al., 1996).

Although there was a significant increase in vagal sensory neuron number in BDNF SM -/- mutants compared to controls, this difference was only significant when both the left and right sides of the nodose ganglia were combined. There was a non-statistically significant trend towards increased vagal sensory neuron number in mutants on the left side (33% increase) in BDNF SM -/- mutant mice. Because there was no statistically significant difference in neuron number in the left ganglion, and there was an increase in IGLE terminals in the intestine of mutants, there are potentially other factors in addition, or alternative to, increased number of vagal sensory neurons that contributed to the increase in IGLE density observed in the mutants compared to controls. Potential alternative explanations for the increased terminals other than increased neuron number are discussed in more detail in the sections below.

Increased Branching of Axons in the Intestine of BDNF SM -/- Mice

Alternatively, the increase in IGLE density and increased number of larger-diameter axon bundles in BDNF SM -/- mice compared to controls could be due to increased branching of axons in the intestine, rather than, or in addition to, the increase in the total number of vagal sensory neurons. This is because after an axon reaches its target destination, it arborizes in order to innervate different target cells (Carmeliet & Tessier-Levigne 2005). The axon terminals direct this arborization of axon fibers through secretion of neurotrophic factors. Local gradients of growth factors also regulate the degree of axon arborization at the nerve terminal (Diamond et al., 1992; Goodman & Shatz 1993; Davies 2000). For example, it has been shown that BDNF and NGF can act as target-derived signals to promote branching of sensory axons at nerve terminals (Kennedy & Tessier-Lavigne, 1995; Patel et al., 2000; Hellard et al., 2004; Gibson & Ma 2011).

As global BDNF KO mice typically show a loss of sensory neurons, the independent roles of BDNF in neuron survival and terminal arborization are difficult to distentangle in the KOs. In order to distinguish the role of BDNF in sensory neuron survival from sensory target innervation, mice were generated with a double deletion of BDNF and the pro-apoptotic protein Bax (Hellard et al., 2004). Double deletion of BDNF and Bax allow for separation of these independent processes, as the loss of Bax allows for neuron survival, as Bax typically promotes apoptosis. Several peripheral sensory ganglia of the double-mutant bdnf(-/-)bax(-/-) mice, such as the petrosal, nodose, and vestibular

ganglia, showed normal numbers of sensory neurons due to the presence of Bax. The axons that project from the peripheral sensory ganglia of the bdnf(-/-)bax(-/-) mice maintained proper axon pathfinding to their targets in the periphery; however, the axons failed to properly innervate the terminals and arborize, indicating branch elongation and arborization depend on BDNF (Hellard et al., 2004). A similar experiment was performed with NGF and similar results were reported: ngf $^{-/-}$; bax $^{-/-}$ double mutant mice also showed normal DRG neuron survival and axon pathfinding to the skin but the axons also failed to innervate the terminal (Patel et al., 2000). Therefore, because neurotrophic factors also regulate axon branching, particularly in the axon terminals, in addition to increased neuron survival, there could be increased axon branching in BDNF SM -/- mutants that result in increased IGLE density in the intestine. However, because the increase in number of axon bundles is specific to the longitudinal orientation rather than the circular orientation, it is not likely an increase in branching of axons rather than survival of neurons in the nodose ganglion is entirely responsible for the increase in IGLE density in BDNF SM -/- mice. If an increase in axon branching occurred in BDNF SM -/- mice, there would likely be an increase in circular fibers and bundles as well as in longitudinal fibers and bundles. Because the increase in number of axon bundles is specific to the longitudinal orientation and there is also an increase in vagal sensory neurons in the nodose ganglion in BDNF SM -/- mutants, it is likely the increase in IGLE density is due at least in part to increased number of

axons that project from the increased number of vagal sensory neurons contained within the nodose ganglion.

Decreased Cell Death and Axon Pruning of Vagal Sensory Neurons in BDNF SM -/- Mice

During development, an excess of neurons are produced which are removed later in a process called axon pruning (Luo & Leary 2005; Low & Cheng 2006; Gibson & Ma 2011). An overabundance of axons is produced early in life in order to ensure the appropriate number and location of axons reaches their target destination. The excess neuronal outgrowth is removed later. Axon pruning is a common process that is observed in almost every part of the developing nervous system. Approximately 50% of developing neurons do not survive until adulthood (Oppenheim 1991; Burek & Oppenheim 1996). Inputs to the target region that are stronger and tend to maintain their connections are reinforced, while weaker connections are more likely to be pruned. This is to ensure the most efficient axons remain for optimal neural circuit structure and function. Malfunction of axon pruning is one explanation for the selective increase in number of longitudinal bundles in BDNF SM -/- mice, while density of circular bundles remained similar in mutants and controls. It is likely that because an increase in axon density was observed in the longitudinal orientation, that the mechanism of proper elimination of long axon collaterals was disrupted in BDNF SM -/- mice. As axons that travel longer distances are more likely to be pruned (Liu et al., 2005; Low & Cheng 2006), this makes the long-reaching longitudinal projections from the nodose

ganglion to the intestine likely candidates for this pruning process. However, it is likely that lack of proper axon pruning occurred in both the longitudinal and circular orientations, and contributed to the increase in IGLE density in BDNF SM -/- mice, as there was a trend toward an increase in the number of circular bundles in the mutant mice, although this was not statistically significant. At the level of the mesentery in the GI tract, longitudinal bundles begin to give off circular bundles, so it is likely that increased longitudinal bundles also give rise to increased circular bundles in BDNF SM -/- mice compared to controls.

Another alternative explanation for the increase in larger diameter longitudinal axon bundles in BDNF SM -/- mice compared to control mice may reflect a decrease in bundle fasciculation, and may not necessarily reflect an increase in axon density. Semaphorins are axon guidance molecules that react to cues in the environment to direct the tip of a growing axon, the growth cone, to its appropriate target. Semaphorins primarily act as repulsive guidance cues, which are important for restricting axon bundles and their nerve terminals to specific regions. The semaphorin 3D (Sema 3D) is expressed in developing vagal afferents and is important for fasciculation of vagal bundles (Taniguchi et al., 1997). For example, in order to determine the role of Sema 3 on axon guidance, Taniguchi et al. (1997) generated mutant mice that lacked Sema 3D. These mice showed aberrant axon pathfinding of many peripheral nerves, including the vagus. Sema 3D mutants displayed dramatic increased nerve thickness and the axons in each nerve were more spread out. In addition, the terminals of the accessory and vagus nerves in all mutant mice analyzed were

also spread out and occupied a wider area, while the nerve bundles and terminals of wt mice were narrowly bundled.

There are also known interactions between neurotrophins and semaphorins, as Sema 3A has been shown to interact with NGF, NT-3, and BDNF to induce cell death of DRG neurons dependent on these neurotrophic factors (Tuttle & O'Leary 1998; Dontchev & Letourneau 2002; Ben-Zvi et al., 2006). Therefore, if the decrease of BDNF in BDNF SM -/- mutants also led to a disruption in Sema 3 signaling, this interaction could result in an increase of vagal sensory neurons and their axon bundles and terminals. If fasciculation of vagal afferent bundles was disrupted due to class 3 Sema molecules, the bundles could have a larger diameter due to defasciculation, rather than an increase in axon density. However, if bundle defasiculation occured in the axon bundles of BDNF SM -/- mice, this should be reflected by an increased number of individual free axons and axon bundles of all diameters measured, including smaller-diameter axon bundles, not just the larger diameter axon bundles as demonstrated in this study. Although it is possible there may be a selective defasciculation of larger bundles - for example, as the number of axons bundled together in an axon increases, they may be less likely to remain tightly bundled. However, in general the evidence does not support decreased fasciculation of axon bundles in BDNF SM -/- mice. This is further substantiated by images of axon bundles as shown in Figures 7 and 8. Axon bundles in BDNF SM -/- mice do not appear to be defasciculated to a greater degree than wt mice, although there is an increased number of larger diameter

axon bundles in the mutants. Because nerve tracers cannot easily discriminate individual fibers within an axon, the diameter of axon bundles has been used as a proxy for the number of axons contained within a bundle. It is assumed larger diameter axon bundles contain an increased number of individual axon fibers. A method of visualizing fine morphological details such as electron microscopy could be used to more clearly delineate individual axon fibers to investigate the degree of defasciculation of vagal bundles in the intestine in BDNF SM -/- mice.

Disrupted p75 and TrkA Receptor Signaling in BDNF SM -/- Mice

A mechanism that could underlie the potential lack of axon pruning that could lead to the increase in axon bundles and IGLE density is disrupted signaling through the p75 receptor. All neurotrophins can signal through the promiscuous low-affinity p75 receptor, in addition to their ascribed specific receptor. The p75 neurotrophin receptor belongs to a family of transmembrane molecules which also act as receptors for the tumor necrosis factor family of cytokines. Neurotrophin signaling involves both positive and negative events through different intracellular signaling pathways triggered by activation of the TrkB receptors or p75. The Trk receptors are thought to play a role in positive processes, such as cell growth and survival, while the p75 receptor signals negative events, such as apoptosis (Chao 1994; Coulson et al., 2008).

As the p75 receptor signals cell death, the decreased BDNF in the BDNF SM -/- mice could lead to decreased binding of BDNF to the p75 receptor. The lack of binding to p75 could lead to a decrease in cell death

necessary for proper development, resulting in an overabundance of neurons, and as a result, an increase in axonal projections and nerve terminal endings. This notion has been shown before in sympathetic innervation of the submandibular salivary gland. Jahad & Kawaja (2005) showed increased sympathetic innervation to the submandibular salivary gland in two different types of knockout mice. An increase in innervation was demonstrated in p75 -/- and p75(-/-)/BDNF-/- double mutants compared to controls. They suggested the lack of p75 receptor expression enhanced the density of these efferent fibers in target tissues in the periphery because the BDNF ligand could not bind to the receptor to initiate proper cell death processes. This interpretation is a potential explanation for the increase in vagal sensory neurons and IGLE density observed in this study, although it is possible efferent sympathetic fibers to the submandibular salivary gland develop through different mechanisms than vagal GI afferents.

There are several different pathways through which disrupted p75 signaling could occur. The precursor form of BDNF, proBDNF, is an apoptotic ligand that induces cell death in sympathetic neurons (Teng et al., 2005). Neurotrophic factors are generally synthesized in an initial precursor form, and yield biologically active mature ligands after enzymatic cleavage (Kolbeck et al., 1994; Lee et al., 2001). It was initially thought the precursor form of neurotrophic factors were not biologically active until cleaved (Huang & Reichardt 2001). However, recent evidence suggests precursor forms of neurotrophic factors are also biologically active, although through different

mechanisms and under different circumstances (Teng et al., 2005; Coulson et al., 2008). For example, neuronal cell death is initiated through binding of the neurotrophin to the p75 receptor. Then, a transmembrane-linked C-terminal fragment (CTF) is generated that contains the cytoplasmic juxtamembrane death domain (Chopper domain) to induce cell death. Next, a second cleavage event occurs that is mediated by release of the intracellular domain from the membrane by γ-secretase, an integral membrane protease, and regulates cell death (Coulson et al., 2000). The death signals initiated by binding of neurotrophins to the p75 receptor use the downstream cell death machinery known as the apoptosome (capase-9/apoptosis protein activating factor) to continue the process of apoptosis (Troy et al., 2002; Coulson et al., 2008).

In addition to disrupted p75 signaling, levels of other Trk receptors could also be dysregulated in BDNF SM -/- mice, allowing for increased IGLE density in the intestine of BDNF SM -/- mice. For example, BDNF may be primarily acting through the TrkB receptor to suppress IGLE innervation in the intestine of BDNF SM -/- mice. Others have suggested BDNF suppression of peripheral sensory receptors may occur through down regulation of the TrkA receptor (Fundin et al., 1997; Wyatt & Davis 1993). Although TrkA is the primary receptor for NGF, which is the least abundant neurotrophin in the nodose ganglion, there is evidence that supports it having a larger role than previously thought (Katz et al., 1990). Katz et al. (1990) reported virtually no vagal sensory neurons were present in culture grown for 24 hr without NGF, while cultures grown in the presence of NGF showed substantial growth of neurons

from nodose ganglia explants. Wyatt & Davis (1993) found TrkA mRNA levels are normally downregulated by BDNF. Therefore, levels of TrkA may not be downregulated properly due to loss of BDNF in BDNF SM -/- mice. As neuron survival is limited by a finite growth factor concentration, potential upregulation of TrkA due to loss of BDNF could increase these defined neurotrophic factor levels, resulting in an increase in NGF ligand, or even other neurotrophic factors to a lesser extent, for the TrkA receptor, which could lead to increased vagal sensory neuron survival which results in increased vagal sensory innervation. It has been well established in the neurotrophin literature that these molecules have a tremendous capacity for plasticity, as the neurotrophic factors interact with each other and/or other receptors in the development of peripheral sensory neurons (Davies et al., 1986; Wyatt & Davis 1993; Erickson et al., 1996; Fundin et al., 1997; ElShamy & Ernfors 1997; Rice et al., 1998; Chen et al., 1999).

Increased Cell Growth in BDNF SM -/- Mice

In contrast to BDNF suppression of vagal sensory neurons and IGLE development that could occur through a lack of axon pruning and binding to p75, there could alternatively be an increase in cell growth in BDNF SM -/- mutants. This could occur by an increase in the birth of new neurons. BDNF has been implicated in neurogenesis, as administration of BDNF leads to an increase in new neurons (Zigova et al., 1998; Pencea et al., 2001; Scharfman et al., 2005; Henry et al., 2007). Although BDNF mRNA is disrupted in mutants compared to controls, substantial levels of BDNF remain in the mutants. The

remaining BDNF in the BDNF SM -/- mice could upregulate and increase neuron proliferation.

Alternatively, increased neuron numbers in BDNF SM -/- mutants could occur through compensation of other neurotrophic factors. Neurotrophins are notorious for cooperating with and compensating for each other, as they share similar structures and have overlapping targets (Kolbeck et al., 1994; Lindsay 1996; Huang & Reichardt 2001). Vagal sensory neurons are no exception to this general feature of neurotrophins, as BDNF, NT-3, NT-4, and to a lesser extent, NGF, all contribute to the survival of vagal sensory neurons. During development, BDNF is responsible for the survival of the largest percentage of vagal sensory neurons, compared with NT-3 or NT-4 (Erickson et al., 1996; ElShamy & Ernfors 1997). Studies utilizing genetic single and double knockouts of neurotrophins have helped in distinguishing the independent and cooperative roles of the neurotrophins. For example, and as stated previously in the introduction, BDNF is responsible for the survival of 60% of vagal sensory neurons in the nodose ganglion and 41% of vagal sensory neurons are dependent on NT-3 for survival (ElShamy & Ernfors 1997). However, double mutant mice with both BDNF and NT-3 knockout show a 66% decrease in vagal sensory neurons, which is a smaller decrease than expected, based on the percent decreases shown by the individual neurotrophin knockouts (ElShamy & Ernfors 1997). A near 100% decrease in vagal sensory neuron numbers would be predicted if neuron loss were additive in the double mutants.

Further bolstering the claim that neurotrophin compensation could lead to increased vagal sensory neuron number and axon outgrowth, expression of the neurotrophic factors themselves have been shown to increase in the absence of a differing neurotrophic factor. For example, protein levels of BDNF were increased in the hippocampus and cerebral cortex of NT-3 and NGF knockout mice (Kolbeck et al., 1999). It is possible that the loss of BDNF during development leads to an increase in NT-3 and/or NT-4 to compensate for the BDNF loss, which could result in an overcompensation of neuronal growth.

Other Mechanisms Potentially Involved in the Effects Observed in BDNF SM -/- Mice

Another developmental process that could be impacted by loss of BDNF in the smooth muscle is disrupted axon guidance from the nodose ganglion to GI targets. There are several reports implicating BDNF and other neurotrophic factors in neuron migration and axon guidance (Kennedy & Tessier-Levigne 1995; Honma et al. 2002; Markus et al., 2002; Pahnke et al., 2004; Mai et al., 2009). An increase in migration of cortical interneurons was found to be stimulated by BDNF and NT-4 (Polleux et al., 2002). Axon growth cones have been shown to respond to extracellular gradients of BDNF, suggesting it has a role in axon pathfinding. Although a direct role for BDNF in axon guidance is lacking, other neurotrophic factors such as GDNF, artemin and neurturin have been shown to play a role in axon guidance cues of enteric, sympathetic and parasympathetic axons (Young et al., 2004). For example, artemin is expressed by cells around developing sympathetic ganglia and smooth muscle

cells of blood vessels. Sympathetic axons grow towards sources of artemin, and contribute to sympathetic axon pathfinding by induction of growth along blood vessels in the smooth muscle (Honma et al., 2002; Yan et al., 2003; Young et al.,2004). Although neurotrophic factors influence axon guidance, axon outgrowth of vagal sensory neurons from the nodose ganglion to their final target destination in the GI tract is not likely to be aberrant in this study. This is because while vagal axon bundles and IGLEs are greater in number, they do appear to reach their appropriate target destinations in the stomach and intestine. Consistent with this, overexpression of NGF in the skin of transgenic mice led to an increase in dorsal root ganglion neurons and significantly more axon fibers, but the organization of the nerve fibers was unaltered and they maintained a path to the appropriate targets in the spinal cord (Mendelson et al., 1996).

Alternatively, there may be no differences in neuron migration and axon guidance of vagal sensory neurons to the target destination in the GI tract, but there may be a change or disruption in the signal for other neurons to migrate out of the nodose ganglion during development in BDNF SM -/- mutants. Peripheral sensory ganglia are derived from two different embryonic tissues: the neural crest and the epibranchial placode. In general, the neural crest gives rise to many diverse cell types, such as melanocytes, craniofacial bones, cartilage, connective tissue, and cardiac smooth muscle cells**,** while the placode gives rise to neurons of the distal geniculate, petrosal, and nodose ganglia (Le Douarin et al., 1986; Zhuo et al., 1997; Crane & Trainor 2006;

Minoux & Rijli 2010). The neural crest-derived cells are highly migratory, while placode-derived cells do not migrate out. This non-migratory characteristic of placode-derived cells makes a disruption in the signal for other neurons to migrate out during the development of the nodose ganglion in BDNF SM -/- mutants unlikely.

Future experiments are necessary to delineate whether any of these explanations are responsible for the increase in vagal sensory innervation observed in the intestine of BDNF SM -/- mutant mice in this study. In order to determine if a lack of the appropriate cell death that is required for normal developmental processes resulted in an overabundance of vagal sensory neurons, a TUNEL assay could be performed. It is hypothesized that the BDNF SM -/- mice would show a decrease in apoptosis compared to the control mice with normal development of vagal sensory neurons and their terminal endings. In contrast, if the increase in neurons within the nodose ganglion in BDNF SM -/- mice was due to an increase in cell growth processes such as replication, proliferation, or differentiation, a bromodeoxyuridine (BrdU) labeling assay could be used to identify proliferating cells. BrdU is a synthetic analogue of thymidine that is incorporated into proliferating cells, allowing for the detection of new cell growth. If the increase in vagal sensory neurons in BDNF SM -/- mutants were due to an increase in cell proliferation, there would be an increase in BrdU labeled cells in the mutants compared to controls.

In addition to a TUNEL assay and a BrdU labeling study to separate out the contributions of cell death and cell growth, mRNA expression of NT-3 and

NT-4 could be quantified in BDNF SM -/- mice and controls. If other neurotrophic factors such as NT-3 and NT-4 are overcompensating for the loss of BDNF in BDNF SM -/- mice, these mutant mice should show an increase in the expression of these genes in the smooth muscle compared to controls. This is a likely contributor to the increase in nodose ganglion cells and IGLE density demonstrated in BDNF SM -/- mice.

Increased Vagal Afferent Innervation is Specific to the Intestine

The increase in IGLE density in BDNF SM -/- mice appears to be specific to the intestine, as IGLE density remained normal in the stomach of BDNF SM -/- mice. Consistent with this, the small intestine of BDNF SM -/- mice demonstrated the greatest decrease in BDNF mRNA levels out of the tissues analyzed (82% decrease), which also included the stomach, prefrontal cortex, and hypothalamus. It was somewhat surprising that the increase in IGLE density was specific to the intestine in this study, rather than to the stomach, as might be expected based on previous reports. It was originally thought that neurotrophins organized the development of the GI tract in an organ-specific manner: NT-4 was hypothesized to be primarily responsible for the development and survival of IGLEs in the intestine, because NT-4 -/- mice demonstrated a 90% decrease in IGLE density in the intestine compared to wt mice, while IGLE density in the stomach remained normal (Fox et al., 2001a). The esophagus appeared to be primarily dependent on NT-3, as there were 65% and 40% decreases in IGLE density observed in the esophagus of NT-3 and TrkC heterozygous mutants, respectively (Raab et al., 2003). Therefore,

as the intestine was primarily dependent on NT-4, and the esophagus on NT-3, it was assumed the stomach was dependent on BDNF. This notion was supported by studies showing BDNF -/- mice had decreased IGLE density in the stomach at P0 (Murphy & Fox 2010). However, Murphy & Fox (2010) concentrated only on the stomach in development, and did not study the effects of BDNF on the development of other GI organs such as the intestine or in adulthood.

It is possible that because BDNF is responsible for the survival of the largest percent of vagal sensory neurons, more than one organ system could be impacted by loss of BDNF. Consistent with this, although high expression levels of both SM22αcre and BDNF lacZ reporters were present in both the stomach and intestine, the extent of the expression of these two promoters was greater in the intestine, primarily due to expression of the SM22α promoter (Fox et al., 2013). This suggests BDNF is responsible for the survival of vagal sensory innervation to the intestine as well as the stomach, and may in fact play a larger role in the intestine than the stomach. Fox et al. (2013) showed there were no changes in IGLE density in the stomach of mutant mice missing one global BDNF allele and one SM22α-targeted BDNF allele, (therefore both BDNF alleles were missing from the smooth muscle, and these mice are known as “SM22α-BDNF KO” mice). Although there was a decrease in vagal sensory neurons in the nodose ganglion in these mutant mice, the decrease was to a much lesser degree than predicted. Based on the number of vagal sensory neurons at birth in homozygous global BDNF KO mice (ElShamy &

Ernfors 1997), a 35% decrease in vagal sensory neurons was expected in the SM22α-BDNF KO mice in the Fox et al. (2013) study. However, surprisingly, only a 9% decrease in vagal sensory neurons was observed in SM22α-BDNF KO mice compared to controls (Fox et al., 2013). This suggested to us at that time there may have been increased survival of vagal sensory neurons in the mutants due to the disruption of one BDNF allele in the smooth muscle by the utilization of the SM22α promoter, which is similar to the findings of the current study, as both BDNF alleles were under the control of the SM22α promoter. Therefore, when one BDNF allele is removed from the smooth muscle under control of the SM22α promoter, as in the Fox et al. (2013) study, there is a 26% increase in vagal sensory neurons. Similarly, in the present study, when both BDNF alleles are under the control of the SM22α promoter, there is a 47% increase in vagal sensory neurons (~ double the increase in sensory neurons observed when one BDNF allele is removed under control of the SM22α promoter).

An alternative explanation for the increase in IGLE density in the intestine is the BDNF SM -/- mutation altered the development of the nodose ganglion itself. If the development of the nodose was disrupted, the normal topographical organization of the neurons contained within the ganglion could be altered. Therefore, if the location of neurons that send their projections to the gut that terminate in IGLEs is altered within the nodose ganglion, the axons and their terminal endings could also have a disorganized pattern. Although it appears the increase in IGLEs is specific to the intestine in this study, this

could be an indirect consequence of the BDNF SM -/- mutation impacting intestine-projecting neurons within the nodose ganglion. This is because although the nerve tracer injections of WGA-HRP into the nodose ganglion may be consistent across genotypes, if the location of intestine-projecting neurons within the ganglion is changed in the mutants, the labeling of different populations of neurons that project to visceral organs may be disrupted. Although the nerve tracer injections appeared to infiltrate the entire ganglion, this alternative interpretation is more likely if WGA-HRP did not reach neurons located in some parts of the nodose ganglion. However, disrupted development of the nodose ganglion itself is unlikely, as the $BDNF^{lox\text{-}lacZ}$ reporter previously demonstrated that the BDNF SM KO was primarily concentrated to the intestine and portions of the antrum and corpus of the stomach (Fox et al., 2013).

As mentioned previously, the nerve tracer utilized in this study does not clearly distinguish terminal size and number, each of which contributes to terminal density. Therefore, the mechanism underlying the increase in vagal sensory innervation remains unclear. BDNF SM -/- mice could have an increased number of IGLEs in the intestine which leads to larger aggregates of IGLE clusters, which could lead to an increase in vagal afferent signaling to the brain due to increased sensory input to the NTS. Alternatively, the mutant mice could have normal numbers of IGLEs in the intestine, but the individual IGLEs could be larger. Increased IGLE size could also lead to increased negative feedback to the brain due to increased IGLE sensitivity, because the size of

each terminal would be increased. Although the neural convergence at the NTS would likely be decreased if IGLE size was increased, there would still be more action potentials sent to the NTS as a result of increased sensitivity due to increased stretch at the larger IGLEs. It is likely both increased terminal number and size may play a role in the increased satiation and satiety observed in BDNF SM -/- mutants. This is because there is an increase in total vagal sensory neurons from both the left and right ganglia, which is consistent with a selective increase in longitudinal axon bundle number. Additionally, although nonsignificant, there is a trend toward increased circular bundles, which would indicate increased axon branching.

Additional nerve tracers could be employed to get a more clear view of how size and number impact the increased IGLE density observed in BDNF SM -/- mice compared to controls. For example, the Dextran tracers have been shown to clearly delineate fine morphological characteristics of individual IGLEs. Dextran tracers are useful to obtain high-definition labeling of vagal afferent axons and terminals after injection into the nodose ganglion (Fox et al., 2001a; Phillips & Powley 2007).

Pathways / Mechanisms Contributing to Increased Satiation and Satiety in BDNF SM -/- Mice

Deficiency of BDNF in the smooth muscle results in decreased total and average meal duration, decreased meal size, increased total IMI and increased satiety ratio in BDNF SM -/- mutant mice compared to control wt mice. These

changes in the feeding behavior of BDNF SM -/- mice suggest increased satiation and satiety occur in the mutant mice compared to controls.

Decreased meal duration alone does not clearly suggest increased satiation, as decreased meal duration could result from an increase in postingestive influences of food intake that control satiation, or a decrease in motivational and/or oropharyngeal influences of food intake. Likewise, oropharyngeal and postingestive controls of food intake combine to produce meal size. As the satiety ratio is derived from the ratio of IMI and the preceding meal size, it is an estimate of how effective a given amount of food is at producing satiety, and not a direct measure of the state of satiety an animal is experiencing. The IMI is another meal pattern parameter associated with satiety, because the extent to which an animal is experiencing satiety influences the time interval until the animal initiates its next meal. However, meal size also needs to be considered when determining the extent to which the IMI influences satiety (as is taken into account in the calculation of the satiety ratio), as differences in meal size also determine the duration of the IMI. Meal duration and IMI meal pattern parameters do not change food intake themselves; however, meal duration and IMI influence meal size and meal number, and it is these meal pattern parameters that influence the actual amount of food ingested. As such, each meal pattern parameter alone cannot definitely determine any mechanisms underlying changes in food intake. However, the meal pattern data, taken together with the meal microstructure

data, provides a strong case for increased satiation and satiety in BDNF SM -/- mice.

The meal microstructure data strengthen the interpretation of increased satiation and satiety in BDNF SM -/- mice, because there were no changes in initial food intake at the start of a meal between mutants and controls. This suggests there were no differences in oropharyngeal factors or motivation to initiate food intake in controls and BDNF SM -/- mice. However, during the latter part of the meal, after the animals start to become satiated at around minute 6, the mutants show increased suppression of food intake compared to wt mice. This decreased food intake during the latter part of the first daily meal in BDNF SM -/- mice corresponds to the postingestive phase of food intake. It is likely there were no changes in palatability to food in BDNF SM -/- mice, as there were no changes in food intake during the first couple of minutes after a 6 hr fast. Therefore, because there were no differences between mutants and controls in palatability or motivation to initiate food intake, the decreased meal duration, decreased meal size, increased IMI and increased satiety ratio suggests increased satiation and satiety in BDNF SM -/- mice.

Although BDNF SM -/- showed increased satiation and satiety, they displayed normal total food intake. Consistent with no change in total food intake, there were no changes in body composition or body weight in BDNF SM -/- mice. This suggests compensation from other meal pattern parameters occurred to result in no net change in food intake or body weight. The BDNF SM -/- mutant demonstrated an increased feeding rate and a trend toward

increased meal frequency that combined to produce compensation for their increased satiation and satiety resulted in no net change in food consumed. Feeding rate affects meal duration and IMI, which acts to influence meal size and number. Therefore, BDNF SM -/- mice were eating at a faster rate during a meal, although the time spent eating during that meal was decreased. They also ate one more meal during the 18 hr meal pattern collection period each day than control mice. Although meal number was not statistically significantly increased in mutants on its own, the combination of the trend toward increased meal number and increased feeding rate in mutants resulted in compensation for the decreased meal duration and size, and the increased IMI and satiety ratio.

The changes in feeding behavior observed in BDNF SM -/- mice are consistent with alteration of vagal signaling, as short-term controls of food intake are primarily under control of vagal regulation, rather than long-term controls of food intake (Moran et al., 2001; Berthoud 2008). As BDNF SM -/- mice show changes in short-term controls of food intake consistent with increased satiation and satiety, and not long term changes in food intake that influence body weight, the mutant mice may have increased vagal satiation signaling. For example, alterations of vagal innervation and vagal feedback signaling have resulted in changes in meal size and duration, both of which are also observed in the current study (Ritter & Ladenheim 1985; Walls et al., 1995; Chavez et al., 1997; Schwartz et al., 1999; Kelly et al., 2000; Fox et al.,

2001a; Chi et al., 2004; Abbott et al., 2005; Powley et al., 2005; Chi & Powley 2007).

The decrease in food intake observed from minutes 6-30 in the meal microstructure analysis is also consistent with a vagal role in the control of food intake in BDNF SM -/- mice. It has been well established that when food is accumulating in the gut after ingestion, which occurs during the postingestive phase of food intake, satiation signals are sent to the brain through vagal afferents (Davis et al., 1975; Kaplan et al., 1992). There were no changes in initial food intake rate at the start of the meal, indicating there were no differences in the oropharyngeal or taste contribution to food intake. This suggests there were no differences between the genotypes in hedonic or motivational influence to obtain food. As the vagus is not typically considered to regulate hedonic influences of food ingestion, but has an identified role in postingestive controls of food intake, this data is consistent with an alteration of vagal signaling in BDNF SM -/- mice.

The increases in satiation and satiety observed in BDNF SM -/- mutants could be due to the increased IGLE density. The relationship between IGLE density and satiation has been demonstrated previously in mice deficient in NT-4, which have a 90% decrease in IGLE density in the duodenum, and also showed increased meal duration on a solid pellet diet, and increased meal size on an Isocal liquid diet (Fox et al., 2001). The inverse relationship has also been demonstrated: Mice with an NT-4 KI showed increased IGLE density in

the intestine, and these mice showed increased satiation, which resulted in decreased meal size (Chi et al., 2004).

The changes in ingestive behavior observed in the BDNF SM -/- mice could be a result of changes in vagal function, such as increased vagal negative feedback signaling to the brain. There are several different processes that could be impacted to result in increased vagal negative feedback signaling. A potential mechanism of altered vagal signaling could occur through maintenance of normal sensory receptor sensitivity, but because there is an increased number of sensory terminals and fibers signaling back to the NTS, there may be increased vagal satiation signaling in mutant BDNF SM -/- mice. The increase in the number of axons could lead to an increase in the summation of neuronal inputs to the NTS. Alternatively, increased vagal afferent signaling could occur through increased sensitivity of the sensory mechanoreceptors themselves, which could result in increased sensitivity to GI stimuli such as distention, and could lead to an increased number and/or duration of action potentials, increased firing rate, or an altered firing pattern in some other way that also results in increased vagal signaling from the intestine to the NTS. Daly et al. (2011) demonstrated changes in vagal signaling through decreased frequency of baseline neuronal impulses of intestinal afferents by whole nerve multiunit extracellular recordings in mice on a high fat diet. Mice on a high fat diet showed a 70% decrease in spontaneous afferent discharge rate arising from isolated segments of jejunum compared to controls. After increased luminal pressure was applied to test the mechanosensitivity of the

afferents, the high fat diet-fed mice also showed a reduction in firing frequency. It is possible similar effects could be seen in BDNF SM -/- mice, although in the opposite direction, as they have increased vagal afferent innervation. Alternatively, or in addition to, alterations in development that can lead to functional changes in vagal signaling that can impact ingestive behavior, the increased satiation and satiety observed in BDNF SM -/- mice compared to controls could also occur through direct functional changes in adulthood. Increased sensitivity of IGLEs to distention in BDNF SM -/- mice could occur in adulthood. Electrophysiological methods should be employed in the future to tease apart any changes in vagal function to the observed increases in satiation and satiety in BDNF SM -/- mice.

An alternative explanation for the increases observed in satiation and satiety in BDNF SM -/- mice compared to controls rather than the proposed explanation of increased vagal afferent innervation in the intestine is because BDNF may be necessary for the survival or development of other targets in the GI tract. In addition to vagal innervation, there other neural inputs to the smooth muscle in the GI tract, such as the sympathetic and enteric nervous systems (Young et al., 2004; Fox et al., 2013). It is possible the loss of BDNF in BDNF SM -/- mice could impact these other targets in the GI tract and result in the changes observed in feeding behavior.

Sympathetic innervation of the GI tract is a possible candidate to be impacted by loss of BDNF from the smooth muscle. However, NGF and NT-3 are primarily responsible for the development of sympathetic innervation of the

GI tract and this innervation is thus not dependent on BDNF for survival (Crowley et al., 1994; Albers et al. 1996; Randolph et al., 2007). Knockout of NGF results in an 80% decrease in the volume of sympathetic SCG neurons compared to wt littermates, while the number of vagal sensory neurons within the nodose ganglion remained normal (Crowley et al., 1994). Meanwhile, NT-3 is responsible for 55% and 53% of DRG and SCG sympathetic neurons, respectively (Ernfors et al., 1994). Knockout of BDNF did not impact SCG density, while the nodose ganglion displayed a 44% decrease in volume at P0 (Jones et al., 1994). Additionally, sympathetic innervation of several peripheral tissues, including the heart, kidneys, and bladder in mice deficient in both BDNF and p75 was determined to be unaltered (Jahed & Kawaja 2005). This study did not investigate GI tissues, leaving open the possibility that sympathetic innervation of the stomach or intestine could be impacted by BDNF. However, severing the splanchnic fibers of the sympathetic innervation to the gut does not affect food intake (Deutsch & Jang Ahn 1986), suggesting the meal pattern and meal microstructure results observed in the current study are not effects due to BDNF loss on the sympathetic nervous system.

The enteric nervous system is another possible tissue in the GI tract that could become altered by loss of BDNF in the smooth muscle. Global heterozygous BDNF mutants (BDNF +/-) showed a 16% decrease in in myenteric plexus cell numbers in the jejunum of the intestine, which is not consistent with the effects observed here, making myenteric neuron targets unlikely to account for the increases in IGLE density, vagal sensory neurons in

the nodose ganglion, and satiation and satiety (Jones et al., 2001). Although it is possible the cell numbers of the myenteric plexus are not equivalent in the jejunum from this example and the duodenum, which was the level of the intestine under investigation in the present thesis. Murphy & Fox (2010) also demonstrated myenteric neuron density remained normal in the stomach of BDNF -/- global KO mice at P0. It is also possible that BDNF contributed to the development or function of enteric or sympathetic innervation of the GI tract and subsequently affected GI reflexes, which could contribute to satiation and satiety. It has been shown that administration of BDNF enhances GI peristalsis by increasing serotonin and calcitonin gene-related peptide (CGRP) (Grider et al., 2006). However, similar effects on GI reflexes through alteration of the enteric and/or sympathetic nervous systems are likely not responsible for the increased satiation and satiety of BDNF SM -/- mice, as the BDNF SM -/- animals showed a decrease of BDNF, rather than an increase of BDNF which resulted in increased GI reflex activity.

Deletion of BDNF from the smooth muscle to study the impact on the vagal afferents innervating this tissue could subsequently affect the development of the smooth muscle tissue itself, in addition to the vagal innervation innervating the tissue. Because BDNF is expressed strongly in the visceral organs, there may be an autocrine role for BDNF in the smooth muscle (Lommatzsch et al., 1999). If BDNF removal from the smooth muscle affects the development of the organs themselves, the visceral organs could become hypotrophic, and this degeneration of the organs could affect vagal innervation

and function indirectly, and could lead to the changes in feeding behavior observed here. An effect similar to this concept has been demonstrated with another organ system and growth factor. For example, NGF reduction in rats leads to severe testicular atrophy. These rats demonstrated reduced testes size and weight, with a 50% decrease in sperm production (Nylén et al., 1989). However, this is unlikely to occur, as neither the receptor for BDNF, trkB, nor its alternate receptor, p75, are expressed in the smooth muscle in mice (Lommatzsch et al., 1999). Additionally, there is no TrkB expression in many GI organs innervated by vagal afferents in humans, such as the esophagus, stomach, small intestine, colon, liver, and pancreas (Shibayama & Koizumi 1996). The BDNF ligand for these receptors and the receptors themselves are only present in the vagal afferent neurons and their projections, and in enteric neurons (Ichikawa 2007; Kashiba et al., 2003; Robinson 1996; Zhuo & Helke 1996; Ernfors et al., 1992). Up to 98% of neurons in the nodose ganglion have been shown to express TrkB mRNA (Kashiba et al., 2003). Based on this collection of evidence, BDNF in the smooth muscle cannot bind to its TrkB or p75 receptors to effect a response.

Effects of SM BDNF on Long-Term Regulation of Food Intake and Body Weight

As reported previously, global and CNS-specific genetic removal of BDNF has typically resulted in hyperphagia and obesity (Kernie et al., 2000; Rios et al., 2001; Unger et al., 2007; Liao et al., 2012; Fox et al., 2013). However, we found no differences in food intake, body weight, or body

composition between BDNF SM -/- mice and controls. There are several explanations for this discrepancy. It is possible that brain-specific removal of BDNF results in hyperphagia and obesity, while peripheral BDNF does not. There may be differences in central and peripheral mechanisms of BDNF regulation. In the smooth muscle, BDNF may play a role in development, rather than act as a feeding signal. However, Kamitakahara and Simerly (2012) similarly found no differences in food intake and body weight in mice with a VMH specific knockout of BDNF, using the promoter of the steroidogenic factor 1 (SF-1) gene, which is restricted to SF-1 neurons in the VMH. In addition, they found a significant increase in axon density to the perifornical region of the LHA from the VMH in mice missing BDNF from the VMH compared to wt mice. Therefore, it seems increasingly likely that BDNF has several different roles in development and metabolic regulation in both the central and peripheral nervous systems.

Additionally, compensatory mechanisms may be acting to maintain normal total food intake and body weight over time in BDNF SM -/- mice. This has been demonstrated in the past by other neonatal genetic ablations of neuropeptides and hormones involved in the regulation of food intake and body weight (Erickson et al., 1996; Luquet et al., 2005; Ring & Zeltser 2010). For example, mice with a developmental KO of AgRP, where the mice are lacking AgRP from birth, showed normal food intake and energy homeostasis, which would suggest AgRP neurons were not important for food intake and energy balance (Erickson et al., 1996). However, it was later observed that deletion of

AgRP neurons in adult animals rapidly reduced food intake, and stimulation of these neurons led to overeating, even in sated animals (Qian et al., 2002; Aponte et al., 2011; Krashes et al., 2013). Therefore, AgRP neurons are important for regulation of food intake, but the acute functions of AgRP neurons were obscured because the original developmental KO of AgRP neurons were compensated for over time (Luquet et al., 2005; Morrison & Munzberg 2012). Because the KO utilized in this study occurred during development, it is possible compensatory mechanisms are responsible for the maintenance of normal total food intake and body weight in BDNF SM -/- mice.

The results presented in this thesis also shed light on some previously unexpected effects of targeting removal of BDNF to the smooth muscle utilizing a slightly different approach compared to the present study (Fox et al., 2013). As mentioned earlier, generation of SM22α-BDNF KO mutant mice resulted in global removal of one BDNF allele, while the other BDNF allele was removed from the smooth muscle. This approach was utilized to ensure high efficiency of BDNF deletion. Theoretically, in these mice approximately 100% BDNF should be removed from the smooth muscle and approximately 50% BDNF should be removed from the brain. This approach surprisingly resulted in mice that exhibited striking early-onset obesity and hyperphagia. One unexpected consequence for interpreting these interesting results was the difficulty in separating out the relative gut and brain contributions to the obesity and hyperphagia observed in SM22α-BDNF KO mice. This is because BDNF levels were reduced by varying amounts in several different tissues that are involved

in regulation of energy balance in these animals. In particular, BDNF mRNA levels in the brain of SM22α-BDNF KO mice in the Fox et al. 2013 study were lower than expected. For example, there was a 90% decrease in the hypothalamus compared to wt mice. This was surprising, as only a 50% decrease was predicted due to the one global BDNF allele missing in those mice. Therefore, it appeared the cre expression driven by SM22α is not as specific to the smooth muscle as had been reported in multiple studies (Li et al., 1996; Zhang et al., 2001; Lepore et al., 2005) and suggested that it was active in hypothalamic cells known to express BDNF (Wetmore et al., 1990; Conner et al., 1997; Xu et al., 2003; Unger et al., 2007). This was verified through the presence of BDNF expression in the hippocampus, anterior-lateral cerebral cortex, and the VMH of $BDNF^{lox\text{-}lacZ}$ reporter mice, indicating BDNF removal from these locations due to the SM22α promoter (Fox et al., 2013). Consequently, it was not possible to distinguish the relative contributions of BDNF loss from the gut and the brain to the hyperphagia and obesity of SM22α-BDNF KO mice.

In the current study, both BDNF alleles were targeted to the smooth muscle, with no global removal of BDNF that had previously complicated interpretation of the increases in food intake and body weight observed in the Fox et al. (2013) study. Interestingly, despite use of the same SM22αcre promoter used in the Fox et al. (2013) study there were no differences in body weight between BDNF SM -/- mice and any other genotypes generated in the present set of experiments. This could imply the unexpected extreme

hyperphagia and obesity demonstrated by the SM22α-BDNF KO mice in the Fox et al. (2013) study were not due solely to the SM22αcre promoter expression that decreased BDNF levels in the anterior-lateral cerebral cortex, hippocampus and VMH. This finding is consistent with previous reports, as Kamitakahara & Simerly (2012) and Dhillon et al. (2006) found VMH-specific BDNF KO mice failed to develop obesity, although the VMH has been implicated as a primary site of BDNF action to regulate food intake within the hypothalamus (Xu et al., 2003; Unger et al., 2007; Wang et al., 2007; Godar et al., 2011). The hyperphagia and obesity as demonstrated by SM22α-BDNF KO mice in the Fox et al. (2013) study was likely due to the combination of 90% decrease in BDNF from the VMH and approximately 50% reductions of BDNF other brain regions (due to the global heterozygous BDNF KO in these mice) that cooperate with the VMH to regulate feeding and body weight.

IGLE Distribution in the Intestine

A novel finding in this study is the similarity of IGLE density throughout the first 8 cm of the duodenum. An initial high density of IGLEs in the proximal segment of the duodenum and a decrease in IGLE density from rostral to caudal down the length of the intestine has typically been reported (Berthoud et al., 1997; Phillips et al., 1997; Fox et al., 2000; Fox et al., 2001a; Wang et al., 2012). However, in the present study, IGLE density was nearly identical in the 0-4 and 4-8 cm segments of duodenum sampled. There are several reasons why the 0-4 cm and the 4-8 cm segments would show very similar densities of IGLEs.

The nodose ganglion is typically considered to be organized in a loosely viscerotopic arrangement, with neurons generally located more anteriorly within the nodose projecting to more anterior organs, and neurons with a more caudal location in the nodose innervating more posterior organs, however little is known about the specific organization of vagal innervation within the nodose (Altschuler et al., 1989; Zhuo et al., 1997). For example, neurons that project to the esophagus and the aortic depressor nerve are located in the rostral part of the nodose ganglion, and neurons that project to the stomach and pancreas are located more caudally within the nodose (Zhuo et al., 1997). However, these distinctions are not well defined, as the specific organization and projection patterns of neurons in the nodose ganglion are still unknown. Because little is known regarding the specific organization of vagal innervation of the GI tract within the nodose ganglion, it is hard to draw conclusions regarding the density and distribution of IGLEs in the stomach and intestine.

The method utilized to label IGLEs in the GI tract in this study and other studies, nodose injections of the nerve tracer WGA-HRP, is a powerful method to label nearly all of the vagal afferents innervating the GI tract. This tracer was utilized in this study because to date it selectively labels the highest percentage of vagal sensory innervation of the GI tract, at almost 100%. However, variables such as injection location within the nodose and experimenter variability could contribute to the different IGLE distribution patterns observed in the current study compared to other studies. Future studies should focus on mapping the exact injection site within the nodose ganglion and where these

neurons project to in the GI tract. It will also be instrumental to study IGLE density throughout the intestine, and include the jejunum and ileum to see if these regions have a higher IGLE density than previously considered.

Separation of Sensory and Motor Vagal Pathways

As discussed previously, the vagus is a mixed nerve, which consists of both sensory and motor components. An additional benefit of a BDNF smooth-muscle specific KO is the ability to disentangle the separate contributions of the sensory and motor components of the vagus. A genetic approach is useful for the selective manipulation of vagal afferents without concomitantly damaging or manipulating the motor component of the vagus nerve, as both sub-diagphragmatic surgical and chemical deafferentations have failed to eliminate the majority of sensory-specific vagal innervation to the GI tract. For example, surgical vagotomy severs both sensory and motor connections between the brain and gut, while application of the chemical neurotoxin capsaicin destroys only a subset of all vagal GI afferents.

In the present study, the KO of BDNF is sensory-specific. This is because BDNF is not necessary for the survival of vagal motor neurons. For example, global KO of BDNF does not impact density of motor DMV neurons; however, there is a significant decrease in vagal sensory neurons in the nodose ganglion (Jones et al., 1994). In addition, Murphy & Fox (2010) showed no change in myenteric neurons or vagal efferents in the stomach of BDNF -/- mice compared to controls. Therefore, the increases in satiation and satiety observed in BDNF SM -/- mice are likely due to changes in vagal sensory

signaling, which is consistent with the increase in IGLE density in these mice. Although it is possible that any changes in sensory signaling can also affect the motor output response, which could contribute to changes in feeding behavior such as GI reflexes. This study is one of the first to provide evidence of vagal satiation signaling without altering vagal motor function or global expression levels of the gene of interest.

Conclusions

Smooth-muscle specific removal of BDNF results in increased vagal afferent innervation to the intestine, as demonstrated by increased IGLE density and increased number of large diameter longitudinal bundles. This effect appears to be mediated by increased survival of vagal sensory neurons, although increased branching of axon bundles may also play a role in the increased IGLE density observed in BDNF SM -/- mutants compared to controls. The increase in IGLE density and vagal bundles in BDNF SM -/- mice is associated with increases in satiation and satiety, as the mutant mice show decreased meal duration, decreased meal size, increased IMI, and increased satiety ratio. Consistent with this, BDNF SM -/- and control mice show the same initial feeding rate after a six hour fast. However, during the postingestive phase of food intake, BDNF SM -/- show increased suppression of food intake. It appears that BDNF's normal role is to suppress the development of sensory vagal innervation in the intestine. This project reveals a novel role for BDNF in the development of vagal afferent innervation to the intestine.

LIST OF REFERENCES

LIST OF REFERENCES

Abbott, C. R., Monteiro, M., Small, C. J., Sajedi, A., Smith, K. L., Parkinson, J. R., . . . Bloom, S. R. (2005). The inhibitory effects of peripheral administration of peptide YY (3-36) and glucagon-like peptide-1 on food intake are attenuated by ablation of the vagal-brainstem-hypothalamic pathway. *Brain Research, 1044*(1), 127-131.

Albers, K. M., Perrone, T. N., Goodness, T. P., Jones, M. E., Green, M. A., & Davis, B. M. (1996). Cutaneous overexpression of NT-3 increases sensory and sympathetic neuron number and enhances touch dome and hair follicle innervation. *The Journal of Cell Biology, 134*(2), 487-497.

Altschuler, S. M., Bao, X., Bieger, D., Hopkins, D. A., & Miselis, R. R. (1989). Viscerotopic representation of the upper gastrointestinal tract in the rat: Sensory ganglia and nuclei of the solitary and spinal trigeminal tracts. *Journal of Comparative Neurology, 283*, 248-268.

Aponte, Y., Atasoy, D., & Sternson, S. M. (2011). AGRP neurons are sufficient to orchestrate feeding behavior rapidly and without training. *Nature Neuroscience, 14*(3), 351-355.

Balkowiec, A., & Katz, D. M. (1998). Brain-derived neurotrophic factor is required for normal development of the central respiratory rhythm in mice. *The Journal of Physiology, 510*, 527-533.

Bariohay, B., Roux, J., Tardivel, C., Trouslard, J., Jean, A., & Lebrun, B. (2009). Brain-derived neurotrophic factor / Tropomyosin-related kinase receptor type B signaling is a downstream effector of the brainstem melanocortin system in food intake control. *Endocrinology, 150*(6), 2646-2653.

Ben-Zvi, A., Yagil, Z., Hagalili, Y., Klein, H., Lerman, O., & Behar, O. (2006). Semaphorin 3A and neurotrophins: a balance between apoptosis and survival signaling in embryonic DRG neurons. *Journal of Neurochemistry, 96*, 585-597.

Berthoud, H.-R. (2008). The vagus nerve, food intake and obesity. *Regulatory Peptides, 149*, 15-25.

Berthoud, H.-R., Kressel, M., Raybould, H. E., & Neuhuber, W. L. (1995). Vagal sensors in the rat duodenal mucosa: distribution and structure as revealed by in vivo DiI-tracing. *Anatomy and Embryology (Berlin), 191*, 203-212.

Berthoud, H.-R., Patterson, L. M., Neumann, F., & Neuhuber, W. L. (1997). Distribution and structure of vagal afferent intraganglionic laminar endings (IGLEs) in the rat gastrointestinal tract. *Anatomy and Embryology, 195*, 183-191.

Berthoud, H.-R. & Powley, T. L. (1992). Vagal afferent innervation of the rat fundic stomach: morphological characterization of the gastric tension receptor. *Journal of Comparative Neurology, 319*, 261-276.

Biddinger, J. E., & Fox, E. A. (2010). Meal parameters and vagal gastrointestinal afferents in mice that experienced early postnatal overnutrition. *Physiology & Behavior, 101*, 184-191.

Blackshaw, L. A., Grundy, D., & Scratcherd, T. (1987). Vagal afferent discharge from gastric mechanoreceptors during contraction and relaxation of the ferret corpus. *Journal of the Autonomic Nervous System, 18*, 19-24.

Boesmans, W., Gomes, P., Janssens, J., Tack, J., & Vanden Berghe, P. (2008). Brain-derived neurotrophic factor amplifies neurotransmitter responses and promotes synaptic communication in the enteric nervous system. *Gut, 57*(3), 314-322.

Bowers, C. Y., Momany, F. A., Reynolds, G. A., & Hong, A. (1984). On the in vitro and in vivo activity of a new synthetic hexapeptide that acts on the pituitary to specifically release growth hormone. *Endocrinology, 114*, 1537-1545.

Broberger, C., Holmberg, K., Shi, T. J., Dockray, G., & Hökfelt, T. (2001). Expression and regulation of cholecystokinin and cholecystokinin receptors in rat nodose and dorsal root ganglia. *Brain Research, 903*(1-2), 128-140.

Burek, M. J., & Oppenheim, R. W. (1996). Programmed cell death in the developing nervous system. *Brain Pathology, 6*, 427-446.

Caleo, M., Menna, E., Chierzi, S., Cenni, M. C., & Maffei, L. (2000). Brain-derived neurotrophic factor is an anterograde survival factor in the rat visual system. *Current Biology, 10*(19),1155-61.

Camerino, C., Zayzafoon, M., Rymaszewski, M., Heiny, J., Rios, M., Hauschka, P. V. (2012). Central depletion of Brain-derived neurotrophic factor in mice results in high bone mass and metabolic phenotype. *Neuroendocrinology, 153*(11), 5394-5405.

Carmeliet, P., & Tessier-Levigne, M. (2005). Common mechanisms of blood and nerve vessel wiring. *Nature, 436*(7048), 193-200.

Carroll, P., Lewin, G. R., Koltzenburg, M., Toyka, K. V., Thoenen, H. (1998). A role for BDNF in mechanosensation. *Nature Neuroscience, 1*, 42-46.

Chao, M. V. (1994). The p75 neurotrophin receptor. *Journal of Neurobiology, 25*(11), 1373-1385.

Chavez, M., Kelly, L., York, D. A., & Berthoud, H.-R. (1997). Chemical lesion of visceral afferents causes transient overconsumption of unfamiliar high-fat diets in rats. *American Journal of Physiology, 272*, R1657-R1673.

Chen, W. P., Chang, Y. C., & Hsieh, S. T. (1999). Trophic interactions between sensory nerves and their targets. *Journal of Biomedical Science, 6*(2), 79-85.

Chi, M. M., Fan, G., & Fox, E. A. (2004). Increased short-term food satiation and sensitivity to cholecystokinin in neurotrophin-4 knock-in mice. *American Journal of Physiology: Regulatory, Integrative and Comparative Physiology, 287,* R1044-R1053.

Chi, M. M., & Powley, T L. (2007). NT-4-deficient mice lack sensitivity to meal-associated preabsorptive feedback from lipids. *American Journal of Physiology: Regulatory, Integrative and Comparative Physiology, 292*, R2124-R2135.

Chien, K. R. (2001). To Cre or not to Cre: the next generation of mouse models of human cardiac diseases. *Circulation Research, 88*(6), 546-549.

Chu, J. Y. S., Cheng, C. Y. Y., Sekar, R., & Chow, B K. C. (2013). Vagal afferent mediates the anorectic effect of peripheral secretin. *Plos One. 8*(5), 1-7.

Clarke, G. D., & Davison, J. S. (1978). Mucosal receptors in the gastric antrum and small intestine of the rat with afferent fibres in the cervical vagus. *The Journal of Physiology, 284*, 55-67.

Conner, J. M., Lauterborn, J. C., Yan, Q., Gall, C. M., & Varon, S. (1997). Distribution of brain-derived neurotrophic factor (BDNF) protein and mRNA in the normal adult rat CNS: evidence for anterograde axonal transport. *The Journal of Neuroscience, 17*, 2295-2313.

Coppola, V., & Tessarollo, L. (2004). Control of hyperphagia prevents obesity in BDNF heterozygous mice. *NeuroReport, 15*(17), 2665-2668.

Cordeira, J. W., Frank, L., Sena-Esteves, M., Pothos, E. N., & Rios, M. (2010). Brain-derived neurotrophic factor regulates hedonic feeding by acting on the mesolimbic dopamine system. *The Journal of Neuroscience, 30*(7), 2533-2541.

Coulson, E. J., May, L. M., Osborne, S. L., Reid, K., Underwood, C. K., Meunier, F. A., . . . Sah, P. (2008). p75 neurotrophin receptor mediates neuronal cell death by activating GIRK channels through phosphatidylinositol 4,5-bisphosphate. *The Journal of Neuroscience, 28*(1), 315-324.

Coulson, E. J., Reid, K., Baca, M., Shipham, K., Hulett, S. M., Kilpatrick, T. J., Bartlett, P. F. (2000). Chopper, a new death domain of the p75 neurotrophin receptor which mediates rapid neuronal cell death. *The Journal of Biological Chemistry, 275*, 30537-30545.

Crane, J. F., & Trainor, P. A. (2006). Neural crest stem and progenitor cells. *Annual Review of Cell and Developmental Biology, 22*, 267-286.

Crowley, C., Spencer, S. D., Nishimura, M. C., Chen, K. S., Pitts-Meek, S, Armanini, M. P., . . . Phillips, H. S. (1994). Mice lacking nerve growth factor display perinatal loss of sensory and sympathetic neurons yet develop basal forebrain cholinergic neurons. *Cell, 76*, 1001-1011.

Daly, D. M., Park, S. J., Valinsky, W. C., & Beyak, M. J. (2011). Impaired intestinal afferent nerve satiety signalling and vagal afferent excitability in diet induced obesity in the mouse. *The Journal of Physiology, 589*, 2857-2870.

Davies, A. M. (2000). Neurotrophins: more to NGF than just survival. *Current Biology, 10*, R374-R376.

Davies, A. M., Thoenen, H., & Barde, Y. A. (1986). The response of chick sensory neurons to brain-derived neurotrophic factor. *The Journal of Neuroscience, 6*(7), 1897-904.

Davis, B. M., Fundin, B. T., Albers, K. M., Goodness, T. P., Cronk, K. M., & Rice, F. L. (1997). Overexpression of nerve growth factor in skin causes preferential increases among innervation to specific sensory targets. *Journal of Comparative Neurology, 387*(4), 489-506.

Davis. J. D. (1998). A model for the control of ingestion – 20 years later. In A. R. Morrison & S. J. Fluharty (Eds.), Progress in psychobiology and physiological psychology (pp. 127-173). San Diego, CA: Academic.

Davis, J. D., Collins, B. J., & Levine, M. (1975). Peripheral control of meal size: Gastrointestinal filling as a negative feedback signal, a theoretical and experimental analysis. *Journal of Comparative and Physiological Psychology, 89*, 985-1003.

Deutsch, J. A., & Jang, A. S. (1986). The splanchnic nerve and food intake regulation. *Behavioral and Neural Biology, 45*(1), 43-47.

Dhillon, H., Zigman, J. M., Ye, C., Lee, C. E., McGovern, R. A., Tang, V., . . .Lowell, B. B. (2006). Leptin directly activates SF1 neurons in the VMH, and this action by leptin is required for normal body-weight homeostasis. *Neuron, 49*(2), 191-203.

Diamond, J., Holmes, M., & Coughlin, M. (1992). Endogenous NGF and nerve impulses regulate the collateral sprouting of sensory axons in the skin of the adult rat. *The Journal of Neuroscience, 12*, 1454-1466.

Dontchev, V. D., & Letourneau, P.C. (2002). Nerve growth factor and semaphorin 3A signaling pathways interact in regulating sensory neuronal growth cone motility. *The Journal of Neuroscience, 22*(15), 6659-6669.

Elitt, C. M., Malin, S. A., Koerber, H. R., Davis, B. M., & Albers, K. M. (2008). Overexpression of artemin in the tongue increases expression of TRPV1 and TRPA1 in trigeminal afferents and causes oral sensitivity to capsaicin and mustard oil. *Brain Research, 1230*, 80-90.

ElShamy, W. M., & Ernfors, P. (1997). Brain-derived neurotrophic factor, neurotrophin-3, and neurotrophin-4 complement and cooperate with each other sequentially during visceral neuron development. *The Journal of Neuroscience, 17*, 8667-8675.

Erickson, J. C., Clegg, K. E., & Palmiter, R. D. (1996). Sensitivity to leptin and susceptibility to seizures of mice lacking neuropeptide Y. *Nature, 381*, 415-421.

Erickson, J. T., Conover, J. C., Borday, V., Champagnat, J., Barbacid, M., Yancopoulos, G., & Katz, D. M. (1996). Mice lacking brain-derived neurotrophic factor exhibit visceral sensory neuron losses distinct from mice lacking lacking NT4 and display a severe developmental deficit in control of breathing. *The Journal of Neuroscience, 16*, 5361-5371.

Ernfors, P., Lee, K. F., Kucera, J., & Jaenisch, R. (1994). Lack of neurotrophin-3 leads to deficiencies in the peripheral nervous system and loss of limb proprioceptive afferents. *Cell, 77*(4), 503-12.

Ernfors, P., Merlio, J.P., & Persson, H. (1992). Cells expressing mRNA for neurotrophins and their receptors during embryonic rat development. *European Journal of Neuroscience, 4*(11), 1140-1158.

Faxen, A., Rossander, L., & Kewenter, J. (1979). The effect of parietal cell vagotomy and selective vagotomy with pyloroplasty on body weight and dietary habits. A prospective randomized study. *Scandinavian Journal of Gastroenterology, 14*(1), 7-11.

Fox, E. A. (2006). A genetic approach for investigating vagal sensory roles in regulation of gastrointestinal function and food intake. *Autonomic Neuroscience, 126-127*, 9-29.

Fox, E. A. (2013). Vagal afferent controls of feeding: a possible role for gastrointestinal BDNF. *Clinical Autonomic Research, 23*, 15-31.

Fox, E. A., & Biddinger, J. E. (2012). Early postnatal overnutrition: Potential roles of gastrointestinal vagal afferents and brain-derived neurotrophic factor. *Physiology & Behavior, 106*(3), 400-412.

Fox, E. A., Biddinger, J. E., Jones, K. R., Worman, A., & McAdams, J. (2013). Mechanism of hyperphagia contributing to obesity in brain-derived neurotrophic factor knockout mice. *Neuroscience, 229*, 176-199.

Fox, E. A., & Byerly, M. S. (2004). A mechanism underlying mature-onset obesity: evidence from the hyperphagic phenotype of brain-derived neurotrophic factor mutants. *American Journal of Physiology: Regulatory, Integrative and Comparative Physiology, 286*(6), R994-1004.

Fox, E. A., & Murphy, M. C. (2008). Factors regulating vagal sensory development: potential role in obesities of developmental origin. *Physiology & Behavior, 94*, 90-104.

Fox, E. A., Phillips, R. J., Baronowsky, E. A., Byerly, M. S., Jones, S., & Powley, T. L.(2001a). Neurotrophin-4 deficient mice have a loss of vagal intraganglionic mechanoreceptors from the small intestine and a disruption of short-term satiety. *The Journal of Neuroscience, 21*, 8602-8615.

Fox, E. A., Phillips, R. J., Byerly, M. S., Baronowsky, E. A., Chi, M. M., & Powley, T. L. (2002). Selective loss of vagal intramuscular mechanoreceptors in mice mutant for steel factor, the c-Kit receptor ligand. *Anatomy and Embryology (Berlin), 205*, 325-342.

Fox, E. A., Phillips, R. J., Martinson, F. A., Baronowsky, E. A., & Powley, T. L. (2000). Vagal afferent innervation of smooth muscle in the stomach and duodenum of the mouse: morphology and topography. *Journal of Comparative Neurology, 428*, 558-576.

Fox, E. A., Phillips, R. J., Martinson, F. A., Baronowsky, E. A., & Powley, T. L. (2001b). C-Kit mutant mice have a selective loss of vagal intramuscular mechanoreceptors in the forestomach. *Anatomy and Embryology, 204*, 11-26.

Fox, E. A., & Powley, T. L. (1985). Longitudinal columnar organization within the dorsal motor represents separate branches of the abdominal vagus. *Brain Research, 341*, 269-282.

Fundin, B. T., Silos-Santiago, I., Ernfors, P., Fagan, A. M., Aldskogius, H., DeChiara, T. M., . . . Rice, F. L. (1997). Differential dependency of cutaneous mechanoreceptors on neurotrophins, trk receptors, and P75 LNGFR. *Developmental Biology, 190*(1), 94-116.

Gibson, D. A., & Ma, L. (2011). Developmental regulation of axon branching in the vertebrate nervous system. *Development, 138*(2), 183-195.

Godar, R., Dai, Y., Bainter, H., Billington, C., Kotz, C. M., & Wang, C. F. (2011). Reduction of high-fat diet-induced obesity after chronic administration of brain-derived neurotrophic factor in the hypothalamic ventromedial nucleus. *Neuroscience, 194*, 36-52.

Goodman, C. S., & Shatz, C. J. (1993). Developmental mechanisms that generate precise patterns of neuronal connectivity. *Cell, 72*(suppl), 77-98.

Grider, J. R., Piland, B. E., Gulick, M. A., & Qiao, L. Y. (2006). Brain-derived neurotrophic factor augments peristalsis by augmenting 5-HT and calcitonin gene-related peptide release. *Gastroenterology, 130*, 771-780.

Hellard, D., Brosenitsch, T., Fritzsch, B., & Katz, D. M. (2004). Cranial sensory neuron development in the absence of brain-derived neurotrophic factor in BDNF/Bax double null mice. *Developmental Biology, 275*, 34-43.

Henry, R. A., Hughes, S. M., & Connor, B. (2007). AAV-mediated delivery of BDNF augments neurogenesis in the normal and quinolinic acid-lesioned adult rat brain. *European Journal of Neuroscience, 25*(12), 3513-3525.

Hill, D. R., Campbell, N. J., Shaw, T. M., & Woodruff, G. N. (1987). Autoradiographic localization and biochemical characterization of peripheral type CCK receptors in rat CNS using highly selective nonpeptide CCK antagonists. *The Journal of Neuroscience, 7*(9), 2067-2076.

Holtwick, R., Gotthardt, M., Skryabin, B., Steinmetz, M., Potthast, R., Zetsche, B., . . . Kuhn, M. (2002). Smooth muscle-selective deletion of guanylyl cyclase-A prevents the acute but not chronic effects of ANP on blood pressure. *Proceedings of the National Academy of Sciences of the United States of America, 99*(10), 7142-7147.

Honma, Y., Araki, T., Gianino, S., Bruce, A., Heuckeroth, R., Johnson, E., & Milbrandt, J. (2002). Artemin is a vascular-derived neurotropic factor for developing sympathetic neurons. *Neuron, 35*(2), 267-282.

Huang, E. J., & Reichardt, L. F. (2001). Neurotrophins: roles in neuronal development and function. *Annual Review of Neuroscience, 24*, 677-736.

Huang, Y., Ko, H., Cheung, Z. H., Yung, K. K., Yao, T., Wang, J. J., . . . Yung, W. H. (2012). Dual actions of brain-derived neurotrophic factor on GABAergic transmission in cerebellar Purkinje neurons. *Experimental Neurology, 233*, 791-798.

Ichikawa, H., Terayama, R., Yamaai, T., Yan, Z., & Sugimoto, T. (2007). Brain-derived neurotrophic factor-immunoreactive neurons in the rat vagal and glossopharyngeal sensory ganglia; co-expression with other neurochemical substances. *Brain Research, 1155*, 93-99.

Jahed, A., & Kawaja, M. D. (2005). The influences of p75 neurotrophin receptor and brain-derived neurotrophic factor in the sympathetic innervation of target tissues during murine postnatal development. *Autonomic Neuroscience, 118*(1-2), 32-42.

Jhaveri, S., Erzurumlu, R. S., Laywell, E. D., Steindler, D. A., Albers, K. M., Davis, B. M. (1996). Excess nerve growth factor in the periphery does not obscure development of whisker-related patterns in the rodent brain. *Journal of Comparative Neurology, 374*, 41-51.

Johnson, E. M., Craig, E. T., & Yeh, H. H. (2007). TrkB is necessary for pruning at the climbing fibre–Purkinje cell synapse in the developing murine cerebellum. *The Journal of Physiology, 582*(2), 629-646.

Jones, K. R., Farinas, I., Backus, C., & Reichardt, L. F. (1994). Targeted disruption of the BDNF gene perturbs brain and sensory neuron development but not motor neuron development. *Cell, 76*, 969-999.

Jones, S., Fox, E. A., & Powley, T. L. (2001). *Neurotrophin-deficient and p75 receptor-deficient mice show altered myenteric neuronal numbers*. Society for Neuroscience Abstract, San Diego, CA.

Kamitakahara, A. K., & Simerly, R. B. (2012). *Ventromedial hypothalamic expression of BDNF is required for normal development of the circuits controlling the counter-regulatory response to hypoglycemia*. Society for Neuroscience Abstract, New Orleans, LA.

Kaplan, J. M., Spector, A. C., & Grill, H. J. (1992). Dynamics of liquid gastric emptying during and after stomach fill. *American Journal of Physiology, 263*, R813-R819.

Kashiba, H., Uchida, Y., & Senba, E. (2003). Distribution and colocalization of NGF and GDNF family ligand receptor mRNAs in dorsal root and nodose ganglion neurons of adult rats. *Brain Research Molecular Brain Research, 110*(1), 52-62.

Katz, D. M. (2005). Regulation of respiratory neuron development by neurotrophic and transcriptional signaling mechanisms. Respiratory Physiology & Neurobiology, 149, 99-109.

Katz, D. M., Erb, M., Lillis, R., & Neet, K. (1990). Trophic regulation of nodose ganglion cell development: Evidence for an expanded role of nerve growth factor during embryogenesis in the rat. *Experimental Neurology, 110*, 1-10.

Kawakami, T., Wakabayashi, Y., Isono, T., Aimi, Y., & Okada, Y. (2002). Expression of neurotrophin messenger RNAs during rat urinary bladder development. *Neuroscience Letters, 329*, 77-80.

Kelly, L., Morales, S., Smith, B. K., & Berthoud, H.-R. (2000). Capsaicin-treated rats permanently overingest low- but not high-concentration sucrose solutions. *American Journal of Physiology: Regulatory, Integrative and Comparative Physiology, 279*, R1805-R1812.

Kennedy, T. E., & Tessier-Lavigne, M. (1995). Guidance and induction of branch formation in developing axons by target-derived diffusible factors. *Current Opinion in Neurobiology, 5*, 83-90.

Kentish, S., Li, H., Philp, L. K., O'Donnell, T. A., Isaacs, N. J., Young, R. L., . . . Page, A. J. (2012). Diet-induced adaptation of vagal afferent function. *The Journal of Physiology, 590*, 209-221.

Kernie, S. G., Liebl, D. J., & Parada, L. F. (2000). BDNF regulates eating behavior and locomotor activity in mice. *EMBO Journal, 19*(6), 1290-1300.

Koda, S., Date, Y., Murakami, N., Shimbara, T., Hanada, T., Toshinai, K., . . . Nakazato, M. (2005). The role of the vagal nerve in peripheral PYY_{3-36}-induced feeding reduction in rats. *Endocrinology, 146*(5), 2369-2375.

Korte, M., Carroll, P., Wolf, E., Brem, G., Thoenen, H., & Bonhoeffer, T. (1995). Hippocampal long-term potentiation is impaired in mice lacking brain-derived neurotrophic factor. *Proceedings of the National Academy of Sciences of the United States of America, 92*, 8856–8860.

Kojima, M., Hosoda, H., Date, Y., Nakazato, M., Matsuo, H., & Kangawa, K. (1999). Ghrelin is a growth-hormone-releasing acylated peptide from stomach. *Nature, 102*, 656-660.

Kolbeck, R., Jungbluth, S., & Barde, Y. A. (1994). Characterisation of neurotrophin dimers and monomers. *European Journal of Biochemistry, 225*, 995-1003.

Kolbeck, R., Bartke, I., Eberle, W., & Barde, Y. A. (1999). Brain-derived neurotrophic factor levels in the nervous system of wild-type and neurotrophin gene mutant mice. *Journal of Neurochemistry, 72*(5), 1930-1938.

Kral, J. G., Paez, W., & Wolfe, B. M. (2009). Vagal nerve function in obesity: therapeutic implications. *World Journal of Surgery, 33*, 1995-2006.

Krashes, M. J., Koda, S., Ye, C. P., Rogan, S. C., Adams, A. C., Cusher, D. S., . . . Lowell, B. B. (2013). Rapid, reversible activation of AgRP neurons drives feeding behavior in mice. *Journal of Clinical Investigation, 121*, 1424-1428.

Krimm, R. F., Davis, B. M., Woodbury, C. J., & Albers, K. M. (2004). NT3 expressed in skin causes enhancement of SA1 sensory neurons that leads to postnatal enhancement of Merkel cells. *Journal of Comparative Neurology, 471*, 352-360.

Kuczewski, N., Porcher, C., Lessmann, V., Medina, I., & Gaiarsa, J.-L. (2009). Activity-dependent dendritic release of BDNF and biological consequences. *Molecular Neurobiology, 39*(1), 37-49.

Lapchak, P. A., & Hefti, F. (1992). BDNF and NGF treatment in lesioned rats: effects on cholinergic function and attenuated weight gain. *NeuroReport, 3*, 405-408.

Laskiewicz, J., Krolczyk, G., Zurowski, G., Sobocki, J., Matyja, A., & Thor, P. J. (2003). Effects of vagal neuromodulation and vagotomy on control of food intake and body weight in rats. *Journal of Physiology and Pharmacology, 54*(4), 603-610.

Le Douarin, M. N., Fontaine-Pérus, J., & Couly, G. (1986). Cephalic ectodermal placodes and neurogenesis. *Trends in Neurosciences, 9*, 175-180.

Lee, R., Kermani, P., Teng, K. K., & Hempstead, B. L. (2001). Regulation of cell survival by secreted proneurotrophins. *Science, 294*, 1945-1948.

LeMaster, A. M., Krimm, R. F., Davis, B. M.. Noel, T., Forbes, M. E., Johnson, J. E., & Albers, K. M. (1999). Overexpression of brain-derived neurotrophic factor enhances sensory innervation and selectively increases neuron number. *The Journal of Neuroscience*, 19, 5919-5931.

Lepore, J. .J., Cheng, L., Min, L. M, Mericko, P. A., Morrisey, E. E., & Parmacek, M. S. (2005). High-efficiency somatic mutagenesis in smooth muscle cells and cardiac myocytes in SM22alpha-Cre transgenic mice. *Genesis, 41*, 179-184.

Levi-Montalcini, R., & Angeletti, P. U. (1968). Nerve growth factor. *Physiological Reviews, 48*, 534-569.

Li, L., Miano, J. M., Cserjesi, P., & Olson, E. N. (1996). SM22α, a marker of adult smooth muscle, is expressed in multiple myogenic lineages during embryogenesis*. Circulation Research, 78*, 188-195.

Li, Y., Wu, X. Y., Zhu, J. X., & Owyang, C. (2001). Intestinal serotonin acts as paracrine substance to mediate pancreatic secretion stimulated by luminal factors. *American Journal of Physiology – Gastrointestinal and Liver, 281*(4), G916-G23.

Liao, G.-Y., An, J. J., Gharami, K., Waterhouse, E. G., Vanevski, F., Jones, K. R., & Xu, B. (2012). Dendritically targeted Bdnf mRNA is essential for energy balance and response to leptin. *Nature Medicine, 18*, 564-572.

Lindsay, R. M. (1988). Nerve growth factors (NGF, BDNF) enhance axonal regeneration but are not required for survival of adult sensory neurons. *The Journal of Neuroscience, 8*(7), 2394-2405.

Lindsay, R. M. (1996). Role of neurotrophins and trk receptors in the development and maintenance of sensory neurons: An overview. *Philosophical Transactions of the Royal Society B: Biological Sciences 351*(1338), 365-373.

Livak, K. J., & Schmittgen, T. D. (2001). Analysis of relative gene expression data using real-time quantitative PCR and the 2(-Delta Delta C(T)) Method. *Methods, 25*(4), 402-408.

Liu, X. B., Low, L. K., Jones, E. G., & Cheng, H. J. (2005). Stereotyped axon pruning via plexin signaling is associated with synaptic complex elimination in the hippocampus. *The Journal of Neuroscience, 25*, 9124-9134.

Lommatzsch, M., Braun, A., Mannsfeldt, A., Botchkarev, V. A., Botchkareva, N. V., Paus, R., . . . Renz, H. (1999). Abundant production of brain-derived neurotrophic factor by adult visceral epithelia. Implications for paracrine and target-derived neurotrophc functions. *American Journal of Pathology, 155*, 1183-1193.

Low, L. K., & Cheng, H.-J. (2006). Axon pruning: an essential step underlying the developmental plasticity of neuronal connections. *Philosophical Transactions of the Royal Society B: Biological Sciences, 361*, 1531-1544.

Luo, L., & O'Leary D, D. (2005). Axon retraction and degeneration in development and disease. *Annual Review of Neuroscience, 28*, 127-156.

Luquet, S., Perez, F. A., Hnasko, T. S., & Palmiter, R. D. (2005). NPY/AgRP neurons are essential for feeding in adult mice but can be ablated in neonates. *Science, 310*(5748), 683-685.

Lyons, W. E., Mamounas, L. A., Ricaurte, G. A., Coppola, V., Reid, S. W., Bora, S. H., . . . Tessarollo, L. (1999). Brain-derived neurotrophic factor-deficient mice develop aggressiveness and hyperphagia in conjunction with brain serotonergic abnormalities. *Proceedings of the National Academy of Sciences of the United States of America, 96*(26), 15239-15244.

Mai, J., Fok, L., Gao, H., Zhang, X., & Poo, M. M. (2009). Axon initiation and growth cone turning on bound protein gradients. *The Journal of Neuroscience, 29*(23), 7450-7458.

Mak, T. W., Penninger, J. M., & Ohashi, P. S. (2001). Knockout mice: a paradigm shift in modern immunology. *Nature Reviews Immunology, 1*(1), 11-19.

Mathis, C., Moran, T. H., & Schwartz, G. J. (1998). Load-sensitive rat gastric vagal afferents encode volume but not gastric nutrients. *American Journal of Physiology, 43*, R280-R286.

Markus, A., Patel, T. D, & Snider, W. D. (2002). Neurotrophic factors and axonal growth. *Current Opinion in Neurobiology, 12*, 523-531.

McDonald, N. Q., Lapatto, R., Murray-Rust, J., Gunning, J., Wlodawer, A., & Blundell, T. L. (1991). New protein fold revealed by a 2.3-Å resolution crystal structure of nerve growth factor. *Nature, 354*(5), 411-414.

Mendelson, B., Albers, K. M., Goodness, T. P., & Davis, B. M. (1996). Overexpression of nerve growth factor in epidermis of transgenic mice preserves excess sensory neurons but does not alter the somatotopic organization of cutaneous nerve projections. *Neuroscience Letters, 211*(1), 68-72.

Mesulam, M.-M. (1978). Tetramethyl benzidine for horseradish peroxidase neurohistochemistry: a noncarcinogenic blue reaction product for visualizing neural afferents and efferents. *Journal of Histochemistry & Cytochemistry, 26*, 106-117.

Minoux, M., & Rijli, F. M. (2010). Molecular mechanisms of cranial neural crest cell migration and patterning in craniofacial development. *Development. 137*, 2605-2621.

Moran, T. H., Ladenheim, E. E., & Schwartz, G. J. (2001). Within-meal gut feedback signaling. *International Journal of Obesity and Related Metabolic Disorders, 25*(Suppl 5), S39-S41.

Mordes, J. P., el Lozy, M., Herrera, M. G., & Silen, W. (1979). Effects of vagotomy with and without pyloroplasty on weight and food intake in rats. *American Journal of Physiology: Regulatory, Integrative and Comparative Physiology, 236*(1), R61-R66.

Morrison, C. D., & Münzberg, H. (2012). Capricious Cre: The devil is in the details. *Endocrinology, 153*(3), 1005-1007.

Murphy, M. C., & Fox, E. A. (2007). Anterograde tracing method using DiI to label vagal innervation of the embryonic and early postnatal mouse gastrointestinal tract. *Journal of Neuroscience Methods, 163*(2), 213-225.

Murphy, M. C., & Fox, E. A. (2010). Mice deficient in brain-derived neurotrophic factor have altered development of gastric vagal sensory innervation. *Journal of Comparative Neurology, 518*, 2934-2951.

Neuhuber, W. L. (1987). Sensory vagal innervation of the rat esophagus and cardia: a light and electron microscope anterograde tracing study. *Journal of the Autonomic Nervous System, 20*, 243-255.

Neuhuber, W. L., & Clerc, N. (1990). Afferent innervation of the rat esophagus in cat and rat. In W. Zenker & W. Neuhuber (Eds.), *The primary afferent neuron: a survey of recent morpho-functional aspects* (pp. 93-107). New York, NY: Plenum Press.

Nonidez, J. F. (1946). Afferent nerve endings in the ganglia of the intramuscular plexus of the dog's esophagus. *Journal of Comparative Neurology, 85*, 177-185.

Nosrat, I. V., Margolskee, R. F., & Nosrat, C. A. (2012). Targeted taste cell-specific overexpression of brain-derived neurotrophic factor in adult taste buds elevates phosphorylated TrkB protein levels in taste cells, increases taste bud size, and promotes gustatory innervation. *The Journal of Biological Chemistry, 287*, 16791-16800.

Nylén, P., Ebendal, T., Eriksdotter-Nilsson, M., Hansson, T., Henschen, A., Johnson, A. C., . . . Olson, L. (1989). Testicular atrophy and loss of nerve growth factor-immunoreactive germ cell line in rats exposed to n-hexane and a protective effect of simultaneous exposure to toluene or xylene. *Archives of Toxicology, 63*(4), 296-307.

Oppenheim, R. W. (1991). Cell death during development of the nervous system. *Annual Review of Neuroscience, 14*, 453-501.

Page, A. J., & Blackshaw, L. A. (1998). An in vitro study of the properties of vagal afferent fibers innervating the ferret oesophagus and stomach. *The Journal of Physiology, 512*, 907-916.

Page, A. J., & Blackshaw, L. A. (1999). $GABA_B$ receptors inhibit mechanosensitivity of primary afferent endings. *The Journal of Neuroscience, 19*(19), 8597-8602.

Page, A. J., Slattery, J. A., Milte, C., Laker, R., O'Donnell, T., Dorian, C., . . . Blackshaw, L. A. (2007). Ghrelin selectively reduces mechanosensitivity of upper gastrointestinal vagal afferents. *American Journal of Physiology – Gastrointestinal and Liver, 292*(5), G1376-G1384.

Pahnke, J., Mix, E., Knoblich, R., Müller, J., Zschiesche, M., Schubert, B., . . . Rolfs, A. (2004). Overexpression of glial cell line-derived neurotrophic factor induces genes regulating migration and differentiation of neuronal progenitor cells. *Experimental Cell Research, 297*(2), 484-494.

Patel, T. D., Jackman, A., Rice, F. L., Kucera, J., & Snider, W. D. (2000). Development of sensory neurons in the absence of NGF/TrkA signaling in vivo. *Neuron, 25*, 345-357.

Pelleymounter, M. A., Cullen, M. J., & Wellman, C. L. (1995). Characteristics of BDNF-induced weight loss. *Experimental Neurology, 131*, 229-238.

Pencea, V., Bingaman, K. D., Wiegand, S. J., & Luskin, M. B. **(**2001). Infusion of brain-derived neurotrophic factor into the lateral ventricle of the adult rat leads to new neurons in the parenchyma of the striatum, septum, thalamus, and hypothalamus. *Journal of Neuroscience, 21*(17), 6706-6717

Peters, J. H., Ritter, R. C., & Simasko, S. M. (2006). Leptin and CCK selectively activate vagal afferent neurons innervating the stomach and duodenum. *American Journal of Physiology: Regulatory, Integrative and Comparative Physiology, 290*, R1544-R1549.

Pezet, S., Malcangio, M., & McMahon, S. B. (2002). BDNF: A neuromodulator in nociceptive pathways? *Brain Research Reviews, 40*, 240-249.

Phillips, R. J., Baronowsky, E. A., & Powley, T. L. (1997). Afferent innervation of gastrointestinal tract smooth muscle by the hepatic branch of the vagus. *Journal of Comparative Neurology, 384*, 247-270.

Phillips, R. J., & Powley, T. L. (2000). Tension and stretch receptors in gastrointestinal smooth muscle: re-revaluating vagal mechanoreceptor electrophysiology. *Brain Research Reviews, 34*, 1-26.

Polleux, F., Whitford, K. L, Dijkhuizen, P. A., Vitalis, T., & Ghosh, A. (2002). Control of cortical interneuron migration by neurotrophins and PI3-kinase signaling. *Development, 129*(13), 3147-3160.

Powley, T. L., Chi, M. M., Baronowsky, E. A., & Phillips, R. J. (2005). Gastrointestinal tract innervation of the mouse: afferent regeneration and meal patterning after vagotomy. *American Journal of Physiology – Regulatory, Integrative and Comparative Physiology, 289*, R563-R574.

Powley, T. L., Spaulding, R. A., & Haglof, S. A. (2011). Vagal afferent innervation of the proximal gastrointestinal tract mucosa: Chemoreceptor and mechanoreceptor architecture. *Journal of Comparative Neurology, 519*, 644-660.

Prechtl, J. C., & Powley, T. L. (1985). Organization and distribution of the rat subdiaphragmatic vagus and associated paraganglia. *Journal of Comparative Neurology, 235*, 182-195.

Prechtl, J. C., & Powley, T. L. (1990). The fiber composition of the abdominal vagus of the rat. *Anatomy and Embryology, 181*, 101-115.

Qian, S., Chen, H., Weingarth, D., Trumbauer, M. E., Novi, D. E., Guan, X., . . . Marsh, D. J. (2002). Neither agouti-related protein nor neuropeptide Y is critically required for the regulation of energy homeostasis in mice. *Molecular and Cellular Biology, 22*, 5027-5035.

Raab, M., Wörl, J., Brehmer, A., & Neuhuber, W. L. (2003). Reduction of NT-3 or TrkC results in fewer putative vagal mechanoreceptors in the mouse esophagus. *Autonomic Neuroscience, 108*, 22-31.

Ramer, L. M., McPhail, L. T., Borisoff, J. F., Soril, L. J. J., Kaan, T. K. Y., Lee, J. H. T., . . . Ramer, M. S. (2007). Endogenous TrkB ligands suppress functional mechanosensory plasticity in the deafferented spinal cord. *Journal of Neuroscience, 27*(21), 5812-5822.

Randolph, C. L., Bierl, M. A., & Isaacson, L. G. (2007). Regulation of NGF and NT-3 protein expression in peripheral targets by sympathetic input. *Brain Research, 1144*, 59-69.

Reichardt, L. F. (2006). Neurotrophin-regulated signalling pathways. *Philosophical Transactions of the Royal Society B: Biological Sciences. 361*(1473), 1545-1564.

Rice, F. L., Albers, K. M., Davis, B. M., Silos-Santiago, I., Wilkinson, G. A., LeMaster, A. M., . . . Fundin, B. T. (1998). Differential dependency of unmyelinated and Aδ epidermal and upper dermal innervation on neurotrophins, trk receptors, and p75 LNGFR. *Developmental Biology, 198*, 57-81.

Rinaman, L., & Levitt, P. (1993). Establishment of vagal sensorimotor circuits during fetal development in rats. *Journal of Neurobiology, 24*(5), 641-659.

Ring, L. E., & Zeltser, L. M. (2010). Disruption of hypothalamic leptin signaling in mice leads to early-onset obesity, but physiological adaptations in mature animals stabilize adiposity levels. *Journal of Clinical Investigation, 120*(8), 2931-2941.

Ringstedt, T., Linnarsson, S., Wagner, J., Lendahl, U., Kokaia, Z., Arenas, E., . . . Ibáñez, C. F. (1998). BDNF regulates reelin expression and Cajal-Retzius cell development in the cerebral cortex. *Neuron, 21*(2), 305-315.

Rios, M., Fan, G., Fekete, C., Kelly, J., Bates, B., Kuehn, R., . . . Jaenisch, R. (2001). Conditional deletion of brain-derived neurotrophic factor in the postnatal brain leads to obesity and hyperactivity. *Molecular Endocrinology, 15*, 1748-1757.

Ritter, R. C., & Ladenheim, E. E. (1985). Capsaicin pretreatment attenuates suppression of food intake by cholecystokinin. *American Journal of Physiology: Regulatory, Integrative and Comparative Physiology, 248*, R501-R504.

Ritter, R. C., Brenner, L. A., & Tamura, C. S. (1994). Endogenous CCK and the peripheral neural substrates of intestinal satiety. *Annals of the New York Academy of Sciences: Cholecystokinin, 713*, 255-267.

Robinson, M., Adu, J., & Davies, A. M. (1996). Timing and regulation of trkB and BDNF mRNA expression in placode-derived sensory neurons and their targets. *European Journal of Neuroscience, 8*(11), 2399-2406.

Rodrigo, J., Hernandez, C. J., Vidal, M. A., & Pedrosa, J. A. (1975). Vegetative innervation of the esophagus. II. Intraganglionic laminar endings. *Acta Anatomica, 92*, 79-100.

Rodrigo, J., de Felipe, J., Robles-Chillida, E. M., Perez Anton, J. A., Mayo, I., & Gomez, A. (1982). Sensory vagal nature and anatomical access paths to esophagus laminar nerve endings in myenteric ganglia. Determination by surgical degeneration methods. *Acta Anatomica, 112*, 47-57.

Rüttimann, E. B., Arnold, M., Hillebrand, J. J., Geary, N., & Langhans, W. (2009). Intrameal hepatic portal and intraperitoneal infusions of glucagon-like peptide-1 reduce spontaneous meal size in the rat via different mechanisms. *Endocrinology, 150*, 1174-1181.

Sanes, J. R., & Lichtman, J. W. (1999). Development of the vertebrate neuromuscular junction. *Annual Review of Neuroscience, 22*, 389-442.

Sang, Q., & Young, H. M. (1998). The origin and development of the vagal and spinal innervation of the external muscle of the mouse esophagus. *Brain Research, 809*(2),253-268.

Scharfman, H., Goodman, J., Macleod, A., Phani, S., Antonelli, C., & Croll, S. (2005). Increased neurogenesis and the ectopic granule cells after intrahippocampal BDNF infusion in adult rats. *Experimental Neurology, 192*(2), 348-356.

Schmidt-Supprian, M., & Rajewsky, K. (2007). Vagaries of conditional gene targeting. *Nature Immunology, 8*(7), 665-668.

Schwartz, G. J., McHugh, P. R., & Moran, T. H. (1991). Integration of vagal afferent responses to gastric loads and cholecystokinin in rats. *American Journal of Physiology, 261*, R64-R69.

Schwartz, G. J., Salorio, C. F., Skoglund, C., & Moran, T. H. (1999). Gut vagal afferent lesions increase meal size but do not block gastric preload-induced feeding suppression. *American Journal of Physiology, 276*, R1623-R1629.

Shibayama, E., & Koizumi, H. (1996). Cellular localization of the Trk neurotrophin receptor family in human non-neuronal tissues. *American Journal of Pathology, 148*(6), 1807-1818.

Smith, G. P. (1996). The direct and indirect controls of meal size. *Neuroscience & Biobehavioral Reviews, 20*(1), 41-46.

Spaeth, A. M., Kanoski, S. E., Hayes, M. R., & Grill, H. J. (2012). TrkB receptor signaling in the nucleus tractus solitaries mediates the food-intake suppressive effects of hindbrain BDNF and leptin. *American Journal of Physiology, Endocrinology and Metabolism, 302*(10), E1252-E1260.

Stearns, A. T., Balakrishnan, A., Radmanesh, A., Ashley, S. W., Rhoads, D. B., & Tavakkolizadeh, A. (2012). Relative contributions of afferent vagal fibers to resistance to diet-induced obesity. *Digestive Diseases and Sciences, 57*, 1281-1290.

Stuckey, C. L., Koltzenburg, M., Schneider, M., Engle, M. G., Albers, K. M., & Davis, B. M. (1999). Overexpression of nerve growth factor in skin selectively affects the survival and functional properties of nociceptors. *The Journal of Neuroscience, 19*, 8509-8516.

Swithers, S. E., Baronowsky, E., & Powley, T. L. (2002). Vagal intraganglionic laminar endings and intramuscular arrays mature at different rates in pre-weanling rat stomach. *Autonomic Neuroscience, 102*(1-2),13-19.

Taicher, G. Z., Tinsley, F. C., Reiderman, A., & Heiman, M. L. (2003). Quantitative magnetic resonance (QMR) method for bone and whole-body composition analysis. *Analytical and Bioanalytical Chemistry, 377*, 990-1002.

Taniguchi, M., Yuasa, S., Fujisawa, H., Naruse, I., Saga, S., Mishina, M., & Yagi, T. (1997). Disruption of *Semaphorin III/D* gene causes severe abnormality in peripheral nerve projection. *Neuron, 19*, 519-530.

Teng, H. K., Teng, K. K., Lee, R., Wright, S., Tevar, S., Almeida, R. D., . . . Hempstead, B. L. (2005). ProBDNF induces neuronal apoptosis via activation of a receptor complex of $p75^{NTR}$ and sortilin. *The Journal of Neuroscience, 25*(22), 5455-5463.

Tinsley, F. C., Taicher, G. Z., & Heiman, M. L. (2004). Evaluation of a quantitative magnetic resonance method for mouse whole body composition analysis. *Obesity Research, 12*, 150-160.

Toriya, M., Maekawa, F., Maejima, Y., Onaka, T., Fujiwara, K., Nakagawa, T., . . . Yada, T. (2010). Long-term infusion of brain-derived neurotrophic factor reduces food intake and body weight via a cortiocotrophin-releasing hormone pathway in the paraventricular nucleus of the hypothalamus. *Journal of Neuroendocrinology, 22*(9), 987-995.

Troy, C. M., Friedman, J. E., & Friedman, W. J. (2002). Mechanisms of p75-mediated death of hippocampal neurons. Role of caspases. *The Journal of Biological Chemistry, 277*, 34295-34302.

Tuttle, R., & O'Leary, D. D. M. (1998). Neurotrophins rapidly modulate growth cone response to the axon guidance molecule, collapsin-1. *Molecular and Cellular Neuroscience, 11*(1-2), 1-8.

Tyler, W. J., & Pozzo-Miller, L. D. (2001). BDNF enhances quantal neurotransmitter release and increases the number of docked vesicles at the active zones of hippocampal excitatory synapses. *The Journal of Neuroscience, 21*, 4249-4258.

Unger, T. J., Calderon, G. A., Bradley, L. C., Sena-Estevez, M., & Rios, M. (2007). Selective deletion of Bdnf in the ventromedial and dorsomedial hypothalamus of adult mice results in hyperphagie behavior and obesity. *The Journal of Neuroscience, 27*(52), 14265-14274.

Vanevski, F., & Xu, B. (2013). Molecular and neural bases underlying roles of BDNF in the control of body weight. *Frontiers in Neuroscience, 7*(37), 1-10.

Walls, E. K., Wang, F. B., Holst, M. C., Phillips, R. J., Voreis, J. S., Perkins, A. R., . . . Powley, T. L. (1995). Selective vagal rhizotomies: a new dorsal surgical approach used for intestinal deafferentations. *American Journal of Physiology, 269*, R1279-R1288.

Wang, C., Bomberg, E., Levine, A., Billington, C., & Kotz, C. M. (2007). Brain-derived neurotrophic factor in the ventromedial nucleus of the hypothalamus reduces energy intake. *American Journal of Physiology: Regulatory, Integrative and Comparative Physiology, 293*, R1037-R1045.

Wang, F. B., Young, Y. K., & Kao, C. K. (2012). Abdominal vagal afferent pathways and their distributions of intraganglionic laminar endings in the rat duodenum. *Journal of Comparative Neurology, 520*, 1098-1113.

Wang, F. B., & Powley, T. L. (2000). Topographic inventories of vagal afferents in gastrointestinal muscle. *Journal of Comparative Neurology, 421*, 302-324.

Wank, S. A., Pisegna, J. R., & de-Weerth, A. (1992). Brain and gastrointestinal cholecystokinin receptor family: structure and functional expression. *Proceedings of the National Academy of Sciences of the United States of America, 89*, 8691-8695.

Wetmore, C., Ernfors, P., Persson, H., & Olson, L. (1990). Localization of brain-derived neurotrophic factor mRNA to neurons in the brain by in situ hybridization. *Experimental Neurology, 109*, 141-152.

Wren, A. M., Small, C. J., Abbott, C. R., Dhillo, W. S., Seal, L. J., Cohen, M. A., . . . Bloom, S. R. (2001). Ghrelin causes hyperphagia and obesity in rats. *Diabetes, 50*(11), 2540-2547.

Wyatt, S., & Davies, A. M. (1993). Regulation of expression of mRNAs encoding the nerve growth factor receptors p75 and trkA in developing sensory neurons. *Development, 119*(3), 635-648.

Xu, B., Goulding, E. H., Zang, K., Cepoi, D., Cone, R. D., Jones, K. R., . . . Reichardt, L. F. (2003). Brain-derived neurotrophic factor regulates energy balance downstream of melanocortin-4 receptor. *Nature Neuroscience, 6*, 736-742.

Yan, H., Newgreen, D. F., & Young, H. M. (2003). Developmental changes in neurite outgrowth responses of dorsal root and sympathetic ganglia to GDNF, neurturin and artemin. *Developmental Dynamics, 227*, 395-401.

Young, H. M., Anderson, R. B., & Anderson, C. R. (2004). Guidance cues involved in the development of the peripheral autonomic nervous system. *Autonomic Neuroscience, 112*, 1-14.

Zagorodnyuk, V. P., Chen, B. N., & Brookes, S. J. H. (2001). Intraganglionic laminar endings are mechanotransduction sites of vagal tension receptors in the guinea-pig stomach. *The Journal of Physiology, 534*, 255-268.

Zermano, V., Espindola, S., Mendoza, E., & Hernandez-Echeagaray, E. (2009). Differential expression of neurotrophins in postnatal C57BL/6 mice striatum. *International Journal of Biological Sciences, 5*, 118-127.

Zhang, J. C., Kim, S., Helmke, B. P., Yu, W. W., Du, K. L., Lu, M. M., . . . Parmacek, M. S. (2001). Analysis of SM22alpha-deficient mice reveals unanticipated insights into smooth muscle cell differentiation and function. *Molecular Cell, 21*(4), 1336-1344.

Zhang, X.-H., & Poo, M.-M. (2002). Localized synaptic potentiation by BDNF requires local protein synthesis in the developing axon. *Neuron, 36*(4), 675-688.

Zhang, Y., Ning, G., Handelsman, Y., & Bloomgarden, Z. T. (2010). Gut hormones and the brain. *Journal of Diabetes, 2*(3), 138-145.

Zhuo, H., & Helke, C. J. (1996). Presence and localization of neurotrophin receptor tyrosine kinase (TrkA, TrkB, TrkC) mRNAs in visceral afferent neurons of the nodose and petrosal ganglia. *Brain Research Molecular Brain Research, 38*, 63-70.

Zhuo, H., Ichikawa, H., & Helke, C. (1997). Neurochemistry of the nodose ganglion. *Progress in Neurobiology, 52*, 79-107.

Zigova, T., Pencea, V., Wiegand, S. J,, & Luskin, M, B. (1998). Intraventricular administration of BDNF increases the number of newly generated neurons in the adult olfactory bulb. *Molecular and Cellular Neuroscience, 11*(4), 234 - 245.

APPENDICES

Appendix A

Table 1

Density of Vagal Elements Quantified in Control and BDNF SM -/- Mice

	Control	BDNF SM -/-
0-4 cm		
Longitudinal fibers	3.39 ± 0.47	3.37 ± 0.47
Longitudinal bundles	5.39 ± 1.31	7.30 ± 1.31
Circular fibers	2.37 ± 0.48	2.54 ± 0.48
Circular bundles	3.098 ± 0.88	4.24 ± 0.88
4-8 cm		
Longitudinal fibers	1.47 ± 0.34	1.48 ± 0.30
Longitudinal bundles	1.98 ± 1.26	3.36 ± 1.19
Circular fibers	1.26 ± 0.33	1.75 ± 0.31
Circular bundles	1.95 ± 1.11	2.83 ± 1.05
Total (0-8 cm)		
Longitudinal fibers	2.59 ± 0.319	2.52 ± 0.31
Longitudinal bundles	4.07 ± 1.11	5.55 ± 1.11
Circular fibers	1.94 ± 0.36	2.23 ± 0.36
Circular bundles	2.60 ± 0.85	3.62 ± 0.85

Table 2

Number of Longitudinal and Circular Bundles in Control and BDNF SM -/- Mice

	Control	BDNF SM -/-
Diameter of longitudinal bundles (μm)		
0.5-1.0	27 ± 8.83	31.11 ± 4.77
1.5-2.0	19 ± 5.04	41.44 ± 9.29
2.5-3.0	6.44 ± 1.96	16.11 ± 4.59
3.5-4.0	1.33 ± 0.37	4.89 ± 1.02
4.5-5.0	0.22 ± 0.15	1.44 ± 0.44
5.5-6.0	0.33 ± 0.17	0.22 ± 0.15
Diameter of circular bundles (μm)		
0.5-1.0	20.56 ± 7.226	24.45 ± 3.56
1.5-2.0	14.12 ± 3.58	24.89 ± 6.429
2.5-3.0	3.39 ± 1.349	9.45 ± 3.54
3.5-4.0	0.78 ± 0.468	3.0 ± 1.218
4.5-5.0	0.12 ± 0.12	0.56 ± 0.24
5.5-6.0	0 ± 0	0.22 ± 0.22

Table 3

Estimated Number of Neurons in the Nodose Ganglia in Control (n = 9) and BDNF SM -/- (n = 14) Mutant Mice and Percentage of Cell Increase in Mutant Mice and Percentage of Cell Increase in Mutants

	Control	BDNF SM -/-	Cell Increase (%)	*p* Value
Right nodose	1737 ± 227	2819 ± 277	62	0.012*
Left nodose	1878 ± 189	2505 ± 292	33	0.129
Total	3615 ± 315	5324 ± 488	47	0.017*

Note. Means ± SEM; see methods for calculations

Table 4

Meal Pattern Parameters in Males and Females

	Control		BDNF SM -/-	
Meal Pattern Parameter	Male	Female	Male	Female
Meal number	9.94±0.63	8.96±0.68	11.05±0.63	10.39±0.58
Meal size (g)	0.38±0.038	0.34±0.033	0.30±0.011	0.28±0.013
Average meal duration (min)	20.73±5.11	23.65±5.52	9.17±5.11	9.04±4.79
Total meal duration (min)	168.95±33.08	181.69±35.74	98.29±33.08	89.21±30.93
Average intermeal interval (min)	64.95±4.12	59.64±2.81	68.69±3.46	68.43±3.26
Total intermeal interval (min)	650.19±50.49	534.98±54.54	741.48±50.49	692.88±47.23
Average feeding rate (g/min)	1.52±0.32	1.17±0.34	2.00±0.32	2.07±0.30
Satiety ratio (min/g)	233.39±21.79	230.133±24.92	284.02±9.38	301.92±15.67

Note. Data shown are means ± SEM averaged over days 5-22.

Appendix B

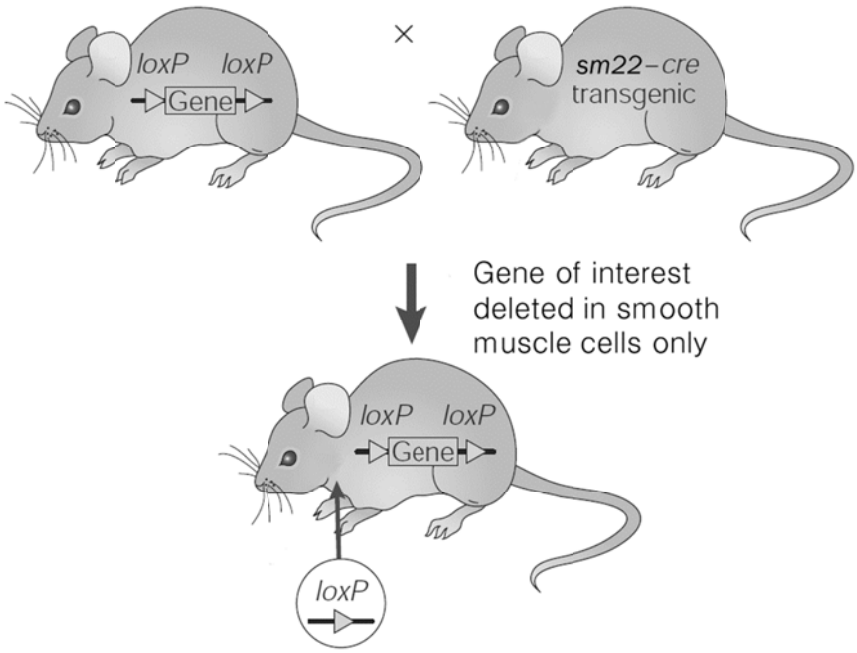

Figure 1. The cre-lox system was employed to target BDNF knockout to the smooth muscle. Target sites called loxP sites are genetically engineered around the gene of interest. Cre recombinase specifically recognizes loxP sites and has been shown to effectively mediate the excision of DNA located between loxP sites. In this study, BDNF is floxed and cre recombinase is expressed under the SM22α promoter, which is expressed only in smooth muscle cells. Therefore, in the progeny, cre recombinase is expressed only in smooth muscle cells and the floxed BDNF gene is deleted specifically from these cells. Image adapted from Mak et al., 2001.

Generation 1:	$SM22\alpha^{cre/cre}$; $BDNF^{+/+}$	X	$SM22\alpha^{+/+}$; $BDNF^{lox/lox}$
Generation 2:	$SM22\alpha^{cre/+}$; $BDNF^{+/lox}$	X	$SM22\alpha^{cre/+}$; $BDNF^{+/lox}$

Generation 3:

$SM22\alpha^{+/+}$; $BDNF^{+/+}$ (wt)

$SM22\alpha^{cre/+}$; $BDNF^{+/+}$ (cre only)

$SM22\alpha^{+/+}$; $BDNF^{lox/lox}$ (double lox)

$SM22\alpha^{+/+}$; $BDNF^{+/lox}$ (single lox)

$SM22\alpha^{cre/+}$; $BDNF^{+/lox}$ (BDNF SM +/-)

$SM22\alpha^{cre/+}$; $BDNF^{lox/lox}$ (BDNF SM -/-)

These initial matings ($SM^{cre/cre}$ x $BDNF^{lox/lox}$) result in all of the offspring being double heterozygotic transgenic mice needed for the next round of mating (Generation 2: $SM^{cre/+}$; $BDNF^{+/lox}$). These mice are then mated among themselves ($SM^{cre/+}$; $BDNF^{+/lox}$ x $SM^{cre/+}$; $BDNF^{+/lox}$) to generate the mice used in the experiments (Generation 3).

Figure 2. Breeding scheme used to generate BDNF SM -/- mice and associated control groups.

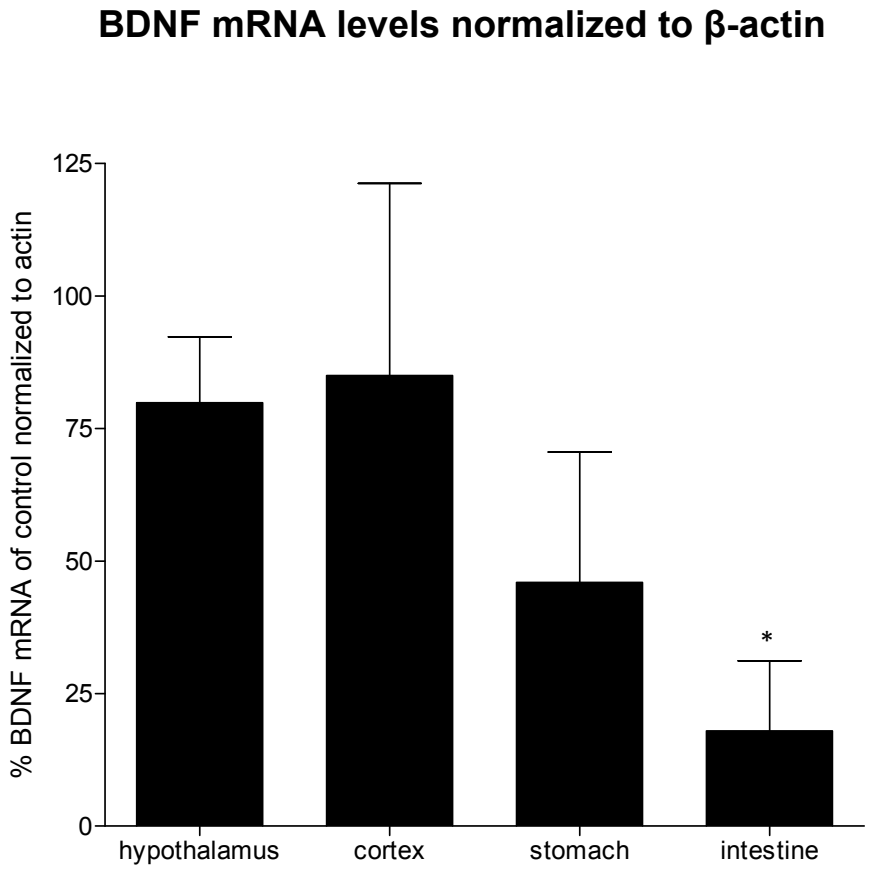

Figure 3. BDNF mRNA levels in BDNF SM -/- were decreased in GI tissues compared to controls, indicating the SM22α promoter successfully targeted KO of BDNF to the smooth muscle. Bars represent relative percent BDNF ± SEM mRNA expression in CNS and GI tissues of BDNF SM -/- mice compared to controls normalized to the reference gene β-actin.

Figure 4. Body weight curves of all genotypes generated from weaning at 3 weeks of age until 4 months of age in males (A) and females (B). Body weight does not differ between any of the genotypes.

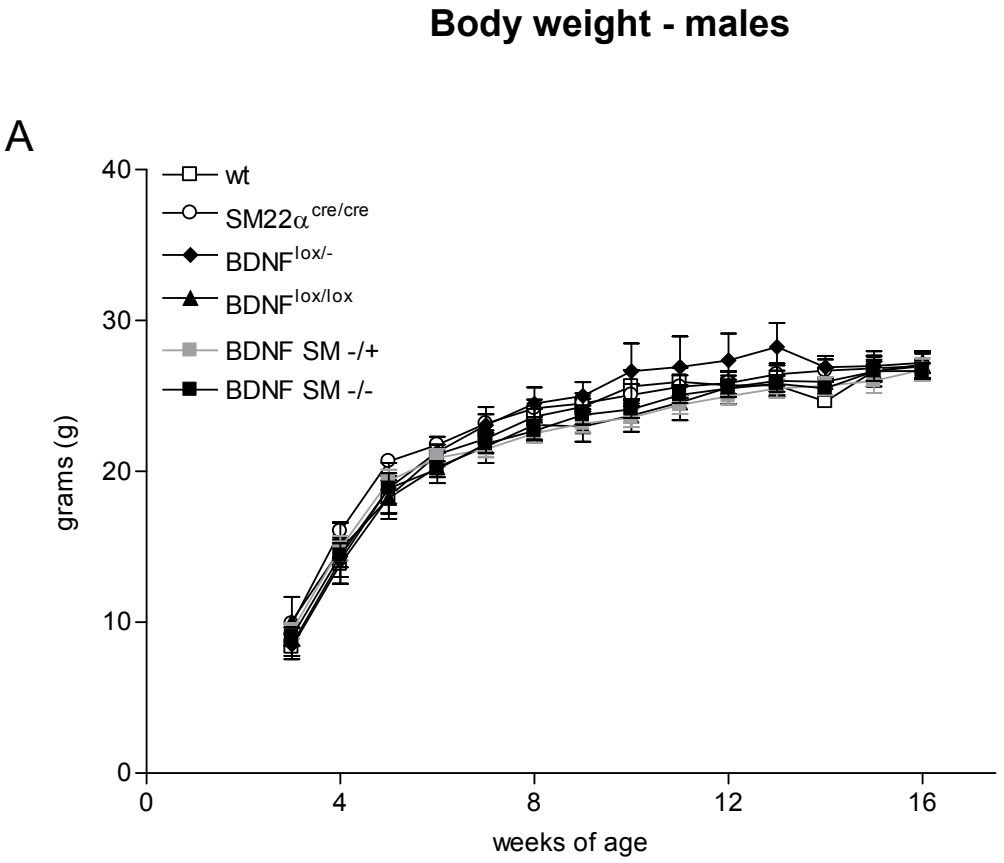
Body weight - males
A
wt
SM22α cre/cre
BDNF lox/-
BDNF lox/lox
BDNF SM -/+
BDNF SM -/-
grams (g)
weeks of age
0
10
20
30
40
0
4
8
12
16

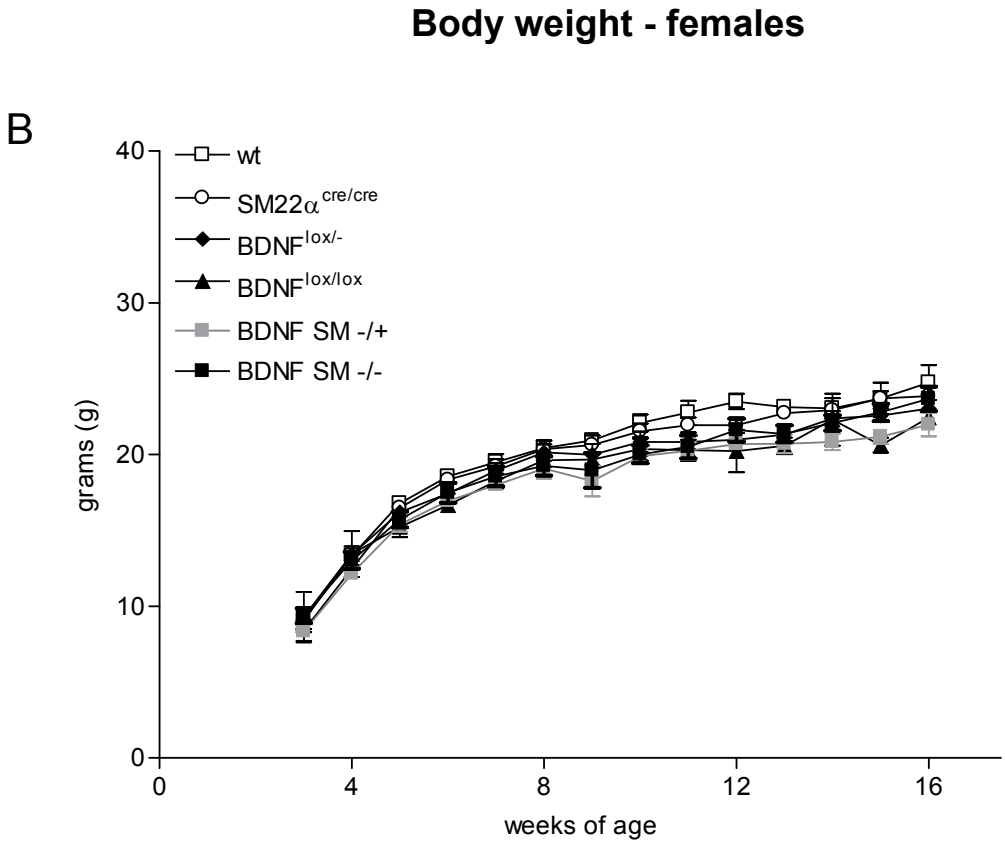
Body weight - females
B
wt
SM22α cre/cre
BDNF lox/-
BDNF lox/lox
BDNF SM -/+
BDNF SM -/-
grams (g)
weeks of age
0
10
20
30
40
0
4
8
12
16

Figure 5. Morphology of IGLEs in the stomach of (A) control and (B) BDNF SM -/- mice. IGLE morphology and density remained normal in BDNF SM -/- mice. Arrows indicate IGLES. Scale bar = 150 µm.

A

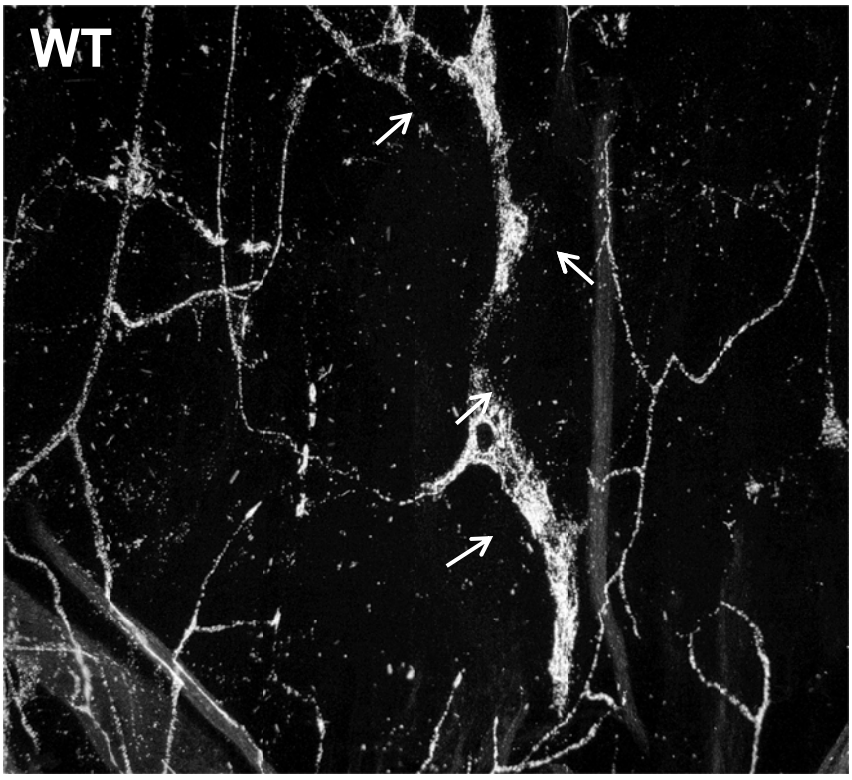

B

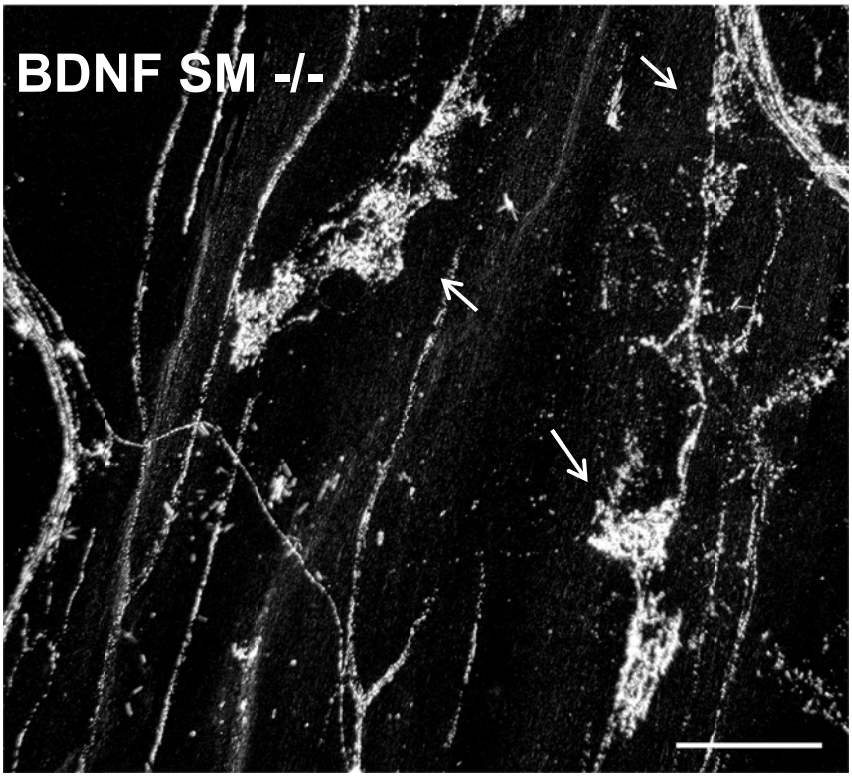

A

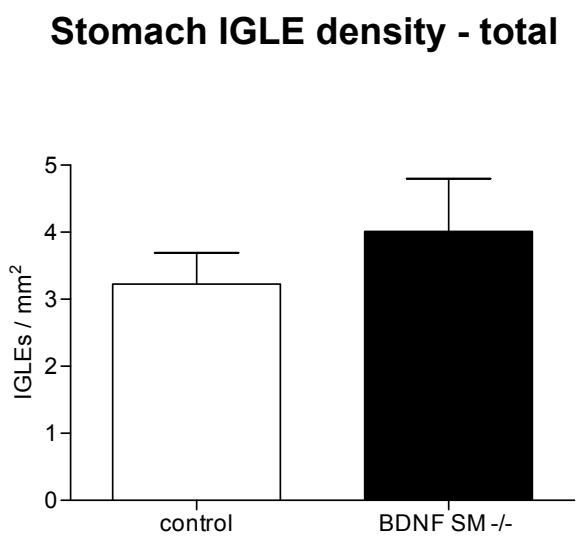

B

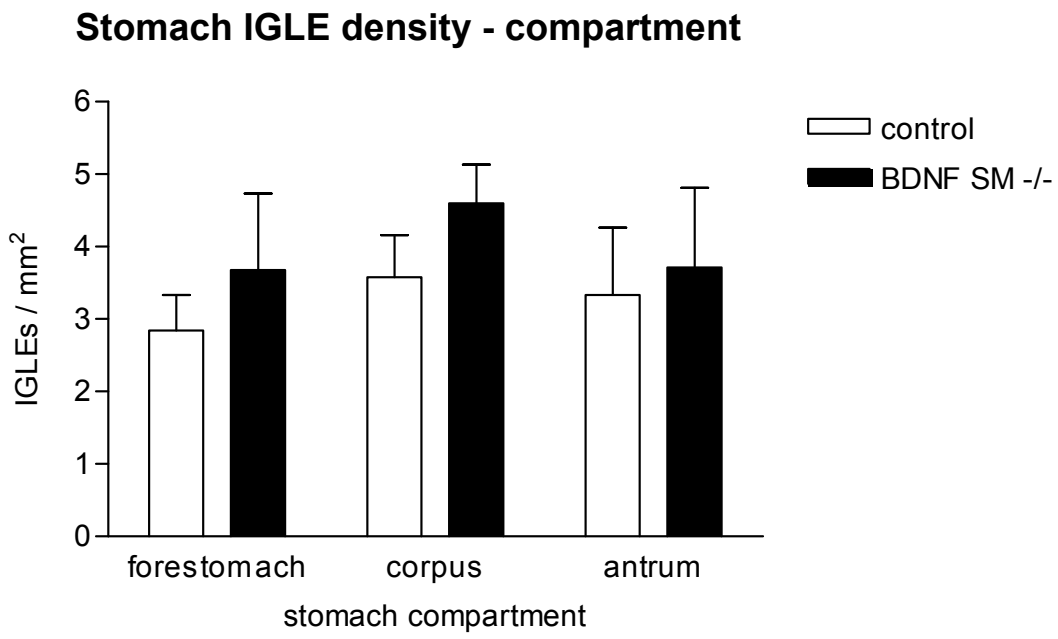

Figure 6. BDNF SM -/- mice displayed normal IGLE density in the stomach compared to controls. (A) Total average IGLE density. (B) IGLE density in each stomach compartment. Values are means ± SEM.

Figure 7. Morphology of IGLEs in the duodenum of (A) control and (B) BDNF SM -/- mice is normal. However, there is a significant increase in IGLE density in the duodenum of BDNF SM -/- mice. Arrows indicate IGLEs. Scale bar = 100 µm.

A

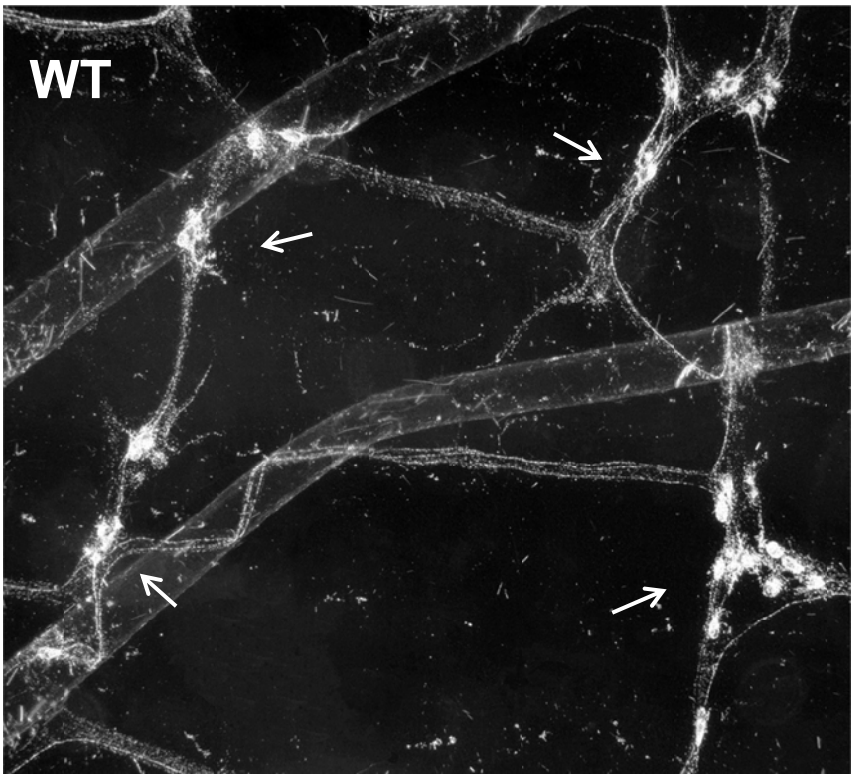

B

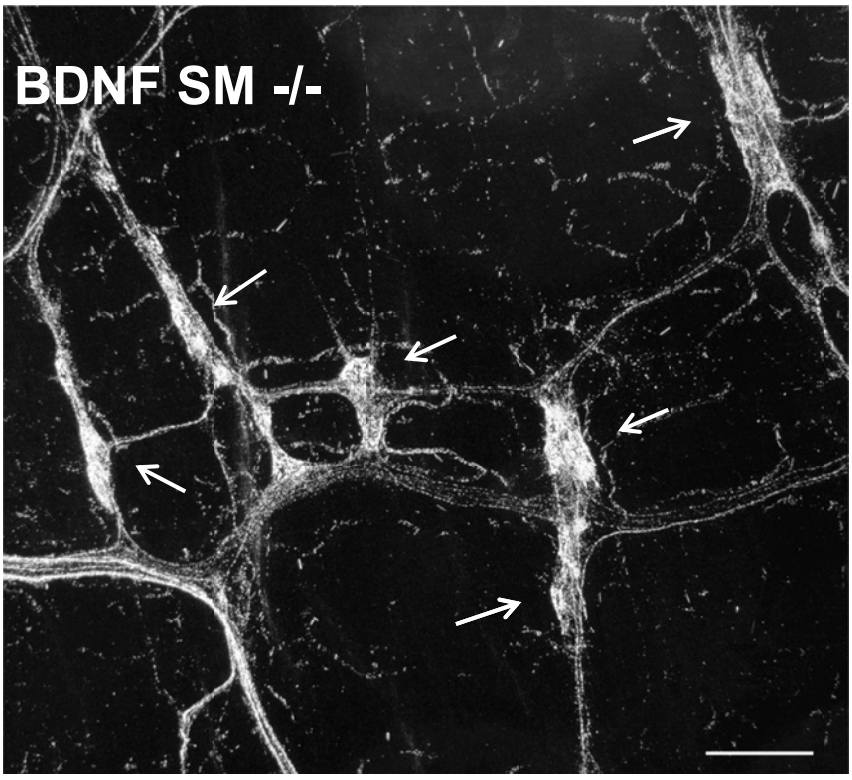

Figure 8. Photomontages of IGLE morphology and density in the intestine of (A) control and (B) BDNF SM -/- mice. BDNF SM -/- mice demonstrated an increase in IGLE density in the intestine compared to controls. Arrows denote IGLEs. Scale bar = 5.0 mm.

A

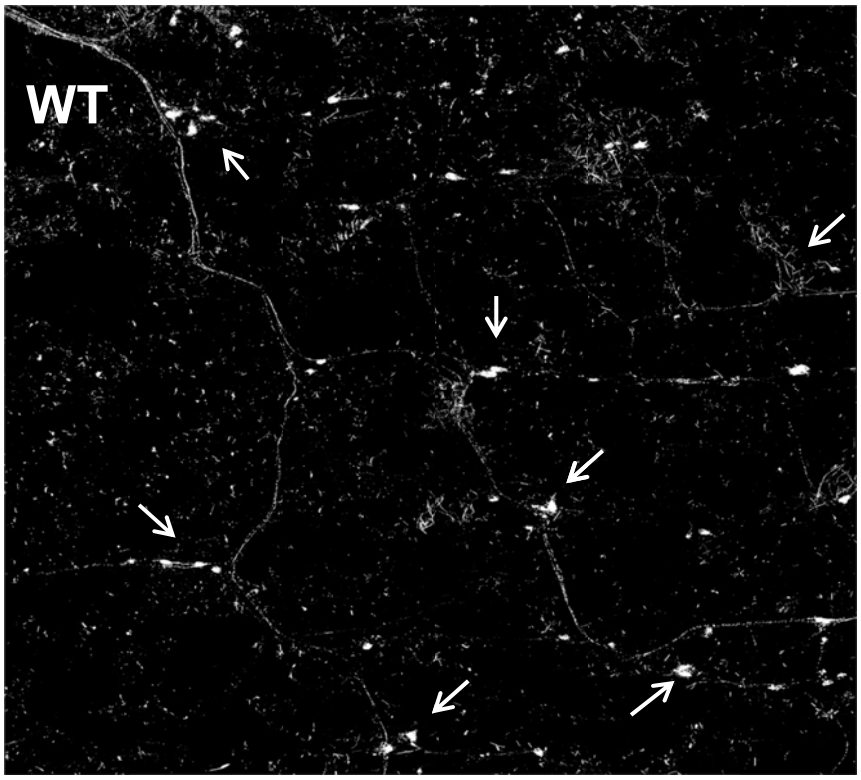

B

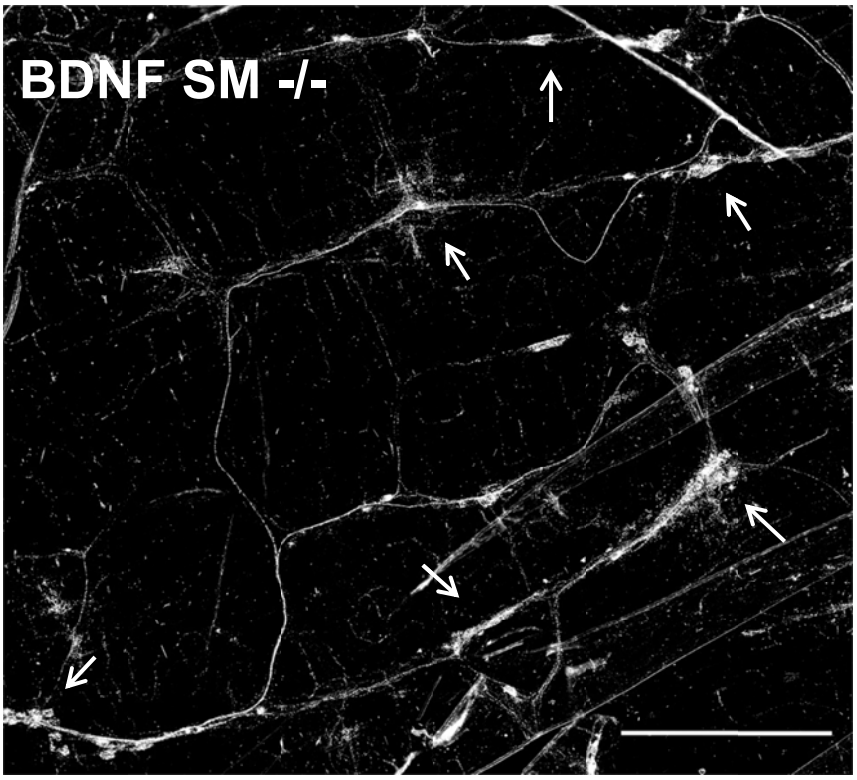

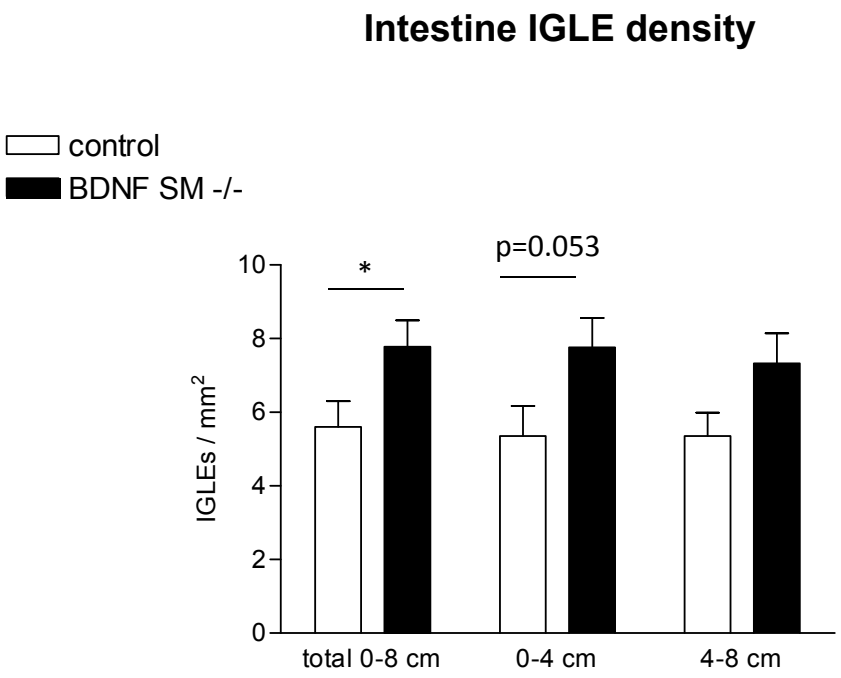

Figure 9. Quantification of vagal afferent innervation shows increased IGLE density across the first 0-8 cm in the intestine of BDNF SM -/- mice compared to controls. Density of IGLEs in the 0-4 and 4-8 cm portions of the duodenum were nearly significant.

Figure 10. BDNF SM -/- mice demonstrated a trend toward increased longitudinal bundle density in the (A) total (0-8 cm) of the duodenum (B) 0-4 cm and (C) 4-8 duodenum of the intestine.

A

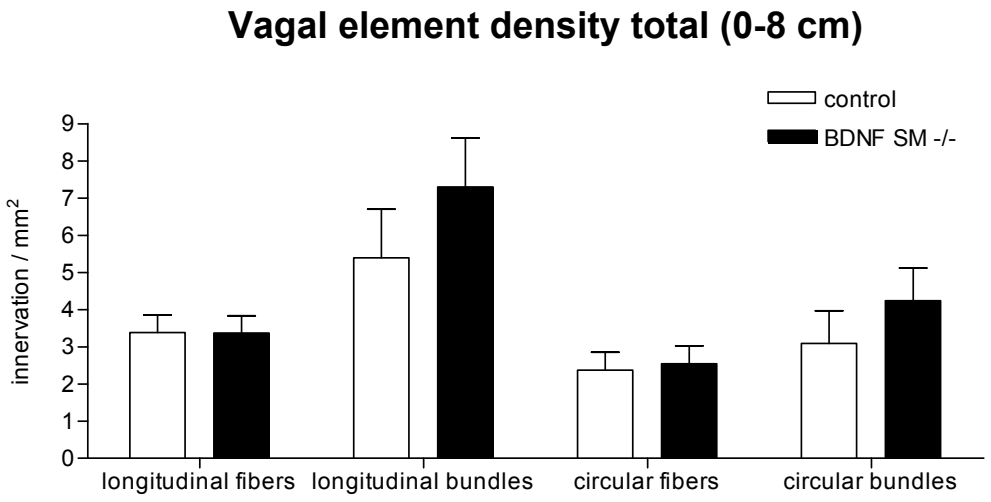
Vagal element density total (0-8 cm)
control
BDNF SM -/-
innervation / mm2
0
1
2
3
4
5
6
7
8
9
longitudinal fibers
longitudinal bundles
circular fibers
circular bundles

B

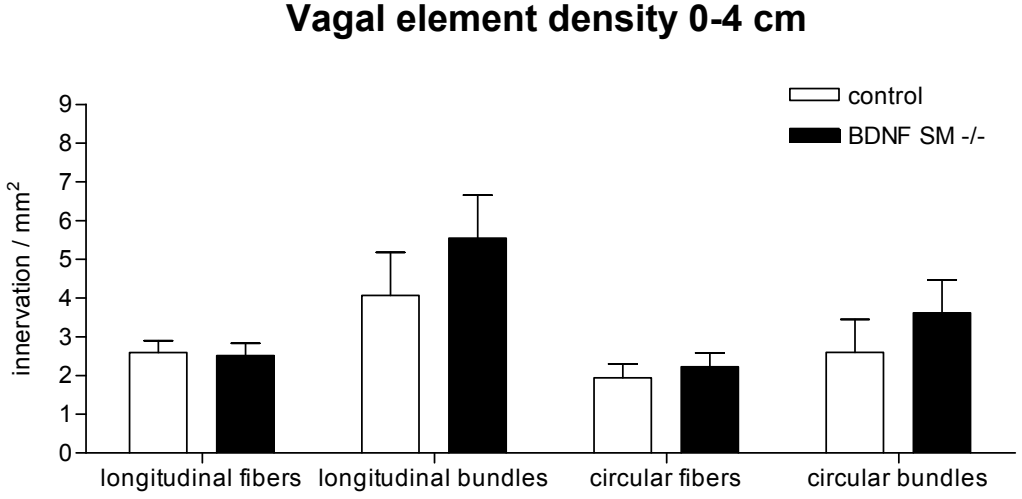
Vagal element density 0-4 cm
control
BDNF SM -/-
innervation / mm2
0
1
2
3
4
5
6
7
8
9
longitudinal fibers
longitudinal bundles
circular fibers
circular bundles

C

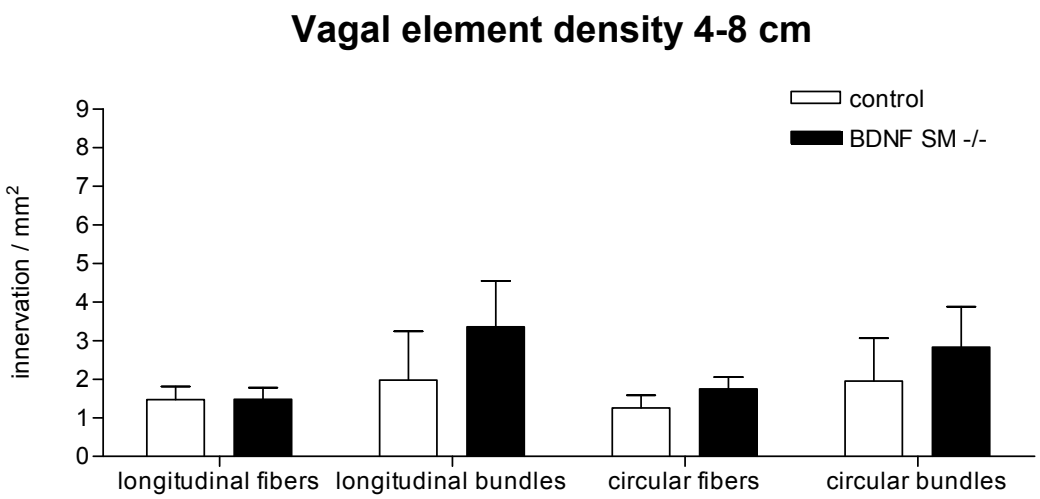
Vagal element density 4-8 cm
control
BDNF SM -/-
innervation / mm2
0
1
2
3
4
5
6
7
8
9
longitudinal fibers
longitudinal bundles
circular fibers
circular bundles

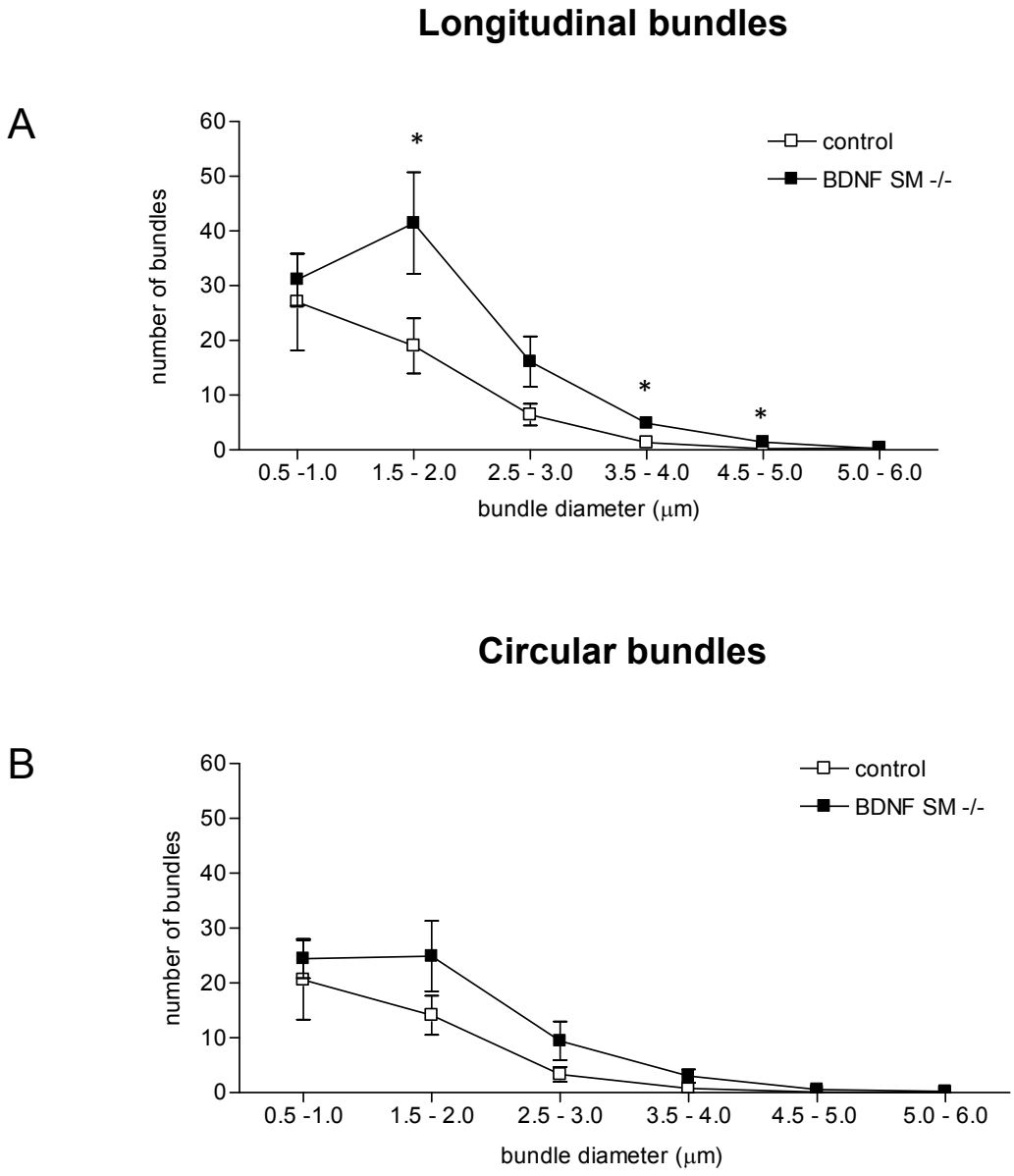

Figure 11. BDNF SM -/- mice demonstrated significantly increased number of larger-diameter longitudinal axon bundles compared to control mice (A), while there was no change in circular bundles (B).

Figure 12. BDNF SM -/- mice showed a significant increase in vagal sensory neurons compared to controls. Images shown are representative examples of nodose ganglia in control (A) and BDNF SM -/- mice (B), while (C) depicts number of vagal sensory neurons on the left and right sides, and the total of both left and ride sides. Scale bar = 250 µm.

A

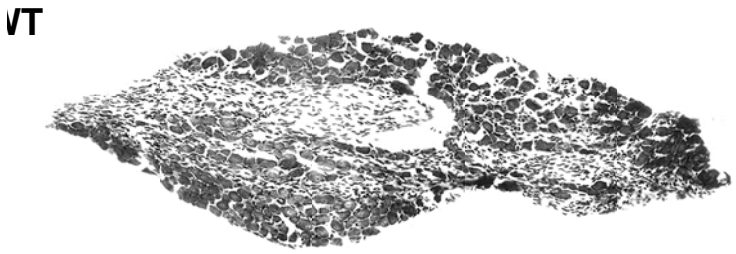
VT

B

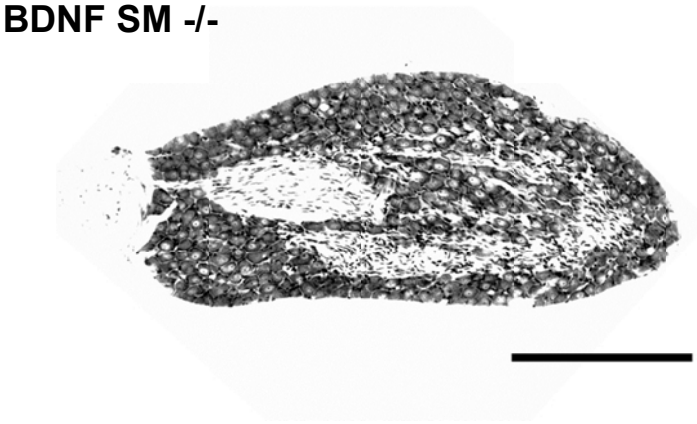
BDNF SM -/-

C

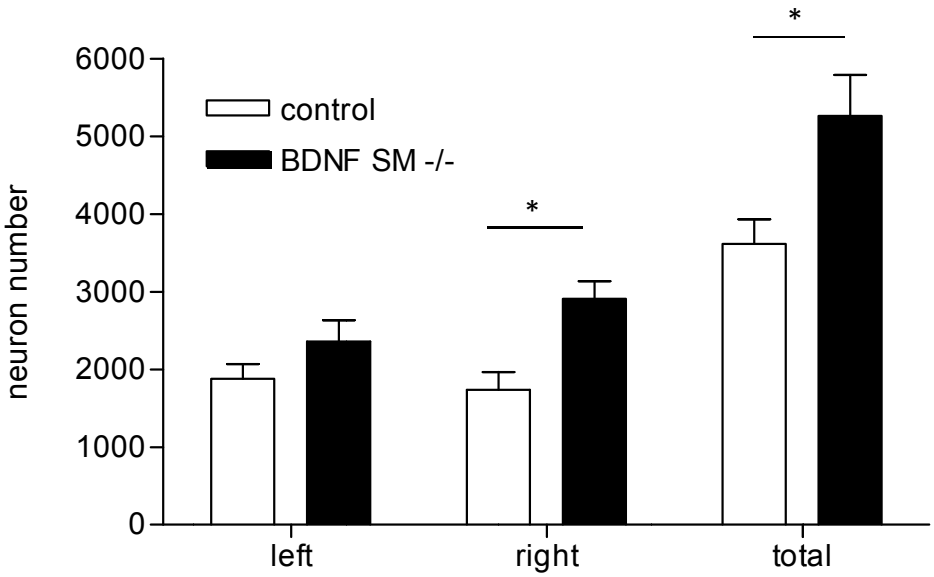
neuron number
6000
5000
4000
3000
2000
1000
0
control
BDNF SM -/-
*
*
left
right
total

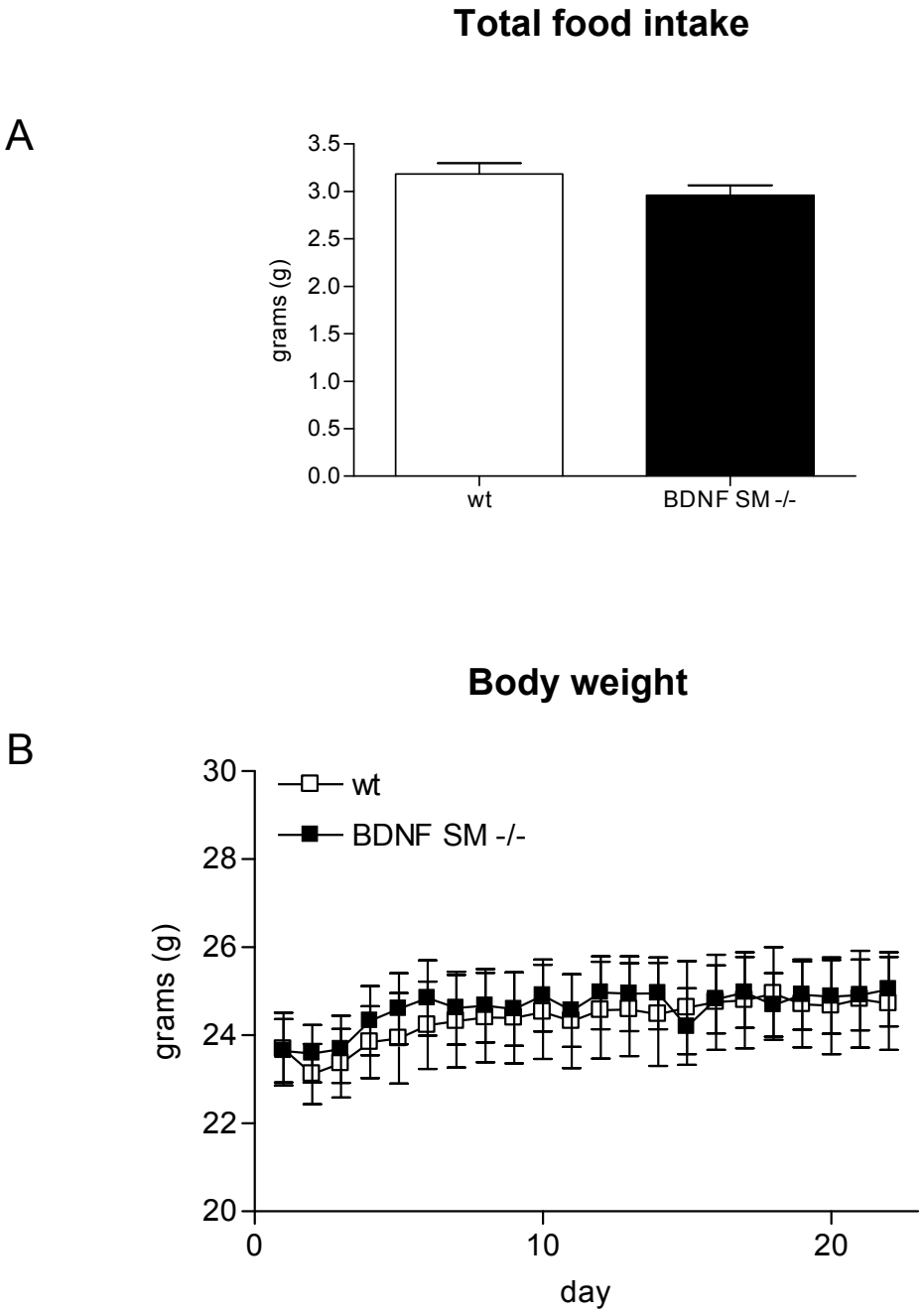

Figure 13. There were no differences in total food intake or body weight during meal pattern collection at 3-4 months of age. (A) Daily food intake over days 5-22 of meal pattern collection on a balanced pellet diet. (B) Daily body weight over days 5-22 of meal pattern collection on a balanced pellet diet.

A

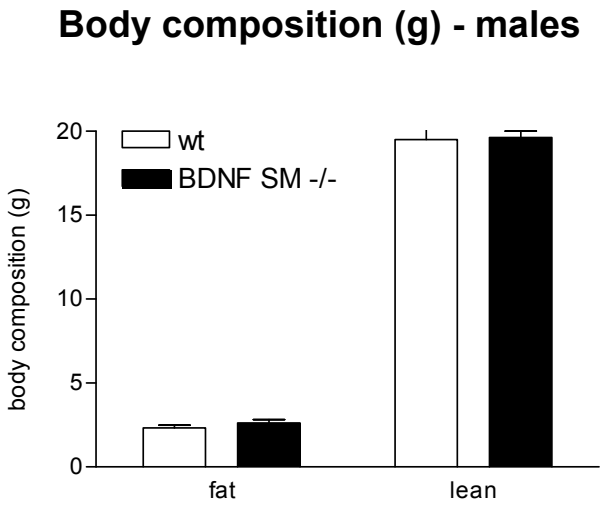

B

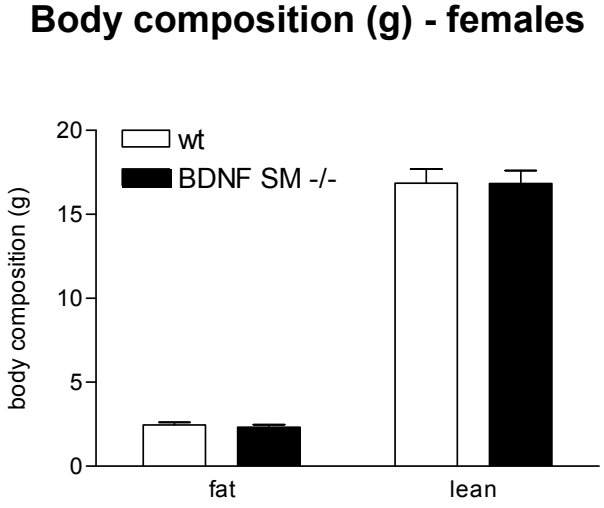

Figure 14. There were no differences in total grams of lean mass or fat mass during meal pattern collection at 3-4 months of age in either males (A) or females (B).

A

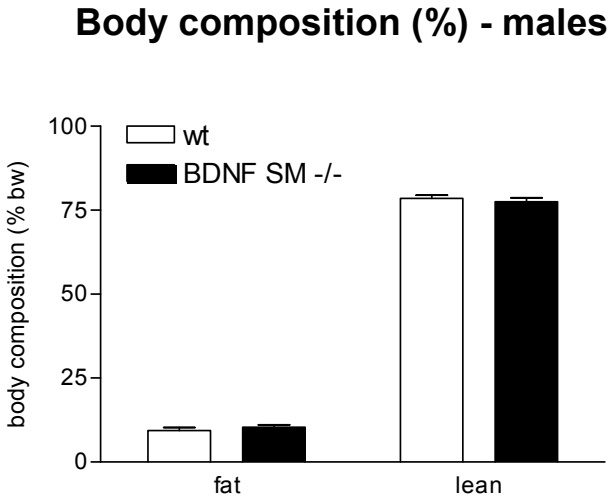

B

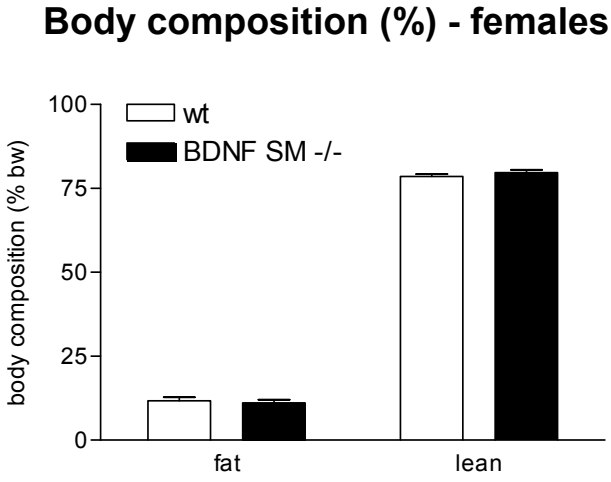

Figure 15. There were no differences in lean mass or fat mass expressed as percent of body mass during meal pattern collection at 3-4 months of age in either males (A) or females (B).

Figure 16. BDNF SM -/- mice showed increased satiation compared to wt mice, as shown by decreased total meal duration (A), decreased average meal duration (B) and decreased meal size (C) compared to wt mice.

A

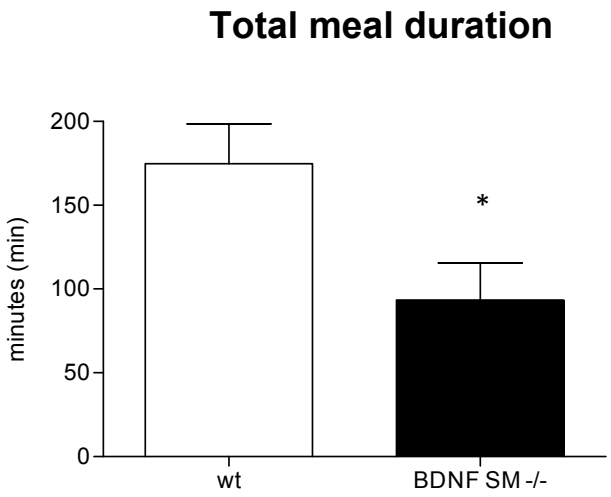
Total meal duration
minutes (min)
200
150
100
50
0
*
wt
BDNF SM -/-

B

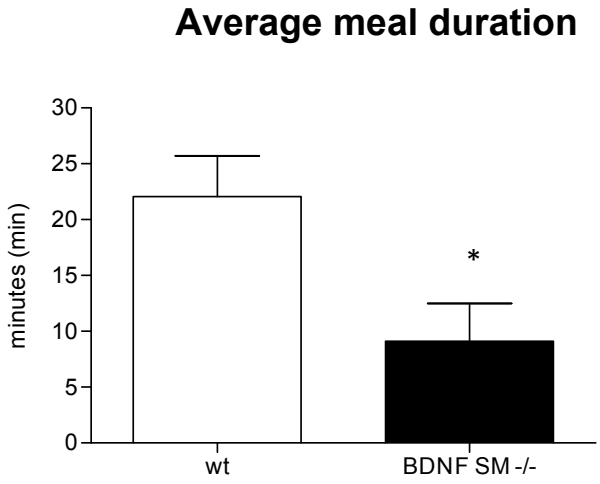
Average meal duration
minutes (min)
30
25
20
15
10
5
0
*
wt
BDNF SM -/-

C

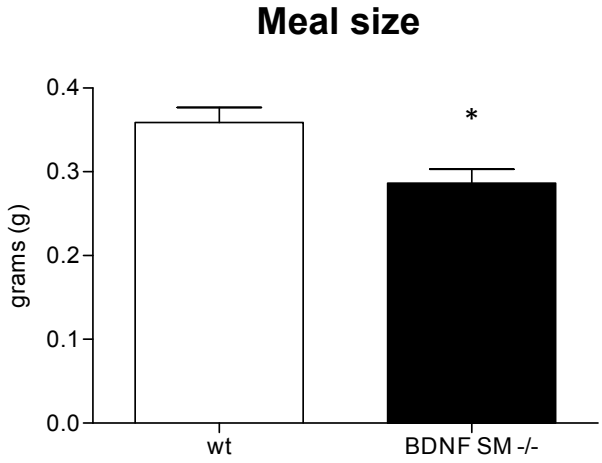
Meal size
grams (g)
0.4
0.3
0.2
0.1
0.0
*
wt
BDNF SM -/-

Figure 17. BDNF SM -/- mice showed increased satiety compared to wt mice, as shown by increased total IMI (A), a trend towards an increased average IMI (B) and increased satiety ratio (C) compared to wt mice.

A

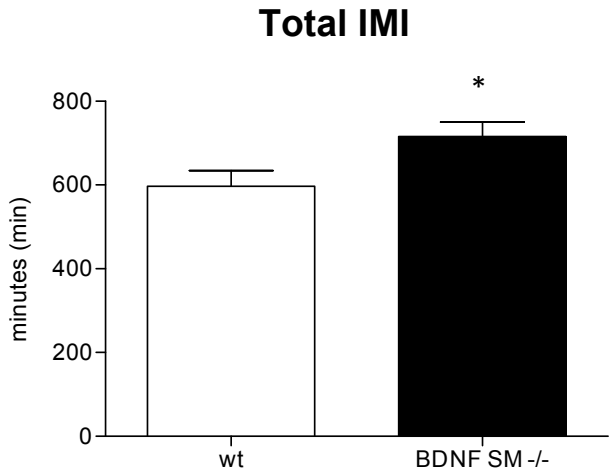
Total IMI
*
800
600
400
200
0
minutes (min)
wt
BDNF SM -/-

B

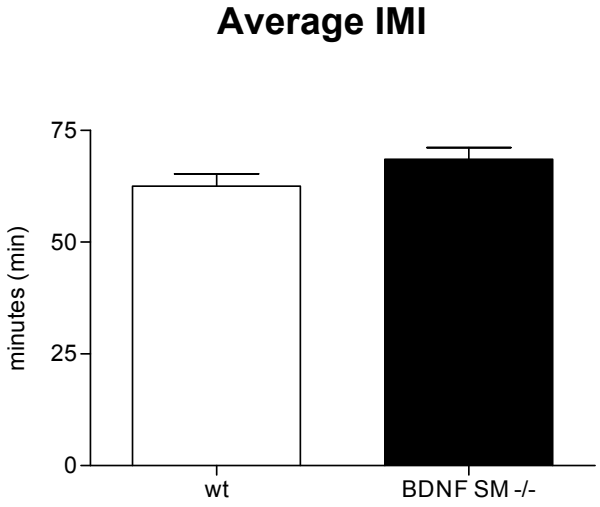
Average IMI
75
50
25
0
minutes (min)
wt
BDNF SM -/-

C

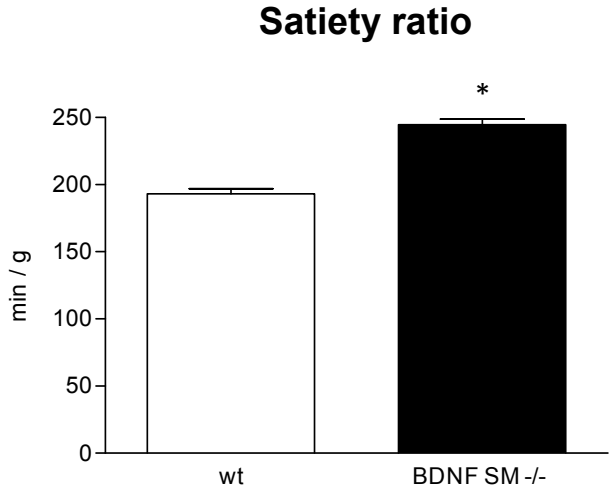
Satiety ratio
*
250
200
150
100
50
0
min / g
wt
BDNF SM -/-

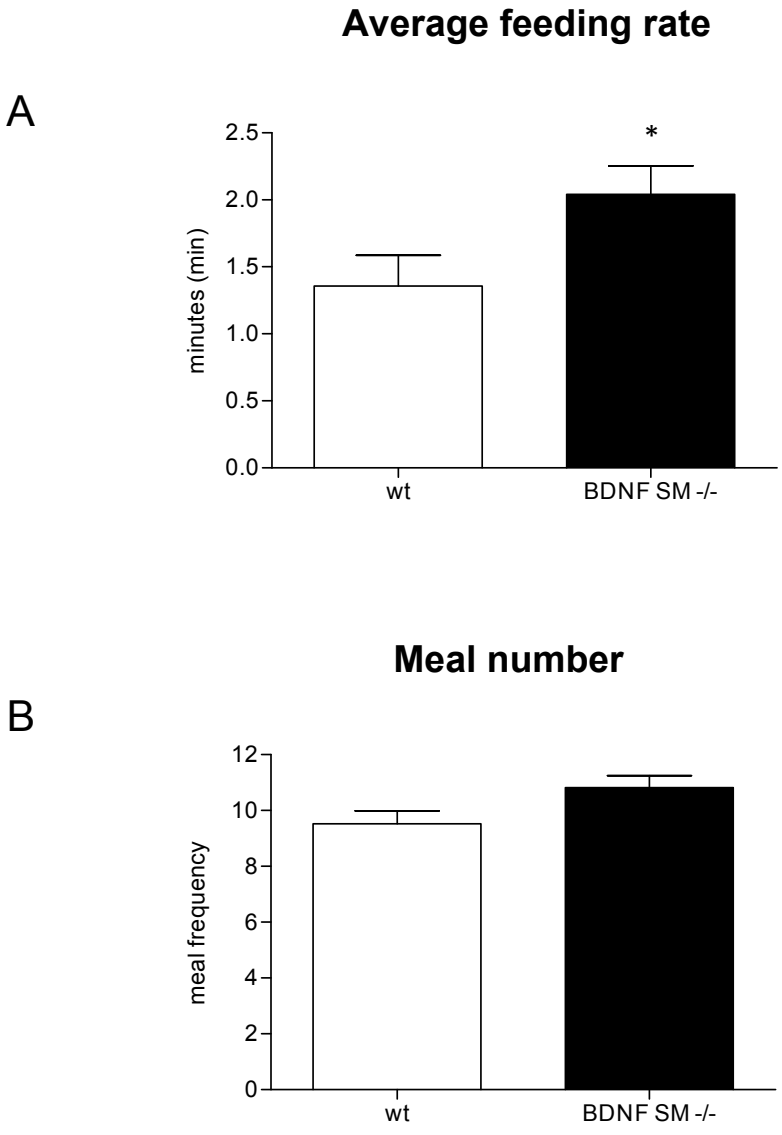

Figure 18. BDNF SM -/- compensated for increased satiation with increased feeding rate (A) and a trend toward increased meal number (B) compared to wt mice.

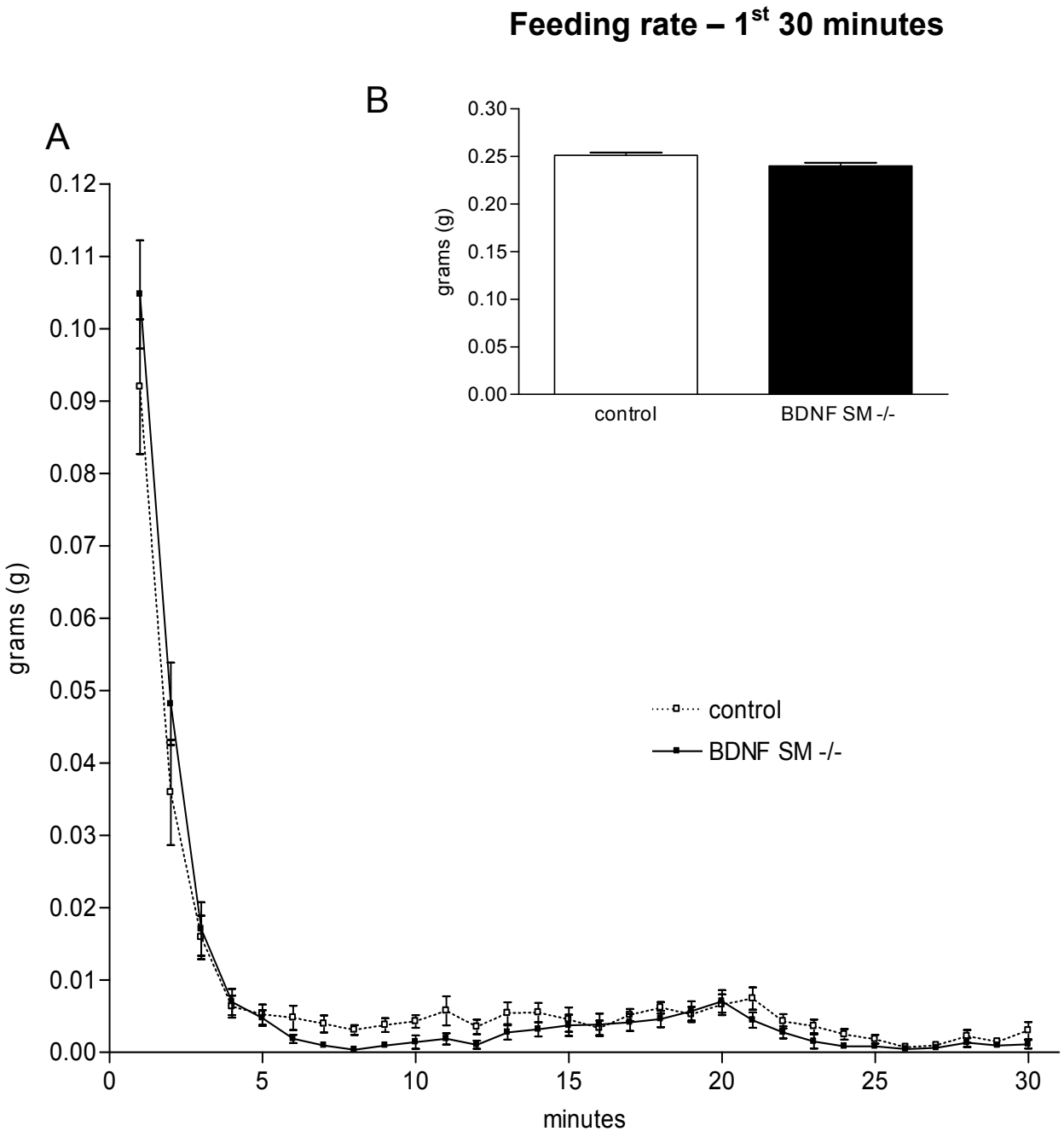

Figure 19. Rate of food intake across the first 30 min meal after a 6 hr fast and averaged across days 5-22 are shown by each minute (A) and averaged across the entire 30 min (inset, B).

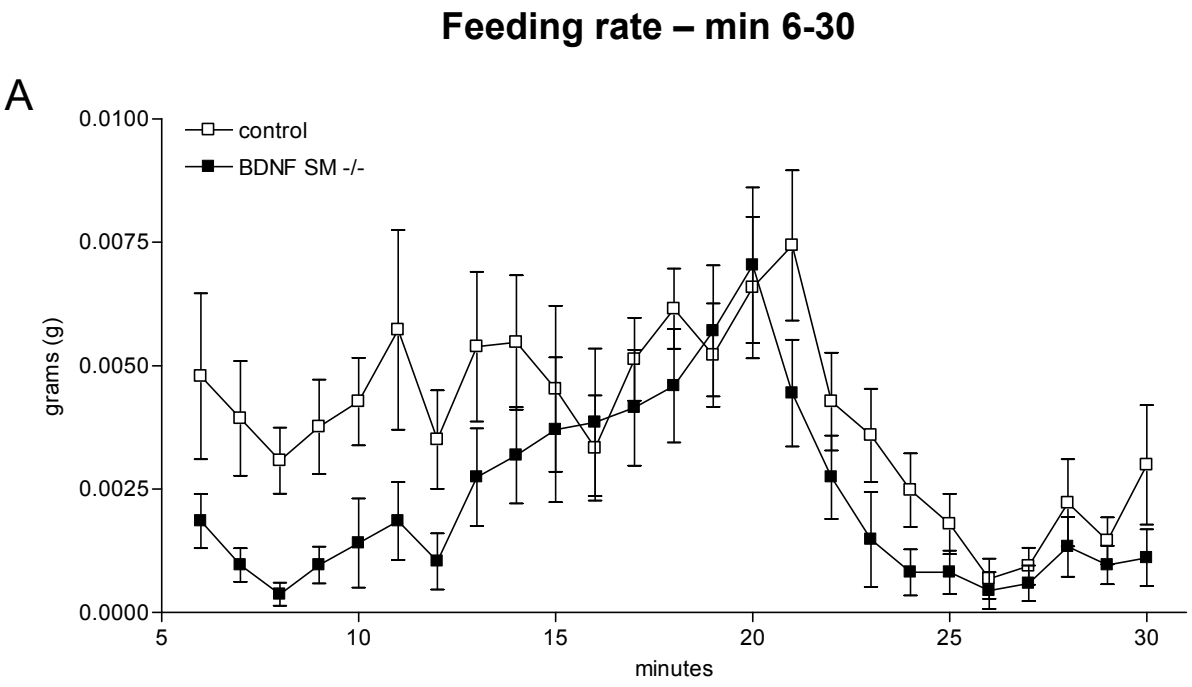

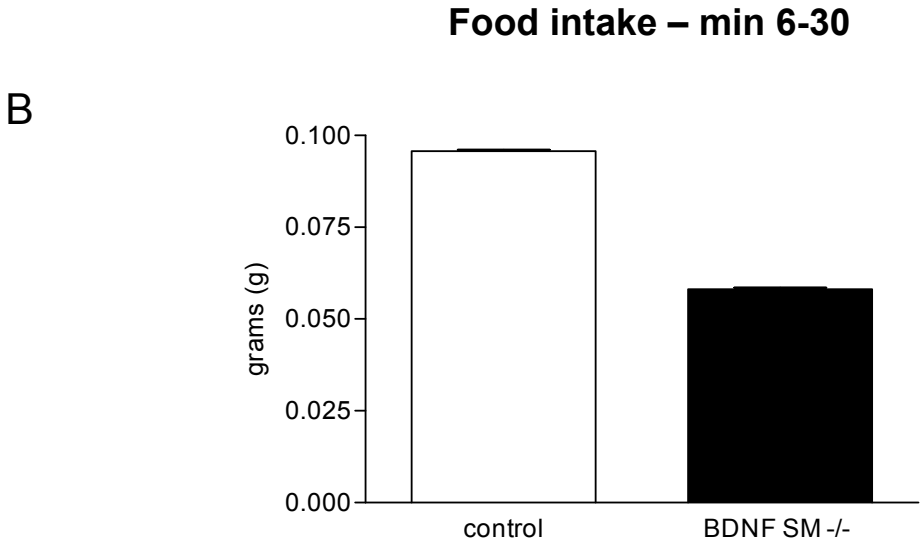

Figure 20. Food intake from minutes 6-30. BDNF SM -/- mice show increased suppression during the late decay phase of food intake. The rate of food intake across minutes 6-30 is shown per minute (A) and as the average food intake across minutes 6-30 (B).

VITA

VITA

Jessica Erin Biddinger
703 3rd Street B150
West Lafayette, IN 47907

Education

The Ohio State University	2004	B.S. Biology
Purdue University	2009	M.S. Behavioral Neuroscience
	2013 (anticipated)	Ph.D. Behavioral Neuroscience

Academic Experience

Purdue University, Graduate Research Assistant	2007 - present
Purdue University, Teaching Assistant	2009 - present

Courses taught (all at Purdue University):

- Introduction to Behavioral Neuroscience
- Neural Systems
- Motivation
- Neuroscience of Motivated Behavior
- Drugs & Behavior
- Ethology
- Research Methods

Industry Experience

Nestlé, Inc., Columbus, OH, Food Microbiologist	2005 - 2007
ConAgra, Columbus, OH, Laboratory Technician	2005 - 2006

Publications

Biddinger, J. E., & Fox, E. A. (2010). Meal parameters and vagal gastrointestinal afferents in mice that experienced early postnatal overnutrition. *Physiology & Behavior*, *101*(1), 184-191.

Fox, E. A., & Biddinger, J. E. (2012). Early postnatal overnutrition: potential roles of gastrointestinal vagal afferents and brain-derived neurotrophic factor. *Physiology & Behavior, 106*(3), 400-412.

Fox, E. A., Biddinger, J. E., Jones, K. R., McAdams, J., & Worman, A. (2013). Mechanism of hyperphagia contributing to obesity in brain-derived neurotrophic factor knockout mice. *Neuroscience*, *229*, 176-199.

Fox, E. A., Biddinger, J. E., Baquet, Z. C., Jones, K. R., & McAdams, J. (2013). Loss of neurotrophin-3 from smooth muscle disrupts vagal gastrointestinal afferent signaling and satiation. *American Journal of Physiology – Regulatory, Integrative and Comparative Physiology* [epub ahead of print].

Awards

NIH Institutional Predoctoral Training Grant Fellow, Ingestive Behavior Research Center, Purdue University, 2011-2013

Most Outstanding Presentation Award, Office of Interdisciplinary Graduate Programs, Purdue University, 2012

Graduate Publication Award (1st place), Department of Psychology, Purdue University, 2011

Ross Fellowship, Ingestive Behavior Research Center, Purdue University, 2007-2009

Marconi Scholarship, Department of Chemistry, The Ohio State University, 2005-2006

Undergraduate Honors Research Award, Department of Chemistry, The Ohio State University, 2005-2006

Scarlet and Grey Scholarship, The Ohio State University, 2002-2004

Affiliations

Society for Neuroscience

Society for the Study of Ingestive Behavior

Ingestive Behavior Research Center

Research Presentations

Biddinger, J. E., & Fox, E. A. (2013). *Increased vagal sensory neuron and intestinal axon bundle number in mice with smooth muscle-knockout (KO) of brain-derived neurotrophic factor (BDNF) may contribute to augmented intestinal mechanoreceptor innervation and satiation*. Society for Neuroscience Annual Meeting, San Diego, CA.

Biddinger, J. E. (2013). *Smooth muscle-specific removal of brain-derived neurotrophic factor (BDNF) results in increased vagal afferent innervation and increased satiation*. Harvard Medical School, Cambridge, MA.

Biddinger, J. E. (2013). *Effects of smooth muscle-specific removal of brain-derived neurotrophic factor on vagal afferent innervation in the gastrointestinal tract and feeding behavior in mice*. Children's Hospital Los Angeles & Saban Research Institute, Los Angeles, CA.

Biddinger, J. E., & Fox, E. A. (2012). *Effects of smooth-muscle specific deletion of brain-derived neurotrophic factor on vagal afferent innervation of the gastrointestinal tract, feeding behavior and body weight.* Society for Neuroscience Annual Meeting, New Orleans, LA.

Biddinger, J. E., & Fox, E. A. (2012). *Gastrointestinal vagal afferent innervation and meal patterns in mice with peripheral BDNF knockout*. Society for the Study of Ingestive Behavior Annual Meeting, Zurich, Switzerland.

Biddinger, J. E., & Fox, E. A. (2012). *Peripheral knockout of brain-derived neurotrophic factor results in increased intestinal vagal afferent innervation in the mouse*. Office of Interdisciplinary Graduate Programs Poster and Awards Reception, Purdue University.

Biddinger, J. E. (2012). *The effects of gastrointestinal brain-derived neurotrophic factor on development and function of vagal afferents, feeding behavior and body weight regulation*. Seminar in Neurobiology, Endocrinology, and Behavior, Purdue University.

Biddinger, J. E., McAdams J., & Fox, E. A. (2011). *Altered feeding patterns of mice with smooth-muscle specific knockout of neurotrophin-3 suggest involvement of vago-vagal gastrointestinal reflexes*. Society for Neuroscience Annual Meeting, Washington, D.C.

Biddinger, J. E. (2011). *Targeted deletion of brain-derived neurotrophic factor results in hyperphagia and obesity: determining the contribution of the vagus*. Seminar in Neurobiology, Endocrinology, and Behavior, Purdue University.

Fox, E. A., Biddinger, J. E., Jones, K. R., Worman, A., & McAdams, J. (2010). *Smooth muscle-specific knockout of brain-derived neurotrophic factor results in hyperphagia and obesity*. Society for Neuroscience Annual Meeting, San Diego, CA.

Biddinger, J. E., & Fox, E. A. (2010). *Meal pattern and microstructure changes underlying hyperphagia and obesity in mice with smooth muscle specific brain-derived neurotrophic factor knockout*. Society for Neuroscience Annual Meeting, San Diego, CA.

Biddinger, J. E. (2010). *Targeted deletion of brain-derived neurotrophic factor and feeding behavior*. Seminar in Neurobiology, Endocrinology, and Behavior, Purdue University.

Biddinger, J. E., Sharp, A. M., & Fox, E. A. (2009). *Effects of early postnatal overnutrition on meal pattern and vagal sensory innervation of the small intestine*. Society for Neuroscience Annual Meeting, Chicago, IL.

Biddinger, J. E. (2009). *Effects of early postnatal overnutrition on vagal innervation in the gastrointestinal tract and meal pattern in the development of obesity*. Seminar in Neurobiology, Endocrinology, and Behavior, Purdue University.

Biddinger, J. E. (2008). *Effect of perinatal nutritional environment on feeding behavior*. Seminar in Neurobiology, Endocrinology, and Behavior, Purdue University.

Biddinger, J. E., He, D., & Parquette, J. R. (2006). *Allosteric chirality transfer throughout a folded dendrimer*. Denman Forum for Undergraduate Honors Research, The Ohio State University, Columbus, OH.